



INTERNATIONAL DOCTORAL
SCHOOL OF THE USC

Luis Arturo
Morán Lara

PhD Thesis

DEVELOPMENT OF LIGANDS
FOR THE PLATELET
RECEPTOR CLEC-2

Santiago de Compostela, 2022

Doctoral Programme in European Joint Doctorate Marie Skłodowska-Curie in Targeting
Platelet Adhesion Receptors in Thrombosis



DEVELOPMENT OF LIGANDS FOR THE PLATELET RECEPTOR CLEC-2

By

Luis Arturo Morán Lara

A thesis submitted to the University of Santiago de Compostela and
the University of Birmingham for European Joint Doctorate Degree.

Escola de Dotouramento Internacional
European Joint Doctorate Marie Skłodowska-Curie in Targeting
Platelet Adhesion Receptors in Thrombosis (TAPAS)
University of Santiago de Compostela, Spain

Institute of Cardiovascular Sciences
College of Medical and Dental Sciences
University of Birmingham, UK

2022



AUTHORSHIP DECLARATION

**DEVELOPMENT OF LIGANDS FOR
THE PLATELET RECEPTOR CLEC-2**

Luis Arturo Morán Lara

I present my PhD thesis following the procedures agreed, and I
declared that:

1. The thesis covers the results generated during my experimental work.
2. The results generated by collaborations are stated.
3. The final version of this thesis is equivalent to the digital version presented.
4. I confirm that this thesis does not incur in any plagiarism activity, not even from my own work to receive any previous qualification

Santiago de Compostela, Spain, 30th of March 2022

Luis A Morán

SUPERVISOR / TUTOR AUTHORISATION
[DEVELOPMENT OF LIGANDS FOR THE PLATELET
RECEPTOR CLEC-2]

Prof. Ángel García Alonso, Prof. Steve P. Watson, Prof. Michael Tomlinson

STATE:

That this thesis corresponds to the work carried out by Mr. Luis Arturo Morán Lara, under our supervision/ tutoring, and hereby authorise its presentation, taking into account that it meets all the relevant requirements stated in the Doctoral Studies Regulations of the USC, and as its director it does not incur in the causes of abstention established in the 40/2015 Law.

In accordance with what is stated in the Regulations for Doctoral Studies, it is also declared that this doctoral thesis can be defended based on the modality of Monographic with reproduction of publications, in which the participation of the PhD student was decisive for its elaboration and the publications adjust to the Research Plan.

In Santiago de Compostela and Birmingham, 19 of May 2022

Acknowledgements

I would like to thank to my supervisors Ángel Garcia from the USC and Steve Watson and Mike Tomlinson (UoB) for their consistent support and guidance during the running of my PhD. I have grown as a professional during my PhD, but more importantly, as human being and you have contributed enormously during this life-changing process. I would also like to thank you for taking me onboard, as a part of TAPAS.

I thank to all the members of the TAPAS consortium; it was a real pleasure to have so many exciting discussions during the TAPAS meetings. I thank to the TAPAS students Hilaire Cheung, Marcin Sowa, Ale Neagoe, Delia Fernandez, Xueqing Wang which I closely worked with, in Santiago or Birmingham. I also want to thank Caroline McKay for their extraordinary support.

I thank to me labmates from the University of Santiago de Compostela, Lidia Hermida, Maria N. Barrachina, and Irene Izquierdo for their friendship and support all these years. Great memories from Santiago and thank you for making me felt at home since the very beginning. I would also give a special thanks to Lidia for always being there to help me and for understanding and listening in the rough times. Thank you, Maria, for always cheer us up! You are wonderful people, thanks for being in my path.

I would also thanks to Eleya Martin, Jo Clark, Ying Di, for your scientific contribution in this project. As well as, Alex Slater, Fay

Damaskinaki. Gina Perrella, Vanesa Ivanova, Lourdes Garcia, Beata Grygielska, Harry Zhi, Sam Montague, Josh Bourne, Martina Colicchia, for their friendship and support. I also thanks to Julie Rayes and Abs Khan, you always have wise advises.

I also thank to the Birmingham platelet group for their support during the difficult times that we have experienced during the COVID-19 pandemic, which started upon my arrival to the UK. I would also like to give a special thanks to Amanda Dalby for proof-reading my thesis, I do not have enough words to thank you for your kindness.

I would also thank to my wonderful wife Brenda Carrero for her unconditional support, for her kind words in the difficult times and for making my life way better than what I was before her. Only you know the behind the scenes of all this experience. You mean the world to me! I give a big thanks to my parents Iyanú and Luis and my brothers Luis Fernando, Luis Raúl, and Luis Adrián for their unconditional support and for making me the person that I am today. There is no distance when I pick the phone to talk to you!

I would also like to thank to the European Union's Horizon 2020 research and innovation program [Marie Skłodowska-Curie grant agreement [No. 766118] for supporting the present PhD thesis and the Targeting Platelet Adhesion Receptors in Thrombosis (TAPAS)

Abstract

Background:

Platelets are anucleate cells derived from megakaryocytes, which play an important role in the regulation of haemostasis and thrombosis at the injury site; however, they are also involved in other physiological processes such as inflammation, during which they interact with other immune cells including leukocytes. However, certain chronic inflammatory diseases may lead to an aberrant prothrombotic response, known as thromboinflammation. This process is modulated by certain platelet immune receptors, including CLEC-2, a C-type lectin-like type II transmembrane receptor.

CLEC-2 is a novel target in thromboinflammatory diseases such as deep vein thrombosis and infection; furthermore, interaction of platelet CLEC-2 with its ligand podoplanin on the surface of cancer cells is involved in the development of thrombosis associated with cancer and metastasis. Additionally, this receptor plays a minor role in physiological haemostasis and has been shown to be involved in thrombus stability in blood perfused over collagen surfaces.

Structural and molecular studies have suggested that clustering of CLEC-2 activates the receptor and leads to platelet aggregation. However, the pharmacological aspects, such as CLEC-2–ligand stoichiometry, required to induce platelet aggregation remain unknown.

Therefore, this study aimed to develop novel ligands for CLEC-2 on the basis of small molecules and nanobodies against CLEC-2 to (1) generate novel blocking agents for CLEC-2 interaction, (2) identify the minimum ligand size required to induce platelet aggregation through CLEC-2, and (3) assess the role of tyrosine kinase dephosphorylation in aggregates formed by CLEC-2 ligands and thus improve the understanding of CLEC-2 activation mechanism and contribute to the design of novel therapeutic agents to prevent or treat thromboinflammation.

Methods:

First, a small-molecule chemical library was screened using the AlphaScreen assay on the basis of the podoplanin–CLEC-2 interaction to identify small-molecule ligands of the receptor. Potential hits were characterised using light transmission aggregometry and western blotting. In the second approach, high-affinity nanobodies raised against human CLEC-2 were screened. The most potent nanobody was multimerised using a short crosslinking sequence of repeated GGGGS, developing dimeric and tetrameric forms. Finally, tyrosine kinase inhibitors were added to platelet aggregates formed by hemi-immunoreceptor-tyrosine-based activation motif ([hem]ITAM) or non-ITAM ligands. Platelet disaggregation was monitored using light transmission aggregometry.

Results:

The experiments identified a polymeric small-molecule ligand that binds to CLEC-2 and induces platelet aggregation in an all-or-none manner. Activation occurs through CLEC-2 phosphorylation mediated by Src and Syk tyrosine kinases.

LUAS, the most efficient of the 48 nanobodies raised against human CLEC-2, blocked the activation of platelets by podoplanin-expressing cells. Surface plasmon resonance showed that LUAS binds to CLEC-2 with an affinity of ~140 nM. Dimerisation increased the affinity to 0.5 nM and generated a potent blocking agent, LUAS-2. However, a tetramer of LUAS (LUAS-4) induced platelet aggregation, which was blocked by Src and Syk kinase inhibitors and by the divalent CLEC-2 antibody fragment AYP1 F(ab)₂, suggesting that activation is mediated by CLEC-2.

This study also showed that platelet aggregate stability is partially and weakly mediated by Src kinases; however, it is likely mediated by signalling independent of the ITAM receptor because similar results have been observed in platelet aggregates formed by the PAR-1 ligand, TRAP-6.

Conclusion:

Polymeric and tetrameric ligands (as katacine or LUAS-4, respectively) are required to induce platelet aggregation and potentially induce clustering of CLEC-2; however, ligand dimerisation does not induce

platelet aggregation. The novel tools will facilitate further research on CLEC-2 function and the mode of activation of CLEC-2.

Introdución:

As plaquetas son células sanguíneas amplamente recoñecidas polo seu papel no mantemento da hemostase e da trombose, formando agregados plaquetarios no lugar da lesión vascular. O papel das plaquetas na hemostase foi descrito hai máis dun século polo científico italiano Giulio Bizzozero. Porén, hoxe en día tamén se recoñece o seu papel noutros procesos fisiolóxicos como a inflamación, onde se demostrou que interactúan con outras células do sistema inmunitario, incluídos os leucocitos.

A interacción entre os procesos inflamatorios e a trombose é relevante pola súa participación en múltiples procesos patolóxicos caracterizados pola presenza de inflamación crónica, que posteriormente ten como resultado a aparición de procesos protrombóticos, onde os pacientes tenden a ter unha resposta deficiente á terapia antiagregante plaquetaria, levando a efectos secundarios letales, asociados a cadros clínicos de hemorraxia grave.

A terapia antiplaquetaria actual caracterízase polo uso de inhibidores da síntese de prostaglandinas a través da ciclooxixenasa, COX-1/2, como é o caso do uso de ácido acetilsalicílico (tamén coñecido como aspirina), ou mediante o uso de inhibidores dos receptores purinéxicos de ADP, como é o caso do uso de axentes antiagregantes, clopidogrel e ticagrelor. Non obstante, en pacientes resistentes á monoterapia

antiplaquetaria, adoitan aplicarse estratexias que inclúen o uso combinado de inhibidores da síntese de prostaglandinas xunto con inhibidores do receptor de ADP. Estas terapias son eficaces, evitando a formación de novos trombos en pacientes con antecedentes ou alto risco cardiovascular, non obstante, o alto risco de presentar cadros hemorráxicos segue a ser unha ameaza latente para o paciente (Guha, Mookerjee et al. 2009, Wang, Ouyang et al 2018).

Por iso, hai moitos anos que existe unha enorme necesidade de desenvolvemento de novas dianas terapéuticas, que se caractericen por unha menor implicación na hemostase e unha maior implicación no desenvolvemento da trombose. Estas características observáronse en receptores tipo ITAM/(hem)ITAM, como é o caso do receptor de coláxeno, GPVI, e do receptor de podoplanina, CLEC-2 (Rayes, Watson et al. 2019). Isto demostrouse en modelos murinos onde a deficiencia ou a redución de GPVI e CLEC-2 non tivo un impacto significativo nos tempos de sangramento. Porén, observouse que teñen unha maior implicación na formación do trombo. No caso de CLEC-2, tamén se observou que ratos deficientes neste receptor estaban protexidos nun modelo de trombose venosa profunda (Haining, Cherpokova et al. 2017, Ahmed, Kaneva et al. 2020).

Outra característica que cabe destacar de CLEC-2 é o feito de que este receptor está moi implicado no desenvolvemento de procesos inmunotrombóticos, agravando os síntomas clínicos destes pacientes.

Por exemplo, CLEC-2 e a súa interacción co podoplanina suxeriuse

como un eixe importante para os procesos inflamatorios presentes nos modelos de sepsis. Tamén se identificou a hemina como un novo ligando de CLEC-2, que podería ser liberado á circulación en procesos hemolíticos (Bourne, Colicchia et al. 2021).

Por todo o anterior, CLEC-2 considérase un obxectivo terapéutico potencial para a prevención e tratamento de enfermidades tromboinflamatorias e trombose venosa profunda. Por iso, neste estudo, dedicámonos a investigar diferentes estratexias para o desenvolvemento de novos ligandos do receptor CLEC-2, co fin de identificar novas ferramentas para o desenvolvemento racional de novos fármacos para este receptor e contribuír a unha mellor comprensión deste receptor.

CLEC-2 é unha proteína transmembrana de 32 KDa, esta proteína pertence á familia das lectinas de tipo C e exprésase en plaquetas, megacariocitos e células dendríticas. CLEC-2 foi identificado en 2006 como o receptor da proteína heterodimérica rodocitina, que está presente no veneno da serpe, *Calloselasma rhodostoma* (Suzuki-Inoue, Fuller et al. 2006).

Estudos estruturais e moleculares suxeriron que o receptor CLEC-2 require a agrupación como mecanismo para a activación do receptor e a posterior agregación plaquetaria. Non obstante, descoñécense aspectos farmacolóxicos como a estequiometría de ligandos e CLEC-2 para inducir a agregación plaquetaria (Hughes, Pollitt et al. 2010).

CLEC-2 coñécese como receptor de tipo hemITAM, xa que só ten un único dominio YxxxL na súa cola citoplásmica. O motivo ITAM (immunoreceptor-tyrosine-based activation motif) fosforíase pola interacción co seu ligando (por exemplo: podoplanina ou rodocitina). A sinalización plaquetaria mediada por CLEC-2 inclúe a fosforilación do receptor pola tirosina quinase Syk e a familia de quinases Src (SFK), Syk despois fosforila a LAT e promove a fosforilación de Btk, PI3K, PLC γ , Vav1/3 e SLP -76, e a unión á proteína LAT. Posteriormente, a PI3K activada induce a formación de PIP3 a partir de PIP2, co fin de favorecer finalmente a formación de diacilglicerol (DAG) e mensaxeiros IP3, levando á liberación de calcio, estimulando a agregación e a desgranulación plaquetaria (Severin, Pollitt et al. 2011, Parguñá, Alonso et al., 2012).

Como se mencionou anteriormente, a activación de CLEC-2 está mediada principalmente pola interacción proteína-proteína (PPI), este tipo de interacción non foi considerada como unha diana terapéutica usando moléculas pequenas durante moitos anos. Non obstante, a pesar dos avances no desenvolvemento de fármacos, os receptores mediados por PPI seguen sendo un dos obxectivos terapéuticos máis desafiantes cando se usan inhibidores convencionais baseados en moléculas pequenas.

En xeral, os principais retos no desenvolvemento de inhibidores de interaccións proteína-proteína son os seguintes:

1) Os PPI carecen dunha bolsa de unión de receptor e ligando definida, o que contrasta con outras dianas terapéuticas convencionais, como as encimas. Isto dificulta o deseño de moléculas pequenas baseadas na estrutura do receptor (Jones e Thornton 1996).

2) As interaccións proteína-proteína están formadas por múltiples interaccións, caracterizadas por unha gran afinidade e aidez, mentres que a aidez das moléculas pequenas tende a ser considerablemente menor (Damaskinaki, Moran et al. 2021).

3) Os ligandos proteicos ocupan grandes superficies (1000-2000 Å²) do receptor, mentres que as moléculas pequenas só ocupan unha pequena área (~300-500 Å²) (Arkin, Tang et al. 2014, De Luca, Agharbaoui et al. 2016).

Non obstante, ata a data describíronse algúns antagonistas non proteicos de CLEC-2. Por exemplo, en 2018, Tsukiji et al., conseguiron identificar que o composto de coordinación cobalto-hematoporfirina (Co-HP) é un inhibidor non peptídico de CLEC-2. Isto fíxose mediante cribado de alto rendemento (HTS) baseado en pequenas moléculas, seguido de procesos de optimización química (Tsukiji, Osada et al. 2018). Os autores demostraron que o Co-HP pode evitar a agregación plaquetaria inducida pola rodocitina ou a podoplanina, nun rango de concentracións micromolar. Tamén mostraron especificidade do receptor, xa que non se observou ningún efecto sobre a agregación plaquetaria, inducida polo coláxeno ou a trombina. Isto suxire que o

efecto de Co-HP pode funcionar ao bloquear a interacción da rodocitina e CLEC-2. Non obstante, sábese que esta substancia pode causar certo grao de toxicidade, polo que é necesario continuar coa investigación para o desenvolvemento de novos inhibidores de CLEC-2.

Chang et al. (2015) tamén identificaron un novo composto de 5-nitrobenzoato non citotóxico, 2CP, capaz de evitar a agregación plaquetaria inducida pola podoplanina a concentración micromolar. Non obstante, non puido evitar a agregación plaquetaria inducida pola rodocitina. Os autores postularon que o 2CP únese ao mesmo sitio de unión para a rodocitina e a podoplanina, aínda que isto contradí o descubrimento de que o 2CP inhibe a agregación inducida pola podoplanina pero non a agregación inducida pola rodocitina (Chang, Hsieh et al. 2015).

Outro enfoque para o desenvolvemento de antagonistas de PPI baséase na xeración de axentes biolóxicos. Por exemplo, o fragmento de anticorpo AYP1 F(ab)₂ xerado contra o receptor CLEC-2 mostrou unha potente inhibición da agregación plaquetaria inducida pola rodocitina ou a podoplanina, o que suxire que pode unirse ao mesmo sitio que estes agonistas (Gitz, Pollitt et al. ., outros 2014).

En xeral, os fragmentos xerados a partir de anticorpos enteiros son axentes bloqueadores eficaces, e algúns deles foron aprobados para uso clínico pola Food and Drug Administration (FDA) dos Estados Unidos. Un exemplo diso é o fragmento de unión ao antíxeno (Fab) do

fragmento quimérico anti-GPIIb/IIIa, tamén coñecido como abciximab, que foi aprobado en 1994 para previr a trombose durante o cateterismo das arterias coronarias (Nelson 2010). Non obstante, o desenvolvemento de novas tecnoloxías asociadas ao desenvolvemento de produtos biolóxicos permitiu a xeración de fragmentos de anticorpos igualmente potentes, pero cunha estabilidade superior. Estes fragmentos xéranse a partir de anticorpos de camélidos e coñécense como nanoanticorpos (*nanobodies*). Os nanoanticorpos tamén son significativamente máis pequenos que os anticorpos e os fragmentos Fab, o que se traduce nun menor risco de inmunoxenicidade.

Os nanoanticorpos son fragmentos de cadea pesada variable única (VHH) derivados de anticorpos funcionais xerados en llamas e/ou camelos. Tamén carecen de cadeas lixeiras (Hamers-Casterman, Atarhouch et al. 1993). Os nanoanticorpos teñen moitas vantaxes sobre os fragmentos de anticorpos tradicionais, incluíndo que son estables nun rango máis amplo de temperatura e pH. Tamén poderían producirse en masa nun sistema bacteriano, debido á súa falta de modificacións post-transdución (Asaadi, Jouneghani et al. 2021); sen embargo, unha das propiedades máis interesantes é a súa idoneidade para a enxeñaría molecular, permitindo a xeración de nanoanticorpos multiméricos, que poden producir opcións de maior avidez en comparación coa versión monomérica e permitir a adición de etiquetas, como o sitio de unión á albúmina para aumentar a súa vida media.

Un exemplo de nanoanticorpos potentes usados clínicamente é o nanoanticorpo divalente caplaxuzimab, que foi aprobado pola FDA para o tratamento da púrpura trombocitopénica trombótica adquirida (Scully, Cataland et al. 2019). Isto demostrou a eficacia e seguridade dos nanoanticorpos para usos clínicos. Polo tanto, a xeración de nanoanticorpos pode representar un medio alternativo prometedor para dirixirse aos receptores baseados en PPI, incluíndo CLEC-2.

Polo tanto, o obxectivo principal da presente tese doutoral é: Desenvolver novos ligandos para CLEC-2 baseados en pequenas moléculas e nanoanticorpos contra CLEC-2 para (1) xerar novos axentes bloqueadores da interacción CLEC-2 e os seus ligandos, (2) comprender o tamaño mínimo do ligando para inducir a agregación plaquetaria a través de CLEC-2, e (3) avaliar o papel da desfosforilación de proteínas tirosina quinases na estabilidade dos agregados plaquetarios formados por ligandos CLEC-2 e xerar así unha mellor comprensión do mecanismo de activación do receptor. Globalmente, todo o anterior contribuiría ao deseño racional de novos axentes terapéuticos para previr ou curar a tromboinflamación.

Métodos:

En primeiro lugar, analizouse unha biblioteca química baseada en moléculas pequenas mediante un ensaio baseado na combinación de estudos in silico e ensaios de liberación de calcio intracelular. Posteriormente, realizouse un segundo cribado de alto rendimento,

pero esta vez, baseado na interacción da podoplanina e CLEC-2 co fin de identificar novos ligandos para o receptore a partir de moléculas pequenas. Os compostos con maior potencial identificados durante o cribado caracterizáronse aínda máis mediante ensaios de agregometría plaquetaria e *western blots*.

Un segundo enfoque baseouse no desenvolvemento de nanoanticorpos. Para iso, xeráronse 48 nanoanticorpos contra CLEC-2 e analizouse a súa actividade mediante citometría de fluxo. A afinidade determinouse mediante a plataforma BiaCORE (SPR). O nanoanticorpo máis potente foi multimerizado usando unha secuencia de reticulación baseada en glicina e serina (GGGS) e, polo tanto, desenvolvéronse formas diméricas e tetrámeras deste nanoanticorpo e posteriormente caracterizáronse bioquímicamente e funcionalmente.

Por outra banda, para estudar o papel das tirosina quinasas na estabilidade dos trombos xerados polos ligandos do receptor tipo ITAM (hem), os agregados plaquetarios formáronse inicialmente tras activación das plaquetas con rodocitina, ligando de CLEC-2 ou utilizando ligandos de GPVI ou PAR-1. Unha vez formados os agregados, engadíronse as inhibidores de quinasas e monitorizouse a desagregación plaquetaria mediante un ensaio de agregometría plaquetaria.

Resultados e discusión:

Cribado de alto rendimento baseado nun ensaio celular

Levou a cabo un primeiro cribado de alto rendimento combinando ensaios in silico e un ensaio baseado na liberación de calcio intracelular. Así, identificouse F1113-0067, unha molécula pequena capaz de inhibir a agregación plaquetaria mediada polos receptores CLEC-2 e GPVI. Non obstante, debido á baixa selectividade desta molécula, considerouse que este composto podería estar inhibindo a agregación plaquetaria mediante unha quinasa común na vía de sinalización destes receptores, polo que se decidiu non continuar coa caracterización deste composto. Non obstante, esta estratexia permitiu recoñecer os retos no desenvolvemento de inhibidores do receptor CLEC-2, e optimizar unha estratexia diferente baseada na interacción proteína-proteína.

Cribado de alto rendimento baseado nun ensaio de inhibición da interacción proteína-proteína

Neste apartado optimizouse un ensaio bioquímico baseado na interacción entre a podoplanina e CLEC-2, co obxectivo de identificar substancias capaces de bloquear a interacción entre o ligando e o receptor mediante a tecnoloxía *ALPHA screen*. Unha vez identificadas as condicións para o ensaio bioquímico, realizouse un novo cribado de alto rendimento baseado na interacción entre podoplanina e CLEC-2, utilizando a quimioteca EU-Open screen (conformada por 5016 compostos) pertencente ao grupo de investigación BioFarma da

Universidade de Santiago de Compostela. Durante este ensaio identificáronse 40 compostos capaces de evitar a interacción entre CLEC-2/podoplanina a unha dose de 10 μ M. Non obstante, un segundo ensaio para determinar a interferencia potencial do ensaio (chamado ensaio TruHit) determinou que só 17 destes compostos poderían ser inhibidores potenciais da interacción ligando-receptor.

A partir deste resultado, elaboráronse curvas dose-resposta para clasificar os compostos segundo a súa potencia. Os compostos máis potentes foron adquiridos comercialmente e probados en ensaios de agregación plaquetaria. Deste xeito, puidose identificar unha "pequena molécula" de natureza polimérica, que se une a CLEC-2 e induce a agregación plaquetaria nun mecanismo "todo ou nada". Esta molécula coñécese co nome de katicina e está amplamente distribuída no reino *plantae*. A katicina pertence á familia das proantocianidinas tipo A, que se atopan na natureza en forma polimérica.

A agregación plaquetaria inducida pola katicina foi completamente bloqueada polos inhibidores das quinasas Src e Syk, como ocorre no caso das agregacións mediadas por receptores ITAM, CLEC-2 ou GPVI.

Do mesmo xeito, observouse que a activación plaquetaria mediada por katicina tamén se asocia coa fosforilación de CLEC-2, suxerindo, a interacción directa entre a katicina e CLEC-2. Non obstante, para comprender o mecanismo polo cal esta molécula é capaz de inducir a

agregación plaquetaria mediante CLEC-2, decidiuse caracterizar a molécula mediante espectrometría de masas, confirmando que a katacina é unha mestura de oligómeros de diferentes tamaños, sendo a forma trimérica a unidade máis pequena observada para esta molécula.

Ademais, os ensaios in silico levados a cabo suxiren que esta molécula podería unirse ao mesmo sitio de unión suxerido para a podoplanina ou a rodocitina. Non obstante, tamén observouse que a katacina podía unirse a un sitio alostérico do receptor CLEC-2, o que podería explicar por qué se observa só unha inhibición parcial cando se usaba un anticorpo anti-CLEC-2. Este estudo tamén analiza a posibilidade de que a katacina poida unirse a outros receptores da membrana das plaquetas, facilitando a agregación plaquetaria.

Desenvolvemento de nanoanticorpos dímeros e tetrámeros

Por outra banda, para comprender a estequiometría do receptor CLEC-2, neste estudo xeráronse 48 nanoanticorpos fronte a CLEC-2 en colaboración con VIB Nanobody Core (Bruxelas, Bélxica). Na caracterización destes nanoanticorpos, demostrouse que o máis eficaz deles, LUAS, é capaz de bloquear a activación das plaquetas por parte das células que expresan podoplanina. LUAS únese a CLEC-2 cunha afinidade de ~ 140 nM como se demostrou mediante a técnica de resonancia plasmática de superficie (SPR).

Posteriormente, procedeuse á dimerización dos nanoanticorpos, observándose un aumento da afinidade a 0,5 nM. Mediante ensaios de

agregación plaquetaria, observouse que o dímero actúa como un potente axente bloqueador da agregación plaquetaria inducida polo veneno de serpe, rodocitina. Esta nova proteína chamouse LUAS-2.

Por outra banda, ao xerar a forma tetramérica de LUAS, denominada LUAS-4, observouse que o novo axente é capaz de inducir unha potente agregación plaquetaria, que está bloqueada polos inhibidores das quinasas Src e Syk, e polo fragmento de CLEC- 2, AYP1 F(ab)2, o que demostra que a activación está mediada polo receptor CLEC-2.

Observáronse resultados similares aos de LUAS-2 cando se trataron plaquetas con fragmentos de anticorpos Fab2 (divalente) ou Fab (monovalente), así como cando se usou podoplanina-Fc (divalente). Mentres, a proteína tetramérica rodocitina, como LUAS-4, inducía unha potente agregación plaquetaria.

Tamén observouse a través da espectroscopia de correlación de fluorescencia (FCS) que LUAS-4 retarda o fluxo de moléculas de CLEC-2-EGFP a través do volume confocal (coeficiente de difusión), o que indica que LUAS-4 permite o agrupamento de varias unidades de CLEC-2, formando grandes complexos CLEC-2. Non se observaron diferenzas significativas neste parámetro cando CLEC-2 estivo asociado con LUAS ou LUAS-2.

Papel das tirosina quinasas no mantemento dos agregados plaquetarios

A presente tese doutoral tamén demostrou que a estabilidade dos agregados plaquetarios mediada polos receptores GPVI e CLEC-2 está

parcialmente mediada pola tirosina quinasa Src, xa que se observou que os agregados plaquetarios estaban parcialmente desagregados cando se engadiron inhibidores de Src. Non obstante, é probable que este feito se deba á sinalización independente do receptor (hem)ITAM, xa que se observaron resultados similares nos agregados plaquetarios formados polo ligando de PAR-1, TRAP-6. Tamén se observou que a fosforilación das tirosina quinases pode revertirse despois da adición dos seus respectivos inhibidores (Syk, Src, Btk), e que a estabilidade do agregado plaquetario é independente dos mediadores secundarios ADP e TxA₂.

Nos ensayos levados a cabo tamén se puido observar que a activación da integrina α IIb β 3 (receptor de fibrinóxeno responsable da agregación plaquetaria) a través do mecanismo de "inside-out" pode revertirse, aínda que non está claro se o mesmo ocorrerá en presenza de altas concentracións de fibrinóxeno, onde a activación realízase polo mecanismo "outside-in".

Conclusiones:

O receptor CLEC-2 require ligandos poliméricos (katicine) e/ou tetrámeros (LUAS-4 o rodocitina) para agrupar suficientes unidades receptoras e inducir a agregación plaquetaria. Os ligandos dímeros dan lugar a potentes inhibidores do receptor con suficiente afinidade para competir cos ligandos proteicos do receptor, como a rodocitina. O desenvolvemento de inhibidores do receptor CLEC-2 utilizando

moléculas pequenas é posible, pero moi limitado debido ás características moleculares da superficie onde se producen as interaccións proteína-proteína.

As novas ferramentas desenvolvidas neste estudo poderían permitir unha maior investigación da función de CLEC-2 e do seu modo de activación así como tamén poderían contribuír ao desenvolvemento racional de novos fármacos dirixidos a CLEC-2 como diana terapéutica para enfermidades tromboinflamatorias ou na prevención e tratamento da trombose venosa profunda.

Table of content

ABBREVIATION LIST	XXXIII
1. GENERAL INTRODUCTION	3
1.1. History of platelets	3
1.2. Platelet morphology and structure	3
1.3. Role of platelets in thrombosis and haemostasis	5
1.4. Platelets in immunothrombosis and thromboinflammation	7
1.5. Platelet receptors and signalling	10
1.5.1. GPIb-IX-V	11
1.5.2. Integrins	12
1.5.3. GPCRs	13
1.5.4. ITAM and hemITAM receptors	16
1.6. Role of (hem)ITAM in thrombus stability	19
1.7. CLEC-2 and thromboinflammation	22
1.8. The CLEC-2 receptor and its ligands	23
1.9. CLEC-2 activation receptor clustering	26
1.10. CLEC-2 antagonists and development challenges	28
1.11. Importance of developing new CLEC-2 ligands	33
2. CHAPTER 2: AIMS AND HYPOTHESIS	37
2.1. General aims	37
2.2. Specific objectives	37
3. CHAPTER 3: MATERIAL AND METHODS	41
3.1. Materials	41
3.2. Methods	43

3.2.1. Preparation of Human Washed Platelets	43
3.2.2. Platelet Functional Assays	44
3.2.2.1. Light Transmission Aggregometry	44
3.2.2.2. Calcium Release Assay	45
3.2.2.3. Flow Cytometry	46
3.2.2.3.1. Evaluation of Platelet Viability	46
3.2.2.3.2. Evaluation of α IIb β 3 Activation	46
3.2.3. Protein Phosphorylation	47
3.2.3.1. Sample Preparation and Western Blot	47
3.2.3.2. Immunoprecipitation	48
3.2.3.3. CLEC-2 and Podoplanin Protein Expression and Purification	49
3.2.3.4. Monobiotinylation of Recombinant Human Podoplanin	50
3.2.4. High-Throughput Screening Based on ALPHAScreen Assay	50
3.2.4.1. Identification of True Hits	51
3.2.5. Dose-Response Curve Generation for Potential Hits	52
3.2.6. High-Throughput Screening Data Analysis	53
3.2.7. Expression and Purification of Nanobodies	53
3.3. Generation of LUAS-2 and LUAS-4	55
3.3.1. Site-Directed Mutagenesis Kit	55

3.3.2. Circularisation of the PCR Product and DNA Template Degradation	56
3.3.3. Bacterial Transformation	57
3.3.4. Ligation of DNA Sequences	58
3.4. CLEC-2 Nanobody Binding With Flow Cytometry	60
3.5. Surface Plasmon Resonance for Binding Studies	61
3.6. Molecular Docking	62
3.7. Mass Spectrometry	62
3.8. Data Analysis	63
4. CHAPTER 4: HIGH THROUGHPUT SCREENING OF SMALL MOLECULE INHIBITORS OF THE PLATELET RECEPTOR CLEC-2	67
4.1. Introduction	67
4.2. Aim:	68
4.3. Results	68
4.3.1. Virtual and cell-based HTS assay to identify potential CLEC-2 inhibitors	68
4.3.1.1. Effect of F1113-0067 on platelet aggregation induced by rhodocytin	70
4.3.1.2. Evaluation of the selectivity of F1113-0067 to prevent platelet aggregation	72
4.3.1.3. Effect of F1113-0067 on platelet viability	76
4.3.1.4. Effect of F1113-0067 on tyrosine phosphorylation mediated by ITAM receptors	77
4.4. Discussion	80

5. CHAPTER 5: BIOCHEMICAL-BASED HTS FOR THE IDENTIFICATION OF A NOVEL CLEC-2 LIGAND	85
5.1. Introduction	85
5.2. Aim	88
5.3. Results	89
5.3.1. Setting-up a podoplanin-CLEC-2 interaction assay based on ALPHA screen	89
5.3.1.1. HTS based on ALPHA screen assay	91
5.3.1.2. Identification of katacine as a CLEC-2 ligand by HTS	97
5.3.1.3. Platelet aggregation induced by katacine is Syk- and Src-dependent and mediated by CLEC-2 activation	99
5.3.1.4. Katacine induces phosphorylation of CLEC-2 and key signalling proteins in the CLEC-2 signalling pathway	101
5.3.1.5. Katacine increased tyrosine phosphorylation levels of CLEC-2	103
5.3.1.6. Katacine structure	104
5.3.1.7. Molecular docking studies predict katacine binds to the same CLEC-2 binding site as podoplanin	108
5.4. Discussion	111
6. CHAPTER 6: DEVELOPMENT OF MULTIMERIC LIGANDS AGAINST HUMAN CLEC-2	119
6.1. Introduction	119
6.2. Aim	120

6.3. Results	120
6.3.1. Initial Screening of Nanobodies Generated Against Human CLEC-2	120
6.3.2. Development of Multimeric Ligands of CLEC-2	124
6.3.2.1. Expression of LUAS-2 and LUAS-4	126
6.3.3. Dimerisation of LUAS Significantly Improves Its Affinity for CLEC-2	128
6.3.4. LUAS-2 Prevents Platelet Aggregation Induced by Rhodocytin	130
6.3.5. LUAS-4 Acts as Potent Agonist of CLEC-2	131
6.3.6. Dimeric and Monomeric Ligands Do Not Induce Human Platelet Aggregation	134
6.3.7. Effect of Monovalent, Divalent, and Tetravalent LUAS on CLEC-2 Clustering	138
6.4. Discussion	140
7. CHAPTER 7: TYROSINE KINASE SIGNALLING IS NOT REQUIRED FOR SUSTAINED PLATELET AGGREGATION MEASURED BY LIGHT TRANSMISSION AGGREGOMETRY	145
7.1. Introduction	145
7.2. Aim	146
7.3. Results	147
7.3.1. Platelet aggregation mediated by CLEC-2 and GPVI receptors is weakly reversed after addition of Src, Syk, and Btk inhibitors	147

7.3.2. Effect of tyrosine kinase inhibitors on phosphorylation	150
7.3.3. Platelet aggregation was sustained in the presence of tyrosine kinase inhibitors combined with apyrase and indomethacin	155
7.3.4. Platelet α IIb β 3 activation is reversed by tyrosine kinase inhibitors, but platelet aggregation is sustained	158
7.4. Discussion	161
8. GENERAL DISCUSSION	167
9. CONCLUSIONS	179
9.1. Generation of new CLEC-2 ligands, based on calcium release or an ALPHA Screen assay in HTS format, using a small molecule based chemical library	179
9.2. Evaluation of the activation mode of CLEC-2 using novel multimeric nanobodies	179
9.3. The role of tyrosine kinases in thrombus stability.	180
10. REFERENCES	181

Illustration list.

Figure 1	Platelet morphology	5
Figure 2	Schematic representation of primary haemostasis	7
Figure 3	Platelet receptors	11
Figure 4	GPVI and CLEC-2 signalling pathway	19
Figure 5	Mapping of the reported binding sites of podoplanin, rhodocytin, and cobalt-hematoporphyrin onto the crystal structure of CLEC-2 (PDB: 26CU)	26
Figure 6	Structure of small molecules inhibitors of CLEC-2	30
Figure 7	Schematic representation of human antibody and their antibody-derived fragments produced by vertebrates (A) and camelid heavy chain antibodies(B).	33
Figure 8	Platelet-based HTS	69
Figure 9	Chemical structure of F1113-0067	70
Figure 10	Dose-response curve of platelet aggregation following platelet incubation with F1113 and stimulated with rhodocytin 100nM	71
Figure 11	F1113-0067 has no effect on platelet aggregation induced by thrombin in washed platelets	73
Figure 12	F1113-0067 is also able to prevent platelet aggregation mediated by GPVI	74

Figure 13	Low doses of F1113-0067 have a higher inhibition on platelet aggregation mediated by rhodocytin than mediated by GPVI	75
Figure 14	F1113-0067 does not affect platelet viability at 12.5 μ M, but higher concentrations may have an impact	77
Figure 15	Effect of F1113-0067 on platelet signalling induced by rhodocytin	78
Figure 16	Effect of F1113-0067 on platelet signalling induced by CRP	79
Figure 17	Schematic representation of an ALPHA screen assay based on podoplanin and CLEC-2 interaction.	87
Figure 18	Matrix of different CLEC-2 and podoplanin concentrations	90
Figure 19	Scatter plot showing the effect of each compound on the ALPHA signal values emitted by a CLEC-2-podoplanin interaction	91
Figure 20	Scatter plot showing TruHits® assay to identify potential false positive compounds on the screening	92
Figure 21	Dose-response curves of potential hits and IC50 of each potential compound	94
Figure 22	Katacine can induce platelet aggregation in an all-or none response mechanism	98

Figure 23	Platelet aggregation induced by katacine is Syk- and Src-dependent and mediated by CLEC-2 receptor	100
Figure 24	Katacine increases tyrosine phosphorylation levels of Syk, LAT, and global protein tyrosine phosphorylation profiles	102
Figure 25	Katacine increases CLEC-2 tyrosine phosphorylation levels	103
Figure 26	Mass spectra of katacine confirm that katacine is a mixture of oligomers with different sizes and has a polar nature, with possible implications on CLEC-2 binding	108
Figure 27	Molecular docking prediction of the katacine binding site for CLEC-2	109
Figure 28	Katacine may bind to an allosteric binding site on CLEC-2	110
Figure 29	Screening of nanobodies against human CLEC-2	121
Figure 30	Surface plasmon resonance (SPR) sensograms of potential nanobodies against CLEC-2	123
Figure 31	SPR sensograms showing AYP1 binding to an immobilised surface of a recombinant CLEC-2-hisx6 tag	124
Figure 32	Agarose gel containing distention products of the clones 1 and 2	126

Figure 33	Chromatograms and SDS-PAGE gels of LUAS-2 and LUAS-4	128
Figure 34	SPR sensograms showing LUAS-2 binding to an immobilised surface of a recombinant CLEC-2-hisx6 tag	129
Figure 35	Divalent LUAS-2 and AYP1 F(ab)2 can prevent platelet aggregation induced by rhodocytin	130
Figure 36	Comparison of the effects of LUAS, LUAS-2, and LUAS-4 on human platelet aggregation	131
Figure 37	LUAS-4 induces platelet aggregation through CLEC-2	132
Figure 38	LUAS-4 increases protein tyrosine phosphorylation in human platelets and can be prevented by Syk and Src inhibitors or AYP1 Fab2	133
Figure 39	Monovalent or divalent forms of AYP1 fail to induce platelet aggregation in human platelets	135
Figure 40	Dimeric podoplanin is unable to cause platelet aggregation in human platelets, whilst podoplanin-expressing cells induce platelet aggregation	137
Figure 41	Membrane dynamics and molecular brightness of CLEC-2 transfected cells stimulated with LUAS, LUAS-2, and LUAS-4 using FCS	139
Figure 42	Kinase inhibitors cannot reverse GPVI and CLEC-2 mediated platelet aggregation	149

Figure 43	Tyrosine phosphorylation is sustained for 50 minutes in GPVI, and CLEC-2 mediated protein phosphorylation	153
Figure 44	Kinase inhibitors reverse GPVI- and CLEC-2-mediated protein phosphorylation	155
Figure 45	Kinase inhibitors together with secondary mediators, antagonists cannot reverse GPVI- and CLEC-2-mediated platelet aggregation	157
Figure 46	Role of the integrin α IIb β 3 activation on the reversal of platelet aggregation by tyrosine kinase inhibitors	159
Figure 47	Kinase inhibitors cannot reverse TRAP6-mediated platelet aggregation	160
Figure 48	Schematic representation of a potential activation mechanism caused by divalent ligands, tetravalent ligands, or the tetrameric complex PF4/FcRIIA on Vaccine-induced immune thrombotic thrombocytopenia (VITT).	173

Table list

Table 1	Agents and volumes used for the site-directed mutagenesis reaction	55
Table 2	PCR conditions for site-directed mutagenesis	56
Table 3	Agents and volumes used for the KLD reaction.	56
Table 4	Agents and volumes used for the double digestion of the new LUAS clones	58
Table 5	Agents and volumes used for the ligation of the vector containing LUAS and (GGGS) ₃ -LUAS-DNA sequence.	59
Table 6	List of potential hits identified on alpha screen.	95
Table 7	Molecular weight and size of the oligomer of katacine calculated based on flavan-3-ol	104

Abbreviation list

5-HT	5-hydroxytryptamine
ACD	Acid-citrate-dextrose
ADP	Adenosine diphosphate
ALPHAScreen	Amplified luminescent proximity homogeneous assay
ATP	Adenosine triphosphate
BSA	Bovine serum albumin
Btk	Bruton's tyrosine kinase
cAMP	Cyclic adenosine monophosphate
CLEC-2	C-type lectin-like receptor-2
Co-HP	Cobalt-hematoporphyrin
CRP	Collagen-related peptide
DAG	Diacylglycerol
DMEM	Dulbecco's Modified Eagle's Medium
DMSO	Dimethyl sulfoxide
DNA	Deoxyribonucleic acid

ECM	Extracellular matrix
EDTA	Ethylenediaminetetraacetic acid
ELISA	Enzyme-linked immunosorbent assay
FACS	Fluorescence-activated cell sorting
FBS	Fetal bovine serum
FcR γ	Fc receptor γ -chain
FCS	Fluorescence correlation spectroscopy
GAPDH	Glyceraldehyde-3-phosphate dehydrogenase
GPCRs	G-protein coupled receptors
GPO	Glycine-proline-hydroxyproline
GPVI	Glycoprotein VI
HEK293T	Human endothelial kidney 293T cells
hemITAM	Hemi-immunoreceptor-tyrosine-based activation motif
HTS	High-throughput screening
IC ₅₀	Half maximal inhibitory concentration
IF	Immunofluorescence
Ig	Immunoglobulin

IP	Immunoprecipitation
IP ₃	Inositol 1,4,5-trisphosphate
IPTG	Isopropyl β-D-1-thiogalactopyranoside
ITAM	Immunoreceptor-tyrosine-based-activation-motif
K _D	Affinity constant
kDa	Kilodalton
KO	Knockout
LAT	Linker of activated T cells
LB	Lysogeny broth
LTA	Light transmission aggregometry
MFI	Median fluorescence intensity
MWCO	Molecular weight cut-off
NO	Nitric oxide
PCR	Polymerase chain reaction
PDB	Protein Data Bank
PDGF	Platelet derived growth factor
PECAM-1	Platelet endothelial cell adhesion molecule-1
PF4	Platelet factor 4

PGI ₂	Prostaglandin I ₂
PI	Phosphatidylinositol
PI3K	Phosphoinositide 3-kinase
PIP ₂	Phosphatidylinositol 4,5-bisphosphate
PKA	Protein kinase A
PKC	Protein kinase C
PLAG	Platelet aggregation-stimulating
PLC β	Phospholipase C- β
PLC γ 2	Phospholipase C γ 2
PPP	Platelet poor plasma
PRP	Platelet-rich plasma
PS	Phosphatidylserine
PVDF	Polyvinylidene difluoride
pY	Phosphotyrosine
RDG	Arginine-glycine-aspartic acid
RPM	Revolutions per minute
S/N	Signal-to-noise
SD	Standard deviation

SDS-PAGE	Sodium dodecyl sulphate–polyacrylamide gel electrophoresis
SFK	Src family kinase
SH2	Src Homology 2
SH3	Src Homology 3
SLP-76	SH2 domain containing leukocyte protein of 76kDa
TAE	Tris-acetate-EDTA
TBS-T	Tris-buffered saline with Tween 20
Tec	Tec family kinase
TPO	Thrombopoietin
TxA ₂	Thromboxane A ₂
vHTS	Virtual High Throughput Screening
VWF	Von Willebrand factor
WB	Western blot
WP	Washed platelet

CHAPTER 1

GENERAL INTRODUCTION

1. General Introduction

1.1. History of platelets

Platelets were recognised as ‘blood dust’ with an unknown function until 1882, when Italian pathologist Giulio Bizzorero described them as the third morphological element of the blood, first calling them *petit plaques* in Italian, or *plaquettes* in French, and later naming them ‘platelets’ in English. Despite others having identified them as a circulating particle in the blood, Bizzorero’s main finding was that platelets play a relevant role in thrombus formation. He observed that when placing light pressure with a needle on rodent arteries, platelets started to adhere to and accumulate at the site of the injury (Ribatti and Crivellato 2007).

1.2. Platelet morphology and structure

Morphologically, platelets are small, anucleate blood cells with a disc shape and are around 2–5 μ m in diameter. They are formed in the bone marrow from megakaryocytes through a process described as thrombopoiesis and released into the bloodstream. A count of 150–400 x 10⁹ platelets/L is maintained, with a half-life ranging from seven to 10 days until clearance.

Platelets have three different types of granules: α -granules, dense granules, and lysosomes. α -granules are the most abundant in the platelet cytosol, found in a range of 50 to 80 per platelet, whilst dense granules have a range of 3 to 8 granules per platelet (Fitch-Tewfik and

Flaumenhaft 2013). The α -granules contain adhesion proteins such as von Willebrand factor (vWF) and fibrinogen; coagulating factors such as factors V and IX; chemokines (e.g., platelet factor 4 (PF4)); growth factors; immune mediators and membrane proteins. In contrast, dense granules are rich in calcium, magnesium, nucleotides such as ADP, ATP, and the amine serotonin (Fitch-Tewfik and Flaumenhaft 2013, Gremmel, Frelinger et al. 2016)

Platelets contain a complex intracellular network of surface-connected membrane channels, named the open canalicular system (OCS) (Behnke 1967), whose main function is the transport of substances to the inside of the platelet, including fibrinogen and tissue factor (Harrison, Wilbourn et al. 1989, Escolar, Lopez-Vilchez et al. 2008) and the release of the platelet granular content (Escolar, Leistikow et al. 1989). Platelets also contain several mitochondria for energetic metabolism, lysosomes for autophagic processes, and Golgi apparatus. Platelet morphology and composition is illustrated in **Figure 1**.

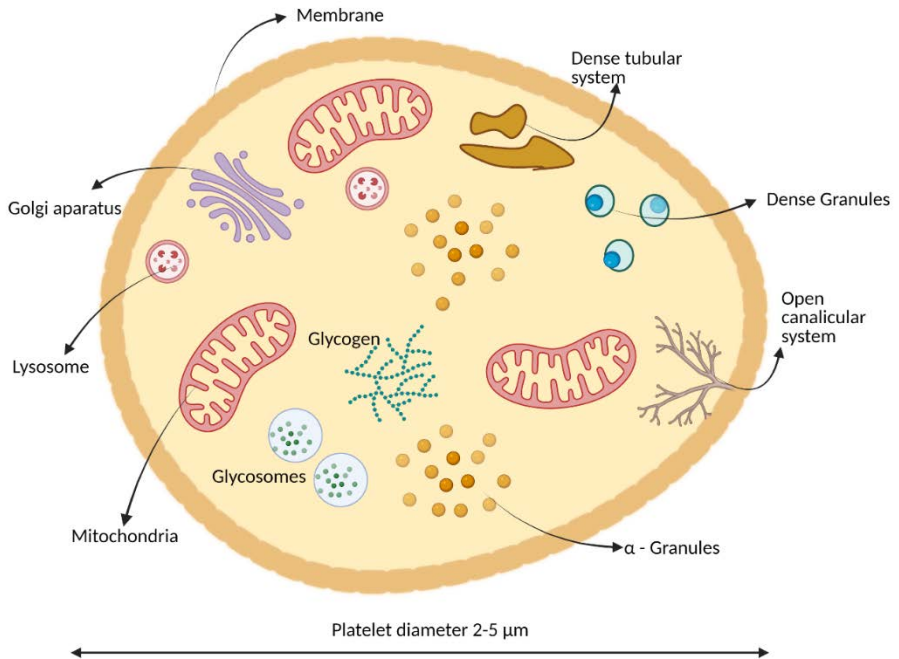


Figure 1. Platelet morphology. Platelets are discoid small blood cells, 2-5µm in diameter. Human platelets are characterised by their lack of a nucleus and the presence of an open canicular system. Mitochondria, Golgi apparatus, lysosomes, and dense and alpha granules are also found in the platelet's cytosol. Created using www.biorender.com

1.3. Role of platelets in thrombosis and haemostasis

Platelets are widely recognised for their roles in haemostasis and thrombosis. Primary haemostasis is the term used to describe several well-orchestrated events between platelets and the sub-endothelial matrix as an initial response when vascular injury occurs. Platelet clot

formation constitutes three main steps: 1) adhesion, 2) activation, and 3) platelet aggregation (**Figure 2**).

Vascular injury leads to the exposure of subendothelial matrix proteins, including collagen (type I or type III), which interacts with membrane receptors of circulating platelets, e.g., glycoprotein VI (GPVI) and integrin $\alpha 2\beta 1$. During this phase, soluble vWF binds to collagen fibres and interacts with glycoprotein Ib (GPIb), which forms the GPIb/IX/V complex, especially under high shear conditions. Through a series of events, known as inside-out signalling, platelet granules release pro-thrombotic proteins, such as ADP and thromboxane, enhancing the signal of the adherent platelet and increasing the overall number of activated platelets.

In the developing thrombus, platelet adhesions are stabilised primarily by the integrin $\alpha \text{IIb}\beta 3$. This integrin is the most abundant receptor on the platelet surface and is responsible for crosslinking activated platelets (Simmons, Sims et al. 1997), forming platelet-to-platelet interactions (Rivera, Lozano et al. 2009). Other membrane proteins associated with thrombus growth and stability include: P-selectin (Merten and Thiagarajan 2000), GPVI (Ahmed, Kaneva et al. 2020) and CLEC-2 (Haining, Cherpokova et al. 2017).

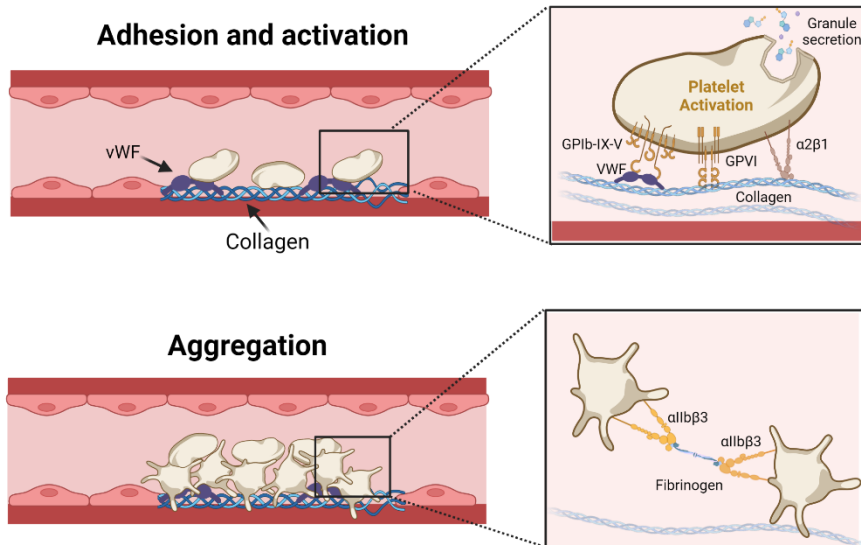


Figure 2. Schematic representation of primary haemostasis. Thrombus formation consists of three main sequential steps. The first step is known as platelet adhesion, here, platelet membrane proteins interact with subendothelial ligands on the injured vessel site. The second step is platelet activation, characterised by the platelet shape change, integrin $\alpha\text{IIb}\beta\text{3}$ activation, and the release of secondary mediators such as ADP and thromboxane. The third step is platelet aggregation (lower panel), this mechanism is mediated by fibrinogen forming a stable platelet plug (Created using www.biorender.com).

1.4. Platelets in immunothrombosis and thromboinflammation

Beyond the recognised roles of platelets in thrombosis and haemostasis, they have also been recognised by their response to inflammatory processes, as a consequence of infections and tissue repair.

Furthermore, it has been observed that platelets contain a wide range of proinflammatory substances, and they contribute to the recruitment and trafficking of leukocytes to the vasculature (Ferreira, Ubatuba et al. 1976, Bult and Bonta 1977, Page 1989, Klinger 1997).

In 2013, Engelmann and Massberg introduced the term immunothrombosis to refer to the immune response associated with intravascular thrombus formation which leads to the recognition, capture and destruction of pathogens (Engelmann and Massberg 2013).

Under normal conditions thrombosis and inflammation both contribute to the effective elimination of harmful agents. However, under severe pathological conditions, characterised by chronic inflammation (Franco, Corken et al. 2015), the sustained activation of endothelial cells, platelets, leukocytes, and the innate immune system, results in a process known as thrombo-inflammation (Schattner, Jenne et al. 2020).

Thrombo-inflammatory processes have been observed in life-threatening diseases, including certain cancer types, where platelet activation is promoted. The active platelets participate in the progression of the cancer and disseminate metastases by stimulating deep venous thrombosis and neutrophil extracellular trap (NET) formations (Palacios-Acedo, Mege et al. 2019).

Thrombo-inflammation has also been shown to play a role in the pathogenesis of severe SARS-COVID-19 infection, with a considerable number of autopsies showing evidence of pulmonary thrombosis. Taus

et al suggested that platelets in COVID-19 pneumonia are responsible for the spread of proinflammatory substances and procoagulant activities in the systemic circulation (Taus, Salvagno et al. 2020). Maiese et. al, also provided an interesting insight on the aetiology of thrombosis associated with COVID-19 infection, proposing this is the consequence of a cytokines storm mediated by viral sepsis, suggesting that the prophylaxis of coagulopathy must be rethought (Maiese, Passaro et al. 2020).

Besides COVID-19 infection, coagulopathy has commonly been observed in other models of acute and chronic sepsis or cancer, thus leading to life threatening complications such as venous thromboembolism (VTE) and disseminated intravascular coagulation (DIC) (Semeraro, Ammollo et al. 2015, Iba, Arakawa et al. 2018). Thromboinflammatory conditions such as sepsis normally require the use of conventional anticoagulant therapies, such as heparin or low-molecular-weight heparins (Martinez, Fernandez et al. 1966, Fan, Jiang et al. 2016). However, despite their potential effectiveness to prevent thrombosis, however, they may favour to a massive bleeding outcome.

Antiplatelet therapy has also been evidenced reducing the thromboinflammatory state on septic patients, preventing coagulation and inflammation. Wang et. al., have listed different clinical studies suggesting and reduction on the mortality of septic patients treated with the COX-1 inhibitor, aspirin or the P2Y₁₂ inhibitors, such as clopidogrel or ticagrelor (Wang, Ouyang et al. 2018). Nevertheless, it is known that

some patients do not response well to these therapies, developing drug tolerance(Guha, Mookerjee et al. 2009), besides, the potential risk of bleeding observed in those patients.

1.5. Platelet receptors and signalling

Platelet receptors are involved in adhesion, interacting with the injured endothelium and platelet activation. They are classified based on their structure and signalling pathway. Some well-recognised receptors are the family of integrins, G protein-coupled receptors (GPCRs), and immunoreceptor tyrosine-based activation motif (ITAM) receptors (**Figure 3**). The platelet membrane is covered with multiple receptors; the most relevant receptors for platelet function include the integrin family (such as α Ib β 3 and α 2 β 1), GPIb-IX-V complex, GPCRs (ADP receptors P2Y_{1/12}, the TXA2 receptor and thrombin receptors, PAR1/4) and the ITAM/hemITAM receptors, GPVI and CLEC-2, respectively.

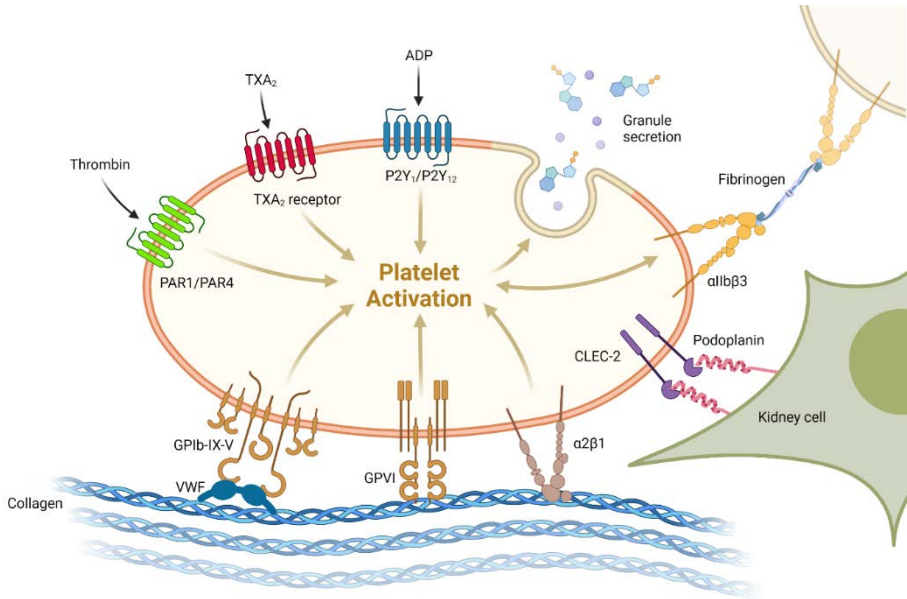


Figure 3. Platelet receptors. This figure illustrates the main receptors found on the platelet membrane and their ligands. Platelet-to-platelet interaction mediated by the integrin αIIbβ3 is also represented (modified figure extracted from www.biorender.com)

1.5.1. GPIb-IX-V

The GPIb-IX-V complex is formed by four transmembrane receptors: GPIb α , GPIb β , GPIIX, and GPV. The prothrombotic role of the GPIb-IX-V complex was first identified through the impaired thrombus formation in Bernard-Soulier syndrome patients (Bernard and Soulier 1948). This complex is important because of its adhesive properties to

vascular vessels walls at the injury site, where collagen fibres are exposed. Subsequently, soluble vWF becomes attached and immobilised to the collagen chains. Circulating platelets quickly bind to the A1 domain of the immobilised vWF, through binding of the GPIb α receptor. This then forms a complex with GPIb β , GPIX and GPV, thus, initiating a cascade of events leading to thrombus formation and haemostasis (Clemetson and Clemetson 1995, Weiss and Lages 1997).

Platelet activation mediated by GPIb-IX-V in response to vWF stimulation is controlled by 14-3-3 proteins, through the interaction with multiple phosphoserine-dependent binding sites on the complex GPIb-IX (Hamers-Casterman, Atarhouch et al. 1993, Chen, Ruggeri et al. 2018). Additionally, tyrosine phosphorylation mediated by Src kinases can also modulate activation mediated by this complex (Wu, Suzuki-Inoue et al. 2001, Ozaki, Asazuma et al. 2005).

1.5.2. Integrins

Integrins are a family of transmembrane glycoproteins composed of α and β subunits. Platelets express five integrins which contribute to platelet-platelet interactions and platelet-extracellular matrix interactions (Bennett 2005).

The integrin α IIb β 3, also known as GPIIb/IIIa, is highly and exclusively expressed on platelets and megakaryocytes. This integrin is recognised

as a fibrinogen, fibronectin and vWF receptor. Integrin $\alpha\text{IIb}\beta\text{3}$ is in a low affinity conformation (inactive) in resting platelets but a conformational change occurs after platelets are exposed to an agonist, resulting in its active or high affinity conformation, as occurs in other integrins from the β1 and β3 family. This conformational change is mediated by an intracellular signalling process referred to as ‘inside-out’ signalling, where the cytoplasmic tails of the integrin interact with intracellular proteins, specifically talin (Nieswandt, Moser et al. 2007). The inside-out signalling can be triggered by soluble ligands, such as ADP, thromboxane A_2 , or thrombin and promotes aggregation, stabilisation, and growth of the thrombus.

1.5.3. GPCRs

The G protein-coupled receptors (GPCRs) are found on the platelet membrane as 7 transmembrane receptors. Their responses are mediated by soluble agonists, including the thromboxane A_2 (TxA_2) receptor, the thrombin receptor (PAR1/4) and the ADP receptor ($\text{P2Y}_{1/12}$). Despite belonging to the same family of receptors, they differ in their activation mechanisms. For example, the activation mechanism of protease activated receptors 1 and 4 (PAR1/4) is distinct among GPCRs, since PARs depend on the proteolytic activity mediated by thrombin to cleave the GPCR N-terminus (Vu, Hung et al. 1991).

Conversely, the TxA₂ and ADP receptors do not require proteolytic cleavage of the receptor after ligand engagement (Offermanns 2006).

In terms of signalling events, PAR1/4 activation promote the release of the associated Gα_q protein, which leads to signalling characterised by phospholipase C (PLC) activation, an increase in Ca⁺² release, and further PKC activation. PARs are also associated with the Gα₁₃ protein, and its release leads to signalling through the Ras homologous A (RhoA) GTPase and Rho-associated protein kinase (ROCK), which are associated with changes in the cytoskeleton by actin. The TxA₂ receptor signals similarly to PARs, since they are both associated with G protein isoforms: Gα₁₃ and Gα_q (Woulfe 2005).

The ADP receptor, P2Y₁ signals exclusively through the Gα_q protein. However, P2Y₁₂ is coupled to a G_{i2} protein, inducing signalling via a different mechanism whereby a reduction in cyclic AMP is observed and the release of diacylglycerol (DAG) and inositol tris-phosphate (IP₃) is promoted. Additionally, intracellular calcium is mobilised from the dense tubular system, promoting cytoskeletal reorganisation (Gachet, Hechler et al. 1997).

ADP and TxA₂ play important roles as positive feedback mediators after platelet activation is induced by other receptors. In the case of ADP, it is released from activated platelets when they interact with other ligands, such as vWF or collagen. On the other hand, TxA₂ is synthesised *de novo* by cyclooxygenases (COX), stimulating further

platelet aggregation, (Rivera, Lozano et al. 2009, Dowal and Flaumenhaft 2010).

Current antiplatelet therapies, such as clopidogrel and aspirin, target ADP receptors or TxA₂ synthesis by cyclooxygenase (COX), respectively. However, the prospective antithrombotic benefits of such therapies are limited by potential bleeding risks (McNeil, Wolfe et al. 2018). This conclusion has been drawn based on patients treated with low dose aspirin, where an increase of gastrointestinal (Stalnikowicz-Darvasi 1995) and extracranial bleeding (Meade, Roderick et al. 1992) has been observed.

ADP inhibitors, such as clopidogrel or prasugrel, used in combination with aspirin have superior antithrombotic effect, compared to when they are used on their own, particularly, in those patients that have shown tolerance to the monotherapy based on P2Y₁₂ inhibitors, such as clopidogrel.(Guha, Mookerjee et al. 2009) However, a marked increase of bleeding cannot be overlooked , since it has been repeatedly reported in patients with acute coronary syndrome (Wiviott, Braunwald et al. 2007, Garcia Rodriguez, Martin-Perez et al. 2016).

The increase of bleeding in patients treated with aspirin and/or P2Y₁₂ is not surprising, since the role of ADP and TxA₂ is essential for the thrombus formation and the maintenance of the haemostasis. Therefore, there is a clear need for the development of novel therapeutics agents targeting receptors which a minor role in the haemostasis, as it has been

observed in other platelet receptor, including (hem)ITAM receptors, CLEC-2 and GPVI.

1.5.4. ITAM and hemITAM receptors

Platelets express three glycoproteins (GPs) which are members of the immunoreceptor tyrosine-based activation motif (ITAM) receptor family. This family of receptors is characterised by the dimeric Fc receptor (FcR) chain, which is non-covalently associated with either the collagen receptor, GPVI, the podoplanin receptor, C-type lectin receptor 2 (CLEC-2) Fc γ RIIA, a low-affinity receptor for immune complexes (Boulaftali, Hess et al. 2014). ITAMs signal via phosphorylation of the two YXXL sequences found in the cytosolic tail, whereas hemITAMs, such as CLEC-2, contain just one YXXL motif.

GPVI is exclusively expressed on platelets and megakaryocytes. For decades, it has been described as the main collagen receptor. The transmembrane domain of GPVI is linked to an intracellular FcR γ -chain homodimer through a salt bridge. Collagen binds to GPVI through the glycine–proline–hydroxyproline (GPO) motifs (Knight, Morton et al. 1999) and has been proven to cause receptor dimerisation and higher-order clustering (Poulter, Pollitt et al. 2017). Fibrin and fibrinogen have also been shown to activate GPVI (Xu, Gauer et al. 2021). The snake venom convulxin has additionally been recognised as a GPVI ligand (Lecut, Arocas et al. 2004); convulxin is also a ligand

for the integrin $\alpha 2\beta 1$ (Jandrot-Perrus, Lagrue et al. 1997, Kanaji, Kanaji et al. 2003).

Collagen or podoplanin binding leads to clustering of GPVI and CLEC-2 respectively and to the subsequent phosphorylation of the ITAM/hemITAM motifs through Src and Syk kinases, as well as the binding of Syk through its SH2 domains. Syk autophosphorylation and phosphorylation by a Src family kinase (SFK) leads to Syk activation. As a consequence, Syk increases phosphorylation of the linker of activated T cells (LAT), which attaches to different protein effectors such as Bruton's tyrosine kinase (Btk), tyrosine-kinase protein Tec and the SH2-domain-containing leukocyte protein of 76 kDa (SLP-76). These events lead to PI 3-kinase (PI3K) and PLC γ 2 activation, with the latter undergoing further phosphorylation by Btk and Tec. The secondary mediators IP3 and DAG generate intracellular Ca²⁺ mobilisation and PKC activation, leading to integrin activation, degranulation, and further release of additional mediators, ADP and thromboxane (**Figure 4**) (Severin, Pollitt et al. 2011, Parguïña, Alonso et al. 2012).

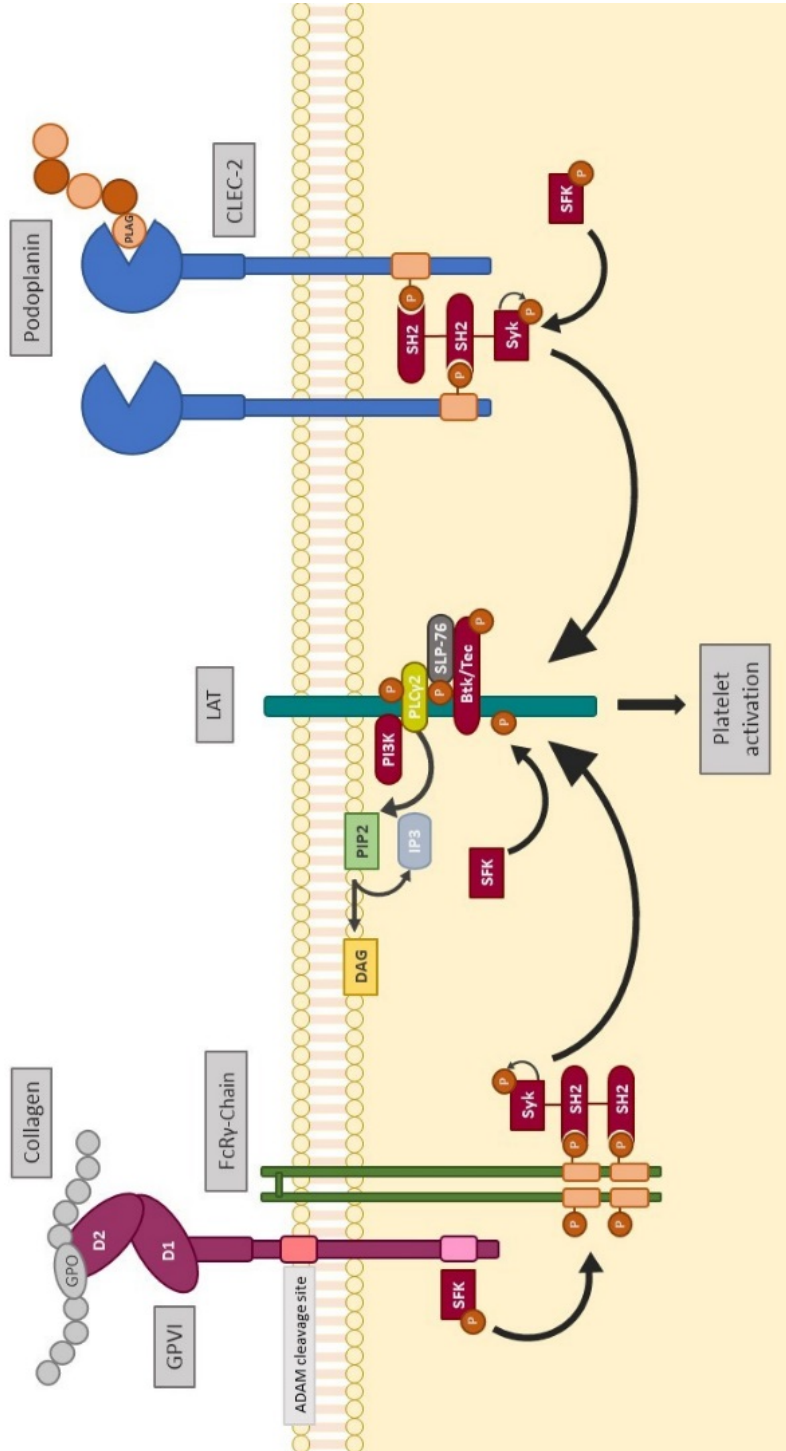


Figure 4. GPVI and CLEC-2 signalling pathways. GPVI/ FcR γ -chain and CLEC-2 follow a similar signalling pathway for platelet activation. ITAM/hemITAM activation is led by Syk and Src phosphorylation. The adaptor protein LAT serves as a scaffold for the binding of effector proteins such as Btk/Tec and SLP-76, which subsequently stimulates PI3K phosphorylation. Secondary mediators are important players as positive feedback of the signalling mediated by CLEC-2.

1.6. Role of (hem)ITAM in thrombus stability

Thrombus stability refers to the capacity of the thrombus to be retained at the injury site. This process is achieved by multiple mechanisms, which includes the formation of a fibrin mesh to prevent displacement by flowing blood. Under physiological conditions, small platelet disaggregates can be eliminated by a fibrinolytic mechanism, mediated by the activation of plasminogen. Altering thrombus stability has been proposed as a potential antithrombotic therapeutic strategy, by promoting this natural fibrinolytic activity (Gorog, Fayad et al. 2017, Gorog 2018). This approach was initially proposed for traditional antithrombotic therapies targeting the ADP receptor, TxA₂ synthesis, or the adhesion receptor α IIB β 3 (Feng, Valiyaveetil et al. 2017). However, the roles of these targets are tightly implicated in haemostasis and can lead to bleeding.

ITAM receptors are interesting potential drug targets, since they have been associated with only a minor role in haemostasis, while playing a major role in the process of thromboinflammation (Rayes, Watson et al.

2019). Furthermore, emerging evidence suggests that GPVI and CLEC-2 have an important role in thrombus formation and stability (Haining, Cherpokova et al. 2017, Ahmed, Kaneva et al. 2020). However, it is not clear whether the role of ITAM receptors in platelet aggregate stability is mediated by direct receptor interactions, or through the role of their related tyrosine kinases.

Recent studies have shown that Syk is necessary for thrombus stabilisation under high shear conditions when blood is flowed over a collagen surface (Andre, Morooka et al. 2011, Perrella, Montague et al. 2022). The role of kinases in thrombus stability was also demonstrated in a study of GPVI signalling, whereby direct blocking of the receptor or inhibition of Src and Syk kinases caused platelet disaggregation on a collagen surface at arterial shear force (Ahmed, Kaneva et al. 2020).

The role of CLEC-2 in platelet aggregate stabilisation has been less explored. However, it has been demonstrated in murine models. For example, May et. al, perfused whole blood from wild type and CLEC-2 deficient mice under arterial shear conditions ($>1000\text{ s}^{-1}$), over a collagen coated surface. It was observed that CLEC-2 deficient platelets were able to adhere to collagen and form large thrombi, through platelet-to-platelet interactions, however, they were rapidly released compared to wild type platelets (May, Hagedorn et al. 2009).

Additionally, a separate CLEC-2-deficient murine model showed normal adhesion and spreading in platelets attached in a collagen,

fibrinogen, laminin, and vWF coated surfaces. The authors also observed an impaired thrombus formation when CLEC-2 deficient blood was flowed on collagen-coated surfaces at a high shear rate (2000 s⁻¹). Thus, they suggested that CLEC-2 may be irrelevant for the initial adhesion to collagen, but it may be involved in the stabilisation of the thrombus (Suzuki-Inoue, Inoue et al. 2010).

Another study demonstrated that the simultaneous depletion of CLEC-2 and GPVI significantly impacts the haemostatic role of platelets. However, independent depletion of each receptor markedly reduced thrombus formation without displaying an impact on haemostasis (Bender, May et al. 2013).

Some years later, Haining et al., proposed that CLEC-2 contributes to thrombus stability *in vivo* independently of hemITAM signalling by using a CLEC-2 receptor knock-in mouse model. The authors mutated the hemITAM motif (Y7A), with the result of rendering its signalling inactive, whilst preserving the extracellular domain of CLEC-2. They observed that the dead-signalling CLEC-2 mice form aggregates similarly to wild types when attached to a collagen coated surfaces. However, blocking the extracellular CLEC-2 by INU1 Fab, surfaces coverage area by platelet aggregates was significantly reduced (Haining, Cherpokova et al. 2017).

The previous studies suggested CLEC-2 as a promising target to prevent pathological thrombus formation without impairing normal haemostasis.

1.7. CLEC-2 and thromboinflammation

Research into platelet glycoprotein receptors have demonstrated that both GPVI and CLEC-2 play important roles in the maintenance of vascular integrity at sites of inflammation (Boulaftali, Hess et al. 2013, Lee and Bergmeier 2016).

Upregulation of CLEC-2 and its ligand, podoplanin, play a significant role in thrombus formation in a model of deep vein thrombosis (DVT) (Payne, Ponomaryov et al. 2017). The importance of CLEC-2 during thromboinflammation was also demonstrated through its role in controlling the innate immunity response after bacterial infections, via the podoplanin-CLEC-2 axis (Rayes, Lax et al. 2017). Thus, CLEC-2 may represent a potential target for thromboinflammatory diseases, as suggested by Vogtle et al. (Vogtle, Cherpokova et al. 2015). However, for the development of new therapeutic agents against CLEC-2 an improved molecular and structural characterisation is needed.

1.8. The CLEC-2 receptor and its ligands

CLEC-2 is a transmembrane receptor with a 229-amino-acid extracellular ligand-binding C-type lectin-like domain, a stalk region, a single transmembrane helix, and a short cytoplasmic tail (Martin, Zuidserwoude et al. 2021). The CLEC-2 receptor is found on the platelet membrane, with an average of 2000-4000 copies per human platelet, as determined by flow cytometry (Gitz, Pollitt et al. 2014) and mass spectrometry (Burkhart, Vaudel et al. 2012). The stimulation of CLEC-2 by its ligands is characterised by a lag phase on human platelet aggregation after ligand engagement, an all-or-none mechanism is also observed (Suzuki-Inoue, Fuller et al. 2006).

The major endogenous ligand of CLEC-2, podoplanin, is a type-I transmembrane sialoglycoprotein, which is expressed as multiple copies on the membrane of renal podocytes, lymphatic endothelium, and various epithelial membranes, including in the lung and choroid plexus. It is known to be up-regulated on hematopoietic cells at sites of inflammation (Rayes, Watson et al. 2019).

Podoplanin is also expressed in a variety of tumour cells and has been related to cancer associated thrombosis. Takagi et al., suggested that platelets promote metastasis and tumour growth by a direct interaction between podoplanin and CLEC-2 (Takagi, Sato et al. 2013). This finding is also supported by the observation that podoplanin is overexpressed in metastatic osteosarcomas, promoting platelet

aggregation and cell migration, while it is absent in healthy osteoblasts (Kunita, Kashima et al. 2011). Zhu et al., observed an increase of the podoplanin plasma levels in patients with fibroadenomas of breast, which was further increased in breast cancer patients (with invasive ductal carcinoma), compared to healthy donors (Zhu, Xu et al. 2020).

The snake venom toxin rhodocytin induces powerful activation of CLEC-2. Rhodocytin is an $(\alpha\beta)_2$ -tetramer comprised of two α - and two β -subunits, and it has been used historically to prove CLEC-2 function on platelets (Suzuki-Inoue, Fuller et al. 2006). Its use has also contributed to our understanding of the CLEC-2 binding site structure and activation mechanism (Watson, Eble et al. 2008). For example, a structural study of CLEC-2 demonstrated that recombinant CLEC-2 undergoes dimerization after rhodocytin engagement (Watson, Christou et al. 2009).

Recently, Bourne et al. (2020) have shown that the iron-coordinated compound heme (hemin), which is released from damaged red blood cells under septic conditions, activates CLEC-2. This finding may be relevant to haemolytic disease (Bourne, Colicchia et al. 2021). This observation was confirmed by Oishi et al., however, they additionally proposed that hemin binds also to GPVI and that hemin-activated platelets induce macrophage extracellular traps (METs). They found that these METs aggravate rhabdomyolysis-induced acute kidney injury, known as RAKI, in a cooperative mechanism involving CLEC-

2 and GPVI (Oishi, Tsukiji et al. 2021). Hemin is the first non-protein agent able to induce platelet aggregation via CLEC-2.

The binding site of the main CLEC-2 ligands (rhodocytin and podoplanin) have been resolved for more than a decade; this data is critical for the rational development of new ligands. In 2008, Watson et al. solved the crystal structure of the CLEC-2 extracellular domain in complex with rhodocytin to 1.6 Å and showed that rhodocytin interacts with four arginine residues: Arg107, Arg118, Arg152, and Arg157 (Watson, Eble et al. 2008). A second study in 2014 by Nagae et al. compared the crystal structure of the extracellular domain of CLEC-2 in complex with rhodocytin and podoplanin. It was observed that the binding interface between both ligands overlapped. None of these studies observed conformational changes induced by the ligand in comparison with the crystal structure of CLEC-2 alone (Nagae, Morita-Matsumoto et al. 2014, Martin, Zuidsherwoude et al. 2021) (**Figure 5**).

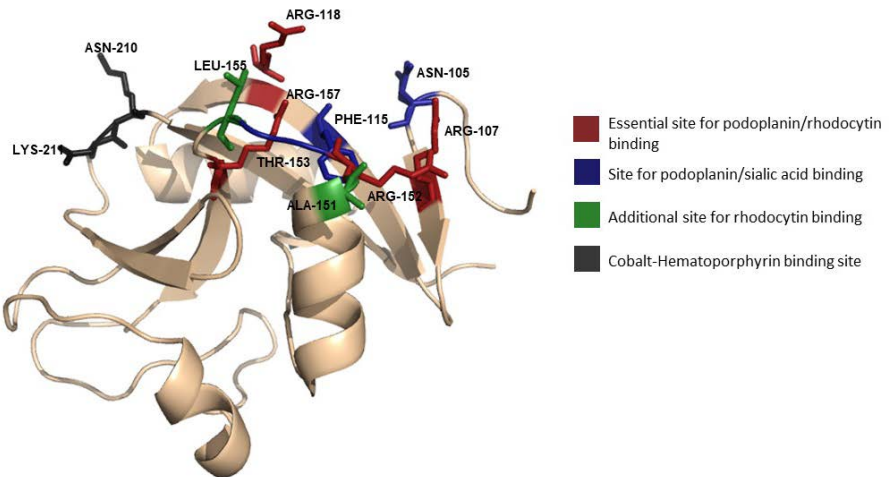


Figure 5. Mapping of the reported binding sites of podoplanin, rhodocytin, and cobalt-hematoporphyrin onto the crystal structure of CLEC-2 (PDB: 26CU). Common binding site for podoplanin and rhodocytin (Arg 107, Arg 118, Arg 152, and Arg 158) (Red); additional binding site for podoplanin (Tyr-153 and His-154) and sialic acid (Asn-105, His-119, and Tyr-129; blue); PDB: 3WSR; additional polar interaction of rhodocytin (PDB: 3WWK; green). The cobalt-hematoporphyrin binding site has been predicted by molecular docking (Asn-210 and Lys-211; grey).

1.9. CLEC-2 activation receptor clustering

In 2014, Pollitt et al., observed that the binding of podoplanin to CLEC-2 on platelets causes signalling via Src family and Syk tyrosine kinases, which results in the formation of receptor macroclusters, promoting platelet adhesion to lymphatic endothelial cells (LECs) at low shear (Pollitt, Poulter et al. 2014). They also showed that the inhibition of

tyrosine kinases downstream of CLEC-2 results in a reduction of cluster formation, resulting in reduced platelet adhesion to LECs (Pollitt, Poulter et al. 2014). This study provided mechanistic insight into how CLEC-2 signalling promotes adhesion to podoplanin, as well as podoplanin regulation.

Receptor clustering seems to be a common mechanism between ITAM receptors. For instance, clustering has also been observed in the Fc- γ receptor I after engaging with the IgG, leading to a rapid tyrosine phosphorylation of Fc- γ chain by SFK and further Syk recruitment (Duchemin, Ernst et al. 1994). Similarly, higher orders of oligomerisation have been observed in GPVI dimer upon collagen binding using advance microscopy techniques(Poulter, Pollitt et al. 2017).

Hughes et al. (2010) have suggested that dimerisation of CLEC-2 is required for Syk phosphorylation and the subsequent signalling pathway. The authors have observed that CLEC-2 is found as a monomer and dimers in unstimulated platelets and higher order of oligomerisation can be form after rhodocytin stimulation. They also proposed a stoichiometry of 2:1 for the CLEC-2 and Syk interaction (Hughes, Pollitt et al. 2010).

These findings indicate the importance of CLEC-2 multimerisation for the modulation of further signalling events and subsequent platelet aggregation. However, there is an absence in the literature that proves

ligand- CLEC-2 receptor stoichiometry. Such knowledge will be relevant for the development of efficient therapeutic CLEC-2 blocking agents.

1.10. CLEC-2 antagonists and development challenges

CLEC-2 activation is mainly mediated by protein-protein interaction (PPI), this kind of interaction were considered undruggable for many years. Despite advances in drug development, receptors mediated by PPIs are one of the most challenging targets using conventional small molecule inhibitors (Damaskinaki, Moran et al. 2021).

Generally, the main challenge of targeting PPIs are the follows:

- 1) The PPIs lack of a clear binding pocket, as observed in other targets, such as enzymes. This makes difficult the small molecule design based on the receptor structure (Jones and Thornton 1996)
- 2) PPI are constituted by multiple interactions, characterised by high affinity and avidity, whilst small molecule avidity tends to be considerably lower (Damaskinaki, Moran et al. 2021)..
- 3) Protein ligands are buried onto large surfaces ($1,000\text{--}2,000 \text{ \AA}^2$) whilst small molecules only occupy a small surface are of the receptor ($\sim 300\text{--}500 \text{ \AA}^2$) (Arkin, Tang et al. 2014, De Luca, Agharbaoui et al. 2016).

In the case of CLEC-2, a single copy of dimeric CLEC-2 can be docked onto the surface across of rhodocytin, burying at least 2305 Å² (Watson, Eble et al. 2008). Therefore, patching this large surface with small molecule inhibitor, seems considerably unlikely.

However, to date, a few antagonists of CLEC-2 have been described. In 2018, Tsukiji et al. identified cobalt-hematoporphyrin (Co-HP), a non-peptide inhibitor, using a small molecule-based high-throughput screening (HTS), followed by chemical optimisation (Tsukiji, Osada et al. 2018). The authors showed that Co-HP can prevent platelet aggregation induced by rhodocytin or podoplanin, at a low micromolar concentration range. They also showed the specificity of the receptor, as no effect on platelet aggregation, induced by collagen or thrombin, was observed. This suggests that the effect of Co-HP may be functioning by blocking the rhodocytin and CLEC-2 interaction. **(Figure 6)**

One interesting finding related to Co-HP, is the possible allosteric binding site predicted by molecular docking, indicating for the first time that amino acids Asn120, Asn210, and Lys211 may have an allosteric effect on the canonical binding site. Despite the speculative nature of the molecular docking studies, the role of Asn120 and Lys211 have been tested, as mutating these residues affects CLEC-2 ligand binding (Tsukiji, Osada et al. 2018). In spite of the promising *in vitro* data, hematoporphyrins are well-known for their cytotoxicity (Lin, Zhang et al. 2020); therefore, its further development as a CLEC-2 inhibitor is

highly unlikely. However, crystallography studies are still needed, which could point to Co-HP as an interesting tool with which to study allosteric inhibition of CLEC-2. Nevertheless, considering the low affinity of Co-HP, obtaining a crystal structure of this complex may be extremely challenging.

Chang et al. (2015) also identified a novel and non-cytotoxic 5-nitrobenzoate compound, 2CP, able to prevent platelet aggregation induced by podoplanin at a high micromolar concentration. However, it was unable to prevent platelet aggregation induced by rhodocytin. The authors posited that 2CP binds to the same binding site for rhodocytin and podoplanin, even though this contradicts the finding that 2CP inhibits podoplanin-induced aggregation but not rhodocytin-induced aggregation (Chang, Hsieh et al. 2015).

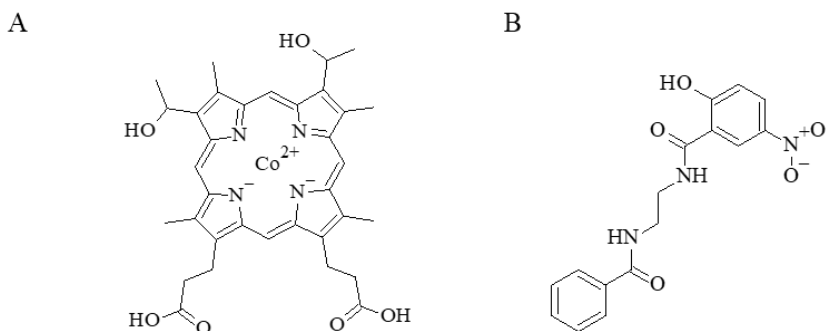


Figure 6. Structure of small molecules inhibitors of CLEC-2. A) the macrocycle cobalt-hematoporphyrin and B) 2CP.

Another approach for the development of antagonists of PPI, is based on the generation of biological agents. For example, the antibody fragment AYP1 F(ab)₂ has been developed against CLEC-2, showing a potent inhibition of platelet aggregation induced by rhodocytin or podoplanin, suggesting that it may bind to the same site as these agonists (Gitz, Pollitt et al. 2014).

Fragments generated from full length antibodies have been shown to be effective blocking agents, and some of them have been approved for clinical usage by the United States food and drug administration (FDA). An example of this is the anti-GPIIb/IIIa chimeric fragment antigen binding (Fab) fragment, also known as abciximab, which has been approved since 1994 to prevent thrombosis during coronary artery catheterisation (Nelson 2010). However, new technology associated with the development of biologics has allowed for the generation of fragments which are equally potent but have superior stability. Such fragments are generated from camelid antibodies and are known as nanobodies. Nanobodies are also significantly smaller in size than antibodies and Fab fragments, which is thought will translate to a lower risk of immunogenicity.

Nanobodies are single variable heavy chain (VHH) fragments derived from functional antibodies generated in llamas, camels and/or sharks. They also lack light chains (Hamers-Casterman, Atarhouch et al. 1993).

Figure 7 shows a structural comparison between a conventional antibody, Fab fragment and camelid nanobody. Nanobodies have many

advantages over traditional antibody fragments, including that they are stable over a wider range of temperature and pH. They could also be mass produced in a bacterial system, due to their lack of post-transduction modifications (Asaadi, Jouneghani et al. 2021). However, one of the most interesting properties is their suitability for molecular engineering, allowing for the generation of multimeric nanobodies, which may produce higher avidity options compared to the monomeric version and allows for the addition of tags, such as the albumin binding site to increase their half-life.

Interest in the development of nanobodies had an exponential increase after the approval of the divalent nanobody, caplacuzimab by the FDA for the treatment of acquired thrombotic thrombocytopenic purpura (Scully, Cataland et al. 2019). This demonstrated the efficacy and safety of nanobodies for clinical uses. Thus, the generation of nanobodies may represent a promising alternative means to target PPI based receptors, including CLEC-2.

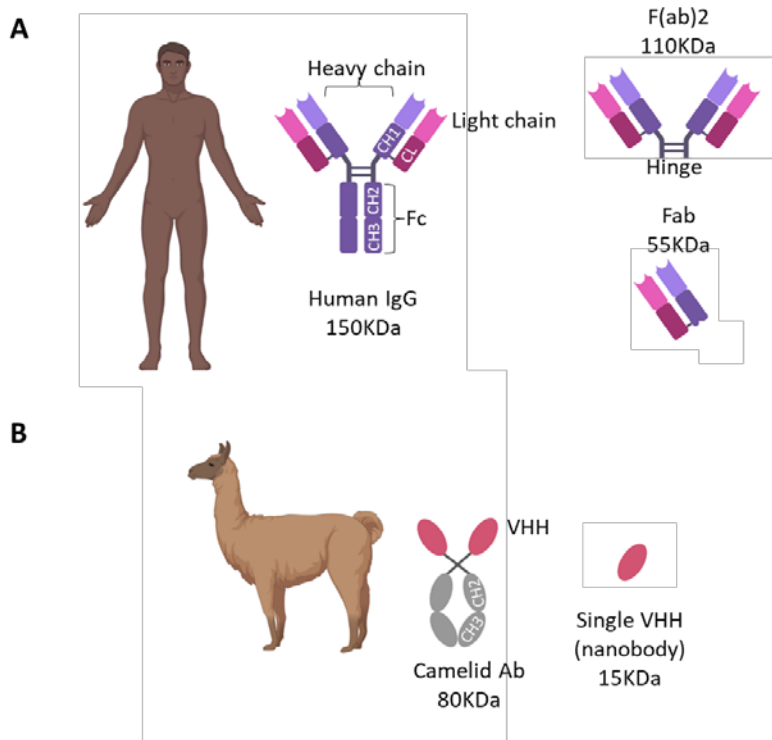


Figure 7. Schematic representation of human antibody and their antibody-derived fragments produced by vertebrates (A) and camelid heavy chain antibodies (B).

1.11. Importance of developing new CLEC-2 ligands

CLEC-2 was identified 15 years ago as the rhodocytin receptor (Suzuki-Inoue, Fuller et al. 2006), and since then, there have been many efforts to fully understand and identify its physiological role during thrombosis and minor role during haemostasis, and in connection to physiological

ligands. Studies have also focussed on its structure and binding site, in addition to the activation mode of the receptor.

After many years of research, its relevance has been understood as a target for a new generation of drugs with a potent antithrombotic effect and lower risk of bleeding (Bender, May et al. 2013). CLEC-2 has a strong implication in the development of venous thrombosis, such as DVT, in thromboinflammatory conditions in severe disease, including cancer, and sepsis (Rayes, Watson et al. 2019).

Nonetheless, to successfully develop potent and selective inhibitors, a deeper understanding of the activation mechanism of CLEC-2 is needed. Therefore, the development of new ligands of CLEC-2 will provide innovative insights into its stoichiometry and identify future inhibitors.

CHAPTER 2

AIMS AND HYPOTHESIS

2. Chapter 2: Aims and hypothesis

The present PhD dissertation aims to answer if it is possible to develop new ligands for the platelet receptor CLEC-2.

2.1. General aims

To achieve the hypothesis of this study, we have established the following general objectives:

1. To identify new ligands for the human CLEC-2 receptor based on a small molecule chemical library.
2. To prove the activation of CLEC-2 using novel multimeric nanobodies
3. To evaluate the role of tyrosine kinases on thrombus stability.

2.2. Specific objectives

To achieve the general aims, we have segmented them into the following specific objectives:

1. To set up a suitable assay for the screening of small molecules against CLEC-2 in a HTS format.
2. To validate any potential candidates identified in the HTS through platelet functional assays
3. To propose a potential mechanism of action of the best ligands identified in the previous point.

4. To multimerise potent nanobodies using molecular biology for further evaluation of CLEC-2 function
5. To evaluate the role of oligomeric ligands on CLEC-2 clustering.
6. To determine the role of tyrosine kinase dephosphorylation on the maintenance of platelet aggregates.

CHAPTER 3

MATERIALS AND METHODS

3. Chapter 3: Material and Methods

3.1. Materials

The platelet agonist rhodocytin was kindly donated by Dr Johannes Eble (University of Münster, Germany), and collagen-related peptide (CRP-XL) was purchased from Cambcol Laboratories (Cambridge, UK). Thrombin was purchased from Merck (Darmstadt, Germany). Katakine was purchased from TargetMol (Boston, MA, USA). Recombinant human podoplanin-rFc and recombinant human CLEC-2-6xHis were expressed in house using HEK293T cells. Recombinant human CLEC-2 was purchased from R&D Systems (Minnesota, USA) to optimise the screening.

The inhibitors indomethacin and apyrase were purchased from Sigma, and Integrilin was purchased from GlaxoSmithKline. The Src inhibitor PP2 was purchased from Sigma-Aldrich (Dorset, UK), and the Syk inhibitor PRT-060318 was purchased from ApexBio (Houston, TX, USA). Ibrutinib was acquired from Sellechem (Germany). AYP1 was expressed and purified from hybridoma cells; fragments of AYP1 were generated in house by Ying Di, research technician at University of Birmingham.

The primary antibodies rabbit anti-phospho-Syk (Y525/526), rabbit anti-FcR gamma and anti-phospho PLC γ 2 pY1217 were obtained from Cell Signalling (Massachusetts, USA); the rabbit anti-phospho LAT(Y200) and anti-phospho Btk pY223 and pY551 were purchased

from Abcam (Cambridge, UK). Monoclonal phosphotyrosine antibody (clone 4G10) was purchased from Upstate Biotechnologies (Lake Placid, NY), and anti-CLEC-2 antibody (AF1718) was obtained from R&D system (Minneapolis, USA). The mouse α -human α -tubulin (Sigma-Aldrich), HRP-conjugated sheep α -mouse, and donkey α -rabbit IgG were purchased from GE Healthcare (Little Chalfont, UK),

For the flow cytometry experiments, Calcein-AM and FITC-conjugated mouse PAC-1 mAb were obtained from Invitrogen.

For protein purification, HiTrap™ Protein A HP column HisPur™ Ni-NTA resin was purchased from GE Healthcare. EZ-Link™ Sulfo-NHS-LC-Biotin was purchased from Thermo Scientific.

For the cell culture experiments, Dulbecco's Modified Eagle Medium (DMEM), antibiotics penicillin and streptomycin, and ultra-low IgG foetal bovine serum were purchased from Gibco. Trypsin-EDTA solution, L-glutamine solution, and poly-L-lysine solution were obtained from Sigma.

For molecular cloning experiments, GenElute™ Gel Extraction Kit, GenElute™ Plasmid Miniprep kit, GenElute™ Plasmid Maxiprep kit, and Luria broth (Miller) were purchased from Sigma-Aldrich. SYBR® Safe DNA gel stain was purchased from Invitrogen. Gel Loading Dye, Purple (6x) buffer; CutSmart buffer; and all restriction enzymes (XmaI and SmaI) were purchased from New England Biolabs.

ALPHAScreen Histidine (Nickel Chelate) Detection Kit and ALPHAScreen TruHits Kit were purchased from PerkinElmer. 1536-well White Polystyrene Not Treated Microplates (3725) were purchased from Corning.

3.2. Methods

3.2.1. Preparation of Human Washed Platelets

Blood collection have been approved by the Comité Autonómico de Ética de la investigación de Galicia (2009/270) from healty donors who have not taken any medication in the previous 10 days.

Whole blood was collected from healthy volunteers in 4.5 mL or 9 mL vacutainers containing 3.2% sodium citrate. Then, 450 μ L or 900 μ L of acid citrate dextrose (ACD; 85 mM sodium citrate, 71 mM citric acid, and 110 mM glucose) was added to the tubes, and the solution was mixed gently.

Samples were centrifuged at $200 \times g$ for 20 min at room temperature. The platelet-rich plasma (PRP) was collected into a Falcon tube, and 0.25 μ g/mL prostacyclin (PGI₂) was added to prevent platelet activation during subsequent centrifugation. Platelets were pelleted by centrifugation of PRP at $1000 \times g$ for 10 min at room temperature.

Platelet pellet was resuspended in 150 μ L of warmed ACD and 1 mL of modified Tyrode's buffer (134 mM NaCl, 2.9 mM KCl, 0.34 mM Na_2HPO_4 , 12 mM NaHCO_3 , 20 mM HEPES, 1 mM MgCl_2 , and 5 mM glucose; pH 7.3). After pellet resuspension, the volume was made up to 25 mL with warmed Tyrode's buffer and 3 mL of ACD; next, 10 μ L of 0.25 μ g/mL PGI_2 was added, and the solution was centrifuged at $1000 \times g$ for 10 min at room temperature. Pellets were resuspended using Tyrode's buffer, and the number of platelets was counted using a Z1 Coulter Particle Counter (Beckman Coulter). Platelet density was adjusted using Tyrode's buffer, and the suspension was rested for 30 min.

3.2.2. Platelet Functional Assays

3.2.2.1. Light Transmission Aggregometry

Washed platelets (300 μ L; 2×10^8 /mL) were transferred to a Chronolog cuvette 312. Platelets were warmed at 37°C in a Chronolog model 700 or 490-X aggregometer (ChronoLog, Havertown, PA, USA) and the stirred at 1200 rpm at 37°C, followed by the addition of the platelet agonist. Platelet aggregation was monitored for at least 8 min after the stimulation. Platelets were pretreated with the inhibitors or potential inhibitors or vehicle for 5 min at 37°C. For platelet disaggregation experiments, inhibitors of tyrosine kinases (PRT-060318 [1 μ M], PP2 [20 μ M], dasatinib [10 μ M], ibrutinib [200 nM]), or secondary mediator

inhibitors (10 μ M indomethacin or 2 U/mL apyrase) were added 150 sec after the agonist, and aggregation was monitored for 20 min.

3.2.2.2. Calcium Release Assay

Washed platelets (2×10^7 /mL) were incubated with freshly prepared FLIPR Calcium 4 reagent (Molecular Devices); probenecid 0.07% was added, and the solution was incubated for 1 h at 37°C in a 384-well transparent-bottom plate. Inhibitors and agonists were automatically dispensed using FDSS7000EX (Hamamatsu). Platelets were incubated for 10 min with 9 μ M eptifibatide (Integrilin®) and small-molecule inhibitors (10 μ M) from the EU-OPENSREEN chemical library provided by the BioFarma facilities at the University of Santiago de Compostela. Dimethyl sulfoxide (DMSO; 0.1%) was used as vehicle control. Then, 100 nM rhodocytin was added to platelets. Changes in fluorescence were measured in real time for 15 min after the addition of rhodocytin, using emission and excitation wavelengths of 480 and 540 nm, respectively.

3.2.2.3. Flow Cytometry

3.2.2.3.1. Evaluation of Platelet Viability

Washed platelets (200 μL ; $2.5 \times 10^6/\text{mL}$) were incubated with the inhibitor or 0.1% (v/v) DMSO for 10 min at 37°C. Triton X-100 (0.01% (v/v)) was used as a cell death control. After pretreatment, 1 μL of 0.1 mg/mL Calcein-AM was added to each sample, and the samples were incubated for 20 min at 37°C in the dark. Samples were analysed using a BD Accuri C6 Plus flow cytometer in the FL1 (530/30 BP) channel. Platelets were identified and gated in an Accuri BD Flow Cytometer (BD Biosciences) according to the forward and side scatter signals. A total of 10,000 platelet events were acquired per sample, and mean fluorescence intensity (MFI) was estimated.

3.2.2.3.2. Evaluation of $\alpha\text{IIb}\beta\text{3}$ Activation

Washed platelets ($2 \times 10^7/\text{mL}$) were incubated with the anti- $\alpha\text{IIb}\beta\text{3}$ activated antibody, PAC-1-FITC, for 20 min and then stimulated with 10 $\mu\text{g}/\text{mL}$ crosslinked collagen-related peptide (CRP-XL) at 37°C. To assess whether Src or Syk inhibitors reverse the $\alpha\text{IIb}\beta\text{3}$ activation, PP2 (20 μM), PRT-060318 (1 μM), or 0.1% DMSO (as vehicle) were added 150 sec after stimulation, and the samples were incubated for 20 min at 37°C. Platelets were identified and gated in an Accuri BD Flow Cytometer (BD Biosciences) according to the forward and side scatter

signals. A total of 10,000 platelet events were acquired per sample, and MFI was estimated.

3.2.3. Protein Phosphorylation

3.2.3.1. Sample Preparation and Western Blot

Washed platelets (300 μ L; 4×10^8 /mL) were incubated in the presence of 9 μ M eptifibatide (Integrilin [®]) for 10 min to prevent the activation of the α IIb β 3 signalling pathway. Then, platelets were warmed for 5 min at 37°C and stirred for 1 min at 1200 rpm at 37°C. Platelets were stimulated for 5 min with the agonist or vehicle. The reaction was stopped by adding 5 \times SDS lysis buffer to each sample, and the sample was quickly transferred to a 1.5 mL Eppendorf microtube and immediately placed at 4°C; then, samples were denatured at 100°C for 5 min.

Platelet lysates were separated using SDS-PAGE, samples were loaded onto 4–12% Bis Tris Plus acrylamide gels (Invitrogen, Paisley, UK) and electrophoresed at 150 V using MOPS buffer. Resolved gels were then transferred to polyvinylidene difluoride membranes preactivated with methanol. Once transfer was complete, membranes were blocked with 4% bovine serum albumin (BSA) for 1 h at room temperature, followed by overnight incubation with the primary antibody in 4% BSA at 4°C.

After primary antibody incubation, membranes were washed thrice with Tris-buffered saline-Tween (TBST-T) for 10 min each, followed

by incubation with the secondary antibody prepared in TBST-T, for 1 h at room temperature. Then, membranes were washed thrice using TBST-T for 10 min each.

Then, TBS-T was completely removed, and membranes were incubated with 1 mL of Pierce ECL western blotting substrate for 1 min; finally, the membranes were developed using Amersham Hyperfilm ECL and further quantitated using ImageJ software.

3.2.3.2. Immunoprecipitation

Washed platelets (4×10^8 /mL) in the presence of 9 μ M eptifibatide (Integrilin®) for 10 min. Then, platelets were warmed for 5 min at 37°C and stirred for 1 min at 1200 rpm at 37°C. Finally, platelets were stimulated with 100 nM rhodocytin, 10 μ M katacine, or vehicle for 5 min, while being stirred at 1200 rpm at 37°C in a Chronolog model 700 aggregometer (ChronoLog, Havertown, PA, USA). Then, platelets were lysed with 2 \times NP-40 lysis buffer in the presence of protease inhibitors (10 μ g/mL aprotinin, 1 μ g/mL pepstatin, 10 μ g/mL leupeptin, 400 μ g/mL 4-(2-aminoethyl)benzenesulfonyl fluoride hydrochloride (AEBFS), 5 mM sodium orthovanadate; pH 7.5). Whole lysates were precleared using Gamma bind Plus Sepharose (Cytiva, USA) and then incubated with 2 μ g of AYP1 antibody for 30 min; the lysate–antibody complex was then incubated for 60 min with Gamma bind Plus Sepharose. Immunoprecipitated proteins were resuspended in SDS lysis buffer

and electrophoresed using SDS-PAGE and western blotted against the 4G10 monoclonal antibody.

3.2.3.3. CLEC-2 and Podoplanin Protein Expression and Purification

Recombinant human CLEC-2 and podoplanin were designed to be expressed in a mammalian system, to ensure that key posttranslational modifications are conserved.

The cDNA sequences of the extracellular domain of human CLEC-2 (residues 55–229) were cloned into pHLSEC (Adegene); this vector allows the insertion of a 6-histidine tag at the C-terminal end of a protein, facilitating protein purification and further coating with ALPHA beads. Human podoplanin cDNA sequence was inserted into a pFUSE-Fc (InvivoGen) expression vector; using this vector results in a fusion protein of podoplanin with an Fc domain, generating a dimeric form of podoplanin and facilitates purification by affinity columns. Both constructs were expressed in house and sequenced for correctness. Vector maps could be found in the appendix section.

To express recombinant human CLEC-2-6xHis and recombinant human podoplanin-rFc, HEK293T cells were transiently transfected with the respective vectors using lipofectamine and polyethylenimine (PEI) in serum-free DMEM. After 4 days, proteins secreted into the

medium were collected. Recombinant human CLEC-2-6xHis and podoplanin-rFc were purified in a gravity purification column using Nickel-NTA resin (Thermo Fisher) and protein A-coated beads (Thermo Fisher), respectively. Characterisation and confirmation of protein expression was performed using SDS-PAGE.

3.2.3.4. Monobiotinylation of Recombinant Human Podoplanin

To ensure that hPodoplanin-Fc bound to streptavidin ALPHAScreen beads, recombinant podoplanin was biotinylated. The protein was incubated with limiting concentrations of 50 $\mu\text{L}/\text{mL}$ EZ-Link™ Sulfo-NHS-LC-Biotin for 30 min at room temperature. The protein was dissolved in PBS at 0.5 mg/mL.

3.2.4. High-Throughput Screening Based on ALPHAScreen Assay

High-throughput screening (HTS) was performed using the miniaturised Amplified Luminescent Proximity Homogeneous Assay (AlphaScreen™) on the basis of the interaction between podoplanin and CLEC-2, which were expressed as described above. The European

Chemical Biology Library (ECBL; pilot library) comprising 5016 compounds was used.

Each of the 5016 chemicals from the library (and 0.1% [v/v] DMSO for vehicle control) were dispensed into 1536-well flat and transparent bottom white plates (Corning® 3725) (Merck, Darmstadt, Germany) using an Echo 525® Liquid Handler (Labcyte, IN, USA). After adding 50 nM of biotinylated h-podoplanin-rFc and 250 nM of h-CLEC-2-6xHis to each well, the plates were incubated for 30 min at 4°C. Then, 40 µg/mL of ALPHAScreen streptavidin donor beads were added, and the plates were incubated for 30 min at room temperature in the dark, followed by an additional incubation under the same conditions with 40 µg/mL nickel coated acceptor beads. The plates were incubated in the dark for 60 min at room temperature and read using an EnVision Multimode Plate Reader (Perkin Elmer, Waltham, USA).

3.2.4.1. Identification of True Hits

False-positive compounds were identified using an ALPHAScreen TruHits kit™. Potentially valuable compounds identified using high-throughput screening were dispensed (10 µM each) into a white 1536-well plate. Biotinylated acceptor beads and streptavidin donor beads (40 µg/mL each) were premixed and incubated for 30 min at room temperature in the dark. The incubated mixture was then added to the plate with the compounds for 10 min at room temperature, and then the

plate was read using an EnVision Multimode Plate Reader (Perkin Elmer, Waltham, USA) at 520/620 nm (ex/em). Compounds with a luminescence signal below the average signal of the beads incubated with DMSO control by more than twice the standard deviation were considered false positive hits.

3.2.5. Dose-Response Curve Generation for Potential Hits

ALPHAScreen assay was used to generate the dose-response curves of lead compounds. Six serial dilutions of the potential candidates ranging from 40 μM to 0.625 μM were prepared. The different dilutions were dispensed using an Echo 525® Liquid Handler (Labcyte, IN, USA), and 50 nM of biotinylated h-podoplanin-rFc and 250 nM of h-CLEC-2-6xHis were added. Because compounds were dissolved in DMSO, different concentrations of DMSO (0.4% to 0.00625%) were used as control during the assay. The mean value of the percentage of inhibition from three independent experiments was calculated and plotted against the log value of the molar concentration. Nonlinear regression analysis of the data were performed to generate dose–response curves using GraphPad Prism 7.

3.2.6. High-Throughput Screening Data Analysis

The signal-to-noise (S/N) ratio was calculated by dividing the mean of the maximum signal (beads coated with the proteins and incubated with 0.1% DMSO) by the mean of the minimum signal (proteins in the presence of rhodocytin, used as inhibitor control).

To evaluate the robustness of the assay, the Z' factor was determined using the following equation:

$$Z' = 1 - \frac{3sd \text{ of max} + 3sd \text{ of min}}{|mean \text{ of max} - mean \text{ of min}|}$$

In the equation, 'max' means the maximum signal from the beads coated with the proteins, and 'min' indicates the minimum signal from the beads in the presence of rhodocytin as an inhibitor of the protein-protein interaction.

Z' values ≥ 0.5 suggests a robust assay.

3.2.7. Expression and Purification of Nanobodies

The nanobodies were received in the pMECS-GG vector from VIB Nanobody Core (Vrije Universiteit Brussels, Belgium); these contain an N-terminal PelB signal sequence that targets the nanobody to the periplasmic space of *Escherichia coli* allowing their extraction from the periplasm.

E. coli WK6 was transformed with the nanobody constructs (provided by VIB). Colonies were grown overnight at 37°C in LB medium (sodium chloride [0.5 g/L]; tryptone [10 g/L], and yeast extract [5 g/L]) supplemented with 100 µg/mL ampicillin. Then, 3.5 mL of overnight cultures was inoculated into 1 L TB (12 g/L tryptone, 24 g/L yeast extract, 9.4 g/L K₂HPO₄, 2.2 g/L KH₂PO₄) supplemented with 100 µg/mL ampicillin and incubated at 37°C at 180 rpm until an optical density (OD) of 0.6–0.9 at 590 nm was reached. Once optimal OD was reached, nanobody expression was induced by adding 1 mM β-D-thiogalactoside (IPTG). Cultures were then incubated at 28°C at 180 rpm for 16 h for protein expression.

E. coli cells containing the nanobodies were collected by centrifugation at 3000 rpm for 15 min, the supernatant was discarded, and the bacterial pellet was resuspended in 12 mL TES buffer (0.2 M tris, pH 8; 0.5 mM EDTA; 0.5 M sucrose) per 1 L of culture. The resuspended pellet was incubated at 4°C with gentle shaking for 1 h.

The suspension was then diluted 2x in diluted TES buffer (TES/4) and incubated at 4°C for 1 h. Then, the suspension was centrifuged at 8000 rpm for 30 min, and the supernatant containing the nanobodies and proteins extracted from the periplasmic space was collected. Nanobodies were purified from the periplasmic extract using affinity columns containing nickel-coated beads and size exclusion chromatography. The concentration of purified nanobodies was

determined by measuring absorbance values at 280 nm using a NanoDrop spectrophotometer.

3.3. Generation of LUAS-2 and LUAS-4

3.3.1. Site-Directed Mutagenesis Kit

The insertion of restriction sites on the LUAS-1 DNA sequence was done using the Q5® Site-Directed Mutagenesis Kit following the manufacturer's instructions. The forward and reverse primers for the mutagenesis were designed using www.nebasechanger.ned.com.

Polymerase chain reaction (PCR) was performed in a total reaction volume of 25 μ L (Table 1).

Table 1: Reaction Mixture (25 μ L) Used for Site-Directed Mutagenesis

Component	
Q5 2\times master mix	12.5 μ L
10 μM forward primer	1.25 μ L
10 μM reverse primer	1.25 μ L
Template DNA	1 μ L (1–20 ng/ μ L)
Nuclease-free water	9 μ L

Detailed conditions of the PCR reaction are shown in Table 2.

Table 2: PCR Conditions for Site-Directed Mutagenesis

Step	Temperature	Time
Initial denaturation	98°C	30 s
25 cycles	98°C	10 s (Per cycle)
	70°C	30 s (Per cycle)
	72°C	3 min 30 s (Per cycle)
Final extension	72°C	2 min
Hold	4°C	

3.3.2. Circularisation of the PCR Product and DNA Template Degradation

After amplification, the PCR product was subjected to the KLD (kinase, ligase, DpnI) reaction for 10 min at room temperature (Table 3) following the manufacturer's instructions.

Table 3: Reaction Mixture Used for the KLD Reaction

Component	Volume
PCR product	1 μ L

2× KLD reaction buffer	5 μ L
10× KLD enzyme mix	1 μ L
Nuclease-free water	3 μ L

3.3.3. Bacterial Transformation

NEB5 α -competent *E. coli* cells were transformed with the products of the KLD reaction. Thus, 5 μ L of the KLD reaction product was added to 50 μ L of chemically competent cells and then incubated for 30 min, followed by a heat shock for 30 sec at 42°C, and immediately incubated on ice for additional 5 min. Then, 950 μ L SOC medium was added, and cells were grown at 37°C at 180 rpm for 1 h and finally seeded in a plate containing LB agar (with ampicillin). The plate was incubated overnight at 37°C.

Positive colonies were identified by DNA sequencing. Picked colonies were mixed with 10 mL LB + 10 μ L ampicillin and incubated at 37°C at 180 rpm for 16 h. On the next day, DNA was extracted and purified using the GeneJET plasmid miniprep kit following the manufacturer's instructions. DNA concentration was estimated using NanoDrop, and DNA sequencing was performed in collaboration with Source Bioscience.

3.3.4. Ligation of DNA Sequences

The clones generated with the DNA vector (LUAS-1 and the vector) and the insert (LUAS-1 and the linker) were digested with XmaI and Sall restriction enzymes (previously inserted in both plasmids). Table 4 shows the reaction mixture used for the double digestion.

Table 4: Reaction Mixture Used for the Double Digestion of the Vector and Insert Plasmids

Component	
DNA	1 µg
10× CutSmart buffer	5 µL
XmaI	1 µL (10 units)
Sall-HF	1 µL (20 units)
Nuclease-free water	To 50 µL

The digested products and the DNA ladder were electrophoresed at 100 V on a 4% agarose gel prepared with tris-acetate-EDTA and supplemented with SYBR™ Safe DNA Gel Stain (1:10,000 dilution). Electrophoresis was stopped when the visible dye had traversed approximately 75% of the gel. Then, the gel was immediately visualised under UV light using a transilluminator. DNA fragments were extracted from the agarose gel using QIAquick Gel Extraction Kit following the

manufacturer's instructions. Purified DNA products were then ligated as indicated in Table 5. This reaction was performed overnight at 4 °C.

Table 5: Reaction Mixture Used for the Ligation of the Vector Containing LUAS and (GGGGS)₃-LUAS DNA sequence

Component	
10× T4 DNA ligase buffer	2 µL
Vector DNA	50 ng
Insert DNA ([GGGGS]₃-LUAS)	37.5 ng
T4 DNA ligase	1 µL
Nuclease-free water	To 20 µL

After ligation, 10 µL ligated DNA was added to 100 µL chemically competent *E. coli* XL1-Blue cells; the cells were incubated on ice for 30 min, then heat shocked at 42°C for 45 s, and incubated on ice for 5 min. Then, 400 µL of LB broth was added, and the cells were further incubated at 37°C at 180 rpm for 1 h. Cell pellet was collected by centrifugation at 100 × *g* for 5 min and the supernatant was removed. Cells were resuspended in 100 µL of LB broth and placed on a LB agar plate (with ampicillin). The plate was incubated overnight at 37°C. Colonies were picked and sequenced in collaboration with Source Bioscience.

The LUAS-4 clone was generated by VIB Nanobody Core. The codons were scrambled to avoid extensive repetition, more specifically in the linkers, and then optimised for *E. coli* while keeping the 5' and 3' cloning enzyme sites intact and removing any interfering sites. The DNA sequences were inserted into a pMECS vector with a C-terminal HA tag and 6xHis tag for bacterial expression. LUAS-2 and LUAS-4 were expressed using the bacterial expression system and purified by Nickel-chelated beads and size exclusion in a manner similar to that used for LUAS.

3.4. CLEC-2 Nanobody Binding With Flow Cytometry

Initial CLEC-2–nanobody binding screening was investigated with flow cytometry. Washed platelet samples ($2.5 \times 10^6/\text{mL}$) were incubated with the nanobodies (7 nM) for 15 min at room temperature, followed by secondary labelling with Alexa Fluor-647 anti-6-His tag antibody (5 $\mu\text{g}/\text{mL}$). Control samples with no staining and only secondary antibody staining were also analysed. The samples were acquired using the fluorescent channel, FL4. Histograms were obtained using cSampler software (BD Biosciences, USA).

3.5. Surface Plasmon Resonance for Binding Studies

The surface plasmon resonance (SPR) experiments were performed to monitor binding and affinity of biological ligands of CLEC-2, namely AYP1 and the novel CLEC-2 nanobodies, LUAS and LUAS-2. These experiments were done in collaboration with Dr Eleya Martin at the University of Birmingham, using a Biacore T200 instrument (GE Healthcare).

For the SPR experiments, one of the binding molecules (the ligand or the receptor) is attached to a glass slide coated by a thin gold film and matrix formed by a hydrophilic-coated surface. In this study, the affinity of CLEC-2 nanobodies was determined using CM5 chips, and the extracellular domain of human CLEC-2 (55-229) was directly immobilised onto the CM5 chip using amine coupling to the carboxymethylated dextran-coated surface.

The SPR experiments were performed under a constant flow rate of 30 $\mu\text{L}/\text{min}$ in HBS-EP running buffer (0.01 M HEPES, pH 7.4; 0.15 M NaCl; 3 mM EDTA; 0.005% [v/v] surfactant P20) at 25°C. Multicycle kinetic assays were used with at least five concentration points between 0.1 \times and 10 \times the affinity constant (K_D). Each concentration of the CLEC-2 ligands was analysed under the following conditions: 120 sec injection, 300 sec dissociation, and 120 sec stabilisation.

To determine the affinity of the AYP1 fragment, AYP1 F(ab) was immobilised directly onto the CM5 chip using amine coupling to the carboxymethylated dextran-coated surface, and reference surfaces were

blocked using 1 M ethanolamine (pH 8). In this case, CLEC-2 ECD 53-229 was flowed under the coated chip as the analyte. The experimental conditions were as follows: 120 sec injection, 300 sec dissociation, and 30 sec regeneration with 10 mM glycine (pH 1.5), followed by a 120 sec stabilisation period.

Biacore T200 Evaluation software was used for the steady state analysis using a 1:1 binding fitting model. The sensograms shown are double reference subtracted; at least two replicates were injected per cycle, and three independent experiments were performed.

3.6. Molecular Docking

AutoDock tools (ADT) was used for protein and ligand preparation, and binding site prediction was done using Autodock Vina (Trott and Olson 2010). The 3D crystal structure of the extracellular domain of human CLEC-2 (PDB: 2C6U) downloaded from RCSB was used, and the 3D structure of katacine was obtained using Chemdraw software. Visualization and binding site analysis were conducted using PyMOL software.

3.7. Mass Spectrometry

To assess the polymeric nature of katacine, 10 μ M of katacine was resuspended in 200 mM ammonium acetate buffer and then infused into a Q-Exactive HF mass spectrometer (ThermoFisher, CA, USA) via nanoelectrospray ionisation (NSI) using a Triversa NanoMate system

(Advion Biosciences, Ithaca, NY) set at 1.4 kV with 0.30 psi backing pressure. The spectra were collected using a source temperature of 250°C and collision energy of 200 V for desolvation and with the resolution setting at 120 K (approximately 25000 FWHM at m/z 1000). These experiments were performed in collaboration with the Dr Todd Mize at the University of Birmingham.

3.8. Data Analysis

Data are presented as mean \pm standard deviation (SD) of the mean with statistical significance taken as $p < .05$ unless otherwise stated. Statistical analysis was performed using Kruskal-Wallis One-Way ANOVA. All statistical analyses were performed using GraphPad Prism 7 (GraphPad Software Inc. La Jolla, USA). IC50 were also calculated using GraphPad Prism 7.

CHAPTER 4

RESULTS

4. Chapter 4: High throughput screening of small molecule inhibitors of the platelet receptor CLEC-2

4.1. Introduction

High throughput screening (HTS) has classically been used for the identification of small molecule inhibitors (SMI) in the drug discovery workflow, evaluating thousands of compounds in a single assay to identify a potential hit, which will probably lead to chemical modifications until a lead compound is identified. A successful HTS mainly depends on two conditions 1) the assay selection (cell based or biochemical based) and 2) the selection of the chemical library.

Conventional chemical libraries are composed of drug-like compounds. This means that most of these compounds follow five criteria for proper absorption, distribution, metabolism, and excretion of the potential drug, thus predicting bioavailability and security (Lipinski, Lombardo et al. 2001). These parameters are known as Lipinski's rule of five, which states that drug-like compounds must have a molecular weight lower than 500Da, a low hydrophobicity ($\text{LogP} < 5$), no more than five hydrogen bond donors, no more than 10 hydrogen bond acceptors, and fewer than 10 routable bonds.

The main challenge of the HTS is that it could be relatively expensive and frequently, the effect of the small molecule could be a consequence of an off-target effects. However, virtual HTS could help to identify

pre-choose potential ligand based on calculation of binding affinity scores, to prechosen to preselect potential molecules from a determined chemical library.

In this chapter, 60,000 compounds from the EU open-screen chemical library were virtually screened based on the crystallised structures of CLEC-2 (PDB: 3wsr and 2c6u), in collaboration with RNASA-IMEDIR, and further validated them using a platelet-based calcium release assay and platelet aggregometry.

4.2. Aim:

The goal of this chapter is to identify small molecule inhibitors of CLEC-2 with potential to become new drugs with primary application as anti-thrombotic.

4.3. Results

4.3.1. Virtual and cell-based HTS assay to identify potential CLEC-2 inhibitors

The AutoDock Vina algorithm (Trott and Olson 2010) was used to rank the top compounds based on AutoDock's affinity score from the chemical library available in the University of Santiago de Compostela. The top compounds (91 molecules) were then screened using the FLIPR

Calcium 4 assay, a cell-based assay to monitor intracellular calcium flux in real time (**Figure 8**).

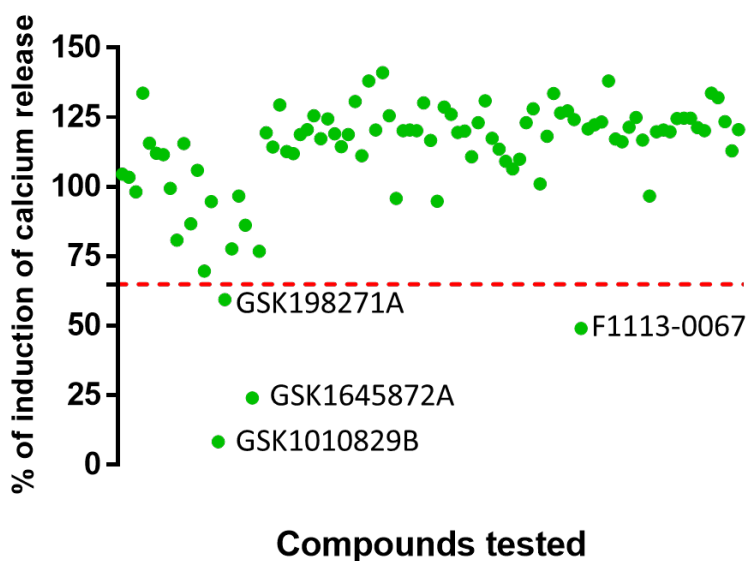


Figure 8. Platelet-based HTS. The scatter plot represents a single-point screening of 91 compounds predicted to bind to CLEC-2 in a virtual HTS. Each compound was dispensed at 10 μM . Four compounds were able to inhibit intracellular calcium release when platelets were stimulated with rhodocytin 100 nM. Each green dot represents the average of three independent experiment for each compound tested; Compounds below the cut-offline (red line) were considered as potential hits based on Zhang's equation.

Four compounds showed a significant inhibition of intracellular calcium release at 10 μM when platelets were stimulated with rhodocytin; three of them were kinase inhibitors GSK198271A $59.49 \pm$

10.2, GSK 16458872A; 24.00 ± 4.7 , GSK1010829B; 8.32 ± 0.1 % calcium release), and the remaining one, F1113-0067 (49.0 ± 4.6 % calcium release) (**Figure 9**), has an unknown biological function. We proceeded to evaluate the effect of F1113-0067 on platelet aggregation, since the other three compounds were not commercially available so we could not test them in further functional experiments.

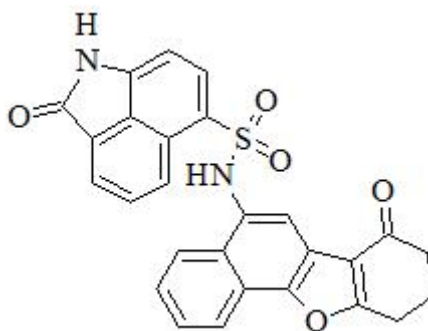


Figure 9. Chemical structure of F1113-0067.

4.3.1.1. Effect of F1113-0067 on platelet aggregation induced by rhodocytin

In the calcium release assay, we observed that platelets stimulated with rhodocytin at 100nM and pre-treated with F1113-0067 10 μ M responded significantly less to rhodocytin compared to platelets pre-treated with DMSO 0.1% only. Therefore, we decided to evaluate if the

compound F1113-0067 was able to prevent platelet aggregation, using a light transmission aggregometry assay.

First, we tested the effects of F1113-0067 at six different concentrations to establish the IC₅₀ of the compound and determine if it was able to prevent platelet aggregation at any of the doses tested. F1113-0067 was able to prevent platelet aggregation induced by rhodocytin in a dose-dependent manner. The dose-response curves model, analysed using GraphPad prism, suggested an IC₅₀ of 8.6 μ M (as shown in **Figure 10**).

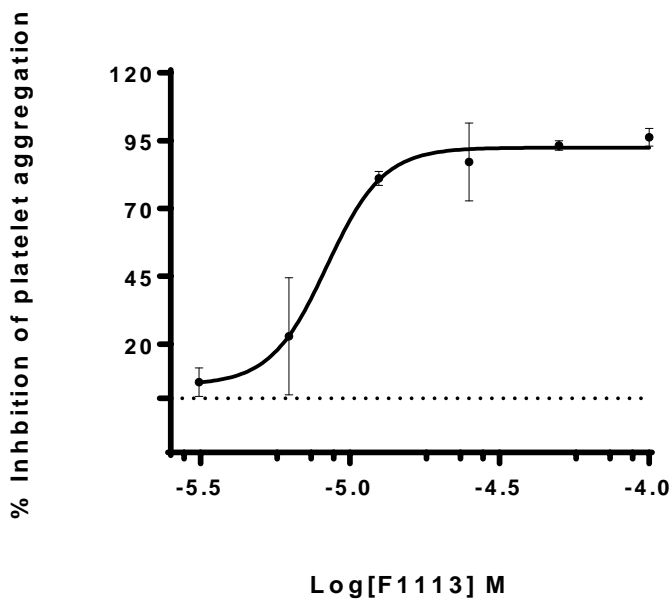


Figure 10. Dose-response curve of platelet aggregation following platelet incubation with F1113-0067 and stimulated with rhodocytin 100nM. Fit curve based on the sigmoidal dose-response model suggested an IC₅₀ of 8.6 μ M for F1113-0067 when platelets are stimulated with 100nM of rhodocytin. GraphPad Prism was used for the analysis of the dose-response curve. The graph shows the mean \pm SD of three independent experiments.

4.3.1.2. Evaluation of the selectivity of F1113-0067 to prevent platelet aggregation

Potential inhibitors must show selectivity for the targeted receptor to prevent off-target effects. Therefore, we decided to test if F1113-0067 was also able to block another ITAM receptor, such as GPVI, or a non-related signalling pathway, as is the case of the GPCR receptors for thrombin, PAR1/4.

Initially, we decided to test if F1113-0067 was able to block platelet aggregation induced by thrombin, and we did not observe any significant effect using 100 to 3.125 μ M, as shown in

. Based on these results, we could assume that F1113 does not interact with any thrombin receptor, or any essential protein related to the PAR-1/4 signalling pathway.

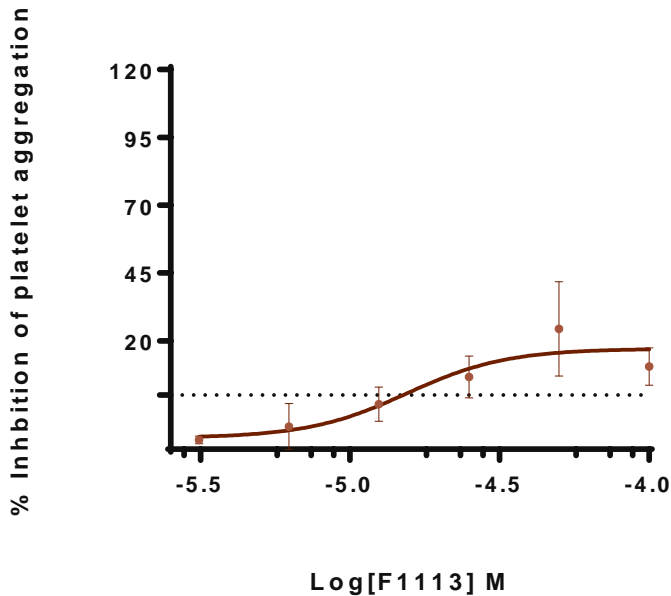


Figure 11. F1113-0067 has no effect on platelet aggregation induced by thrombin in washed platelets. Six different concentrations (100, 50, 25, 12.5, 6.25, and 3.125 μM) were tested to assess the effect of F1113 in platelet aggregation induced by 0.5 U/mL of thrombin. The graph shows the mean \pm SD of three independent experiments.

Then we proceeded to evaluate if F1113-0067 was able to prevent platelet aggregation mediated by a similar signalling pathway, as is the case for the ITAM receptor GPVI. Thus, we evaluated the effect of F1113-0067 at different concentrations, before stimulating platelets with 3 $\mu\text{g}/\text{mL}$ collagen-related peptide (CRP), and a dose-response curve was established (**Figure 12**). We observed that F1113-0067 was

able to block platelet aggregation mediated by GPVI with an IC₅₀ of 10 μ M, suggesting that the effect of F1113-0067 blocking CLEC-2 and GPVI is mediated by a common protein in the signalling pathway, rather than by a direct interaction with the receptor.

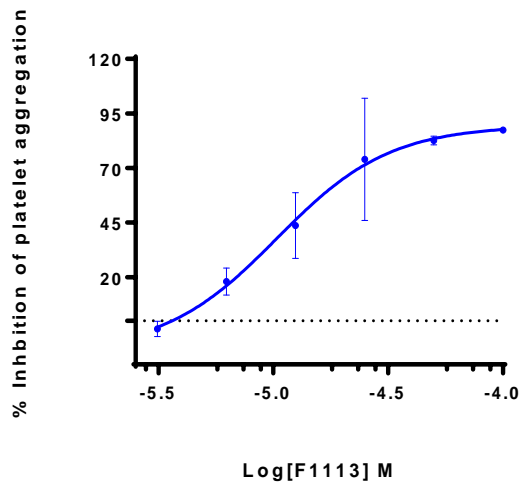


Figure 12. F1113-0067 prevents platelet aggregation mediated by GPVI. Six different concentrations of F1113-0067 (100, 50, 25, 12.5, 6.25, and 3.125 μ M) were tested to prove the effect of F1113-0067 in platelet aggregation induced by 3 μ g/mL of CRP. The fit curve based on the sigmoidal dose-response model suggested an IC₅₀ of 10 μ M. The graph shows the mean \pm SD of three independent experiments.

We further evaluated if a lower dose of F1113-0067 could prevent platelet aggregation with higher selectivity for one of the two ITAM receptors studied. We found that 12.5 μ M F1113-0067 can significantly

prevent platelet aggregation induced by rhodocytin ($81.5 \pm 21.1\%$ of inhibition) compared to controls, whilst platelets stimulated with CRP $3\mu\text{g}/\text{mL}$ showed less inhibition ($38.2 \pm 14.1\%$). The effect of $12.5\mu\text{M}$ of F1113-0067 in platelets treated with thrombin was negligible ($5.75 \pm 1.06\%$ of inhibition), as shown in **Figure 13**.

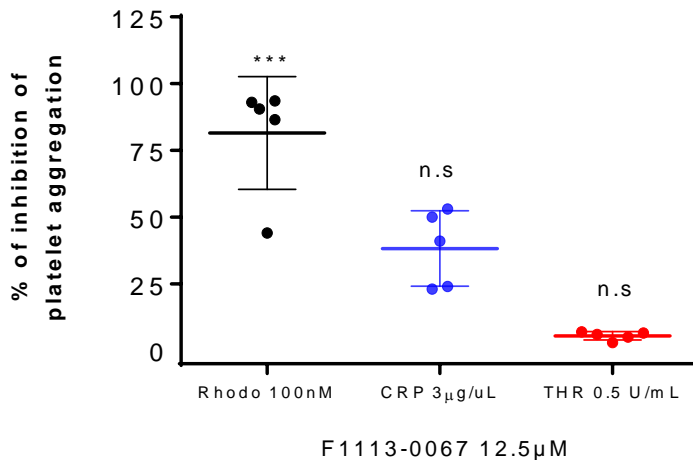


Figure 13. Low doses of F1113-0067 have a higher inhibition on platelet aggregation mediated by rhodocytin compared to GPVI. Washed platelets were preincubated with $12.5\mu\text{M}$ of F1113-0067 for 10 minutes and then stimulated with rhodocytin 100nM , CRP $3\mu\text{g}/\text{mL}$, or thrombin $0.5\text{U}/\text{mL}$. (n.s. = not significant differences; *** $p < 0.0001$; data analysis performed using one-way ANOVA [Kruskal Wallis]; $N=5$).

4.3.1.3. Effect of F1113-0067 on platelet viability

In the development of new pharmacological agents, it is important to understand possible toxicity issues in an early stage of development of a new drug. Therefore, we decided to determine if the concentration used for the *in vitro* studies had any effect on platelet viability. To do so, we incubated platelets with calcein-AM, a marker of viability. Healthy platelets internalise and cleave calcein-AM, which is retained in the cytosol and can be measured by flow cytometry. Platelets were gated according to their size; those untreated with F1113-0067 were considered as a positive control of viability, and platelets treated with 0.5% of DMSO were used as a basal condition. We tested the effect of 12.5 μ M and 25 μ M of F1113-0067 but did not observe significant differences in platelet viability at 12.5 μ M concentrations (81.1 ± 10.4 %) compared with the DMSO control ($89.6\% \pm 9.1$). However, the higher concentration of F1113-0067 tested did reduce platelet viability ($66.2 \pm 14.3\%$; **Figure 14**). Therefore, we used the lower concentration for the rest of our experiments, since 12.5 μ M is enough to prevent platelet aggregation induced by rhodocytin and does not significantly alter platelet viability.

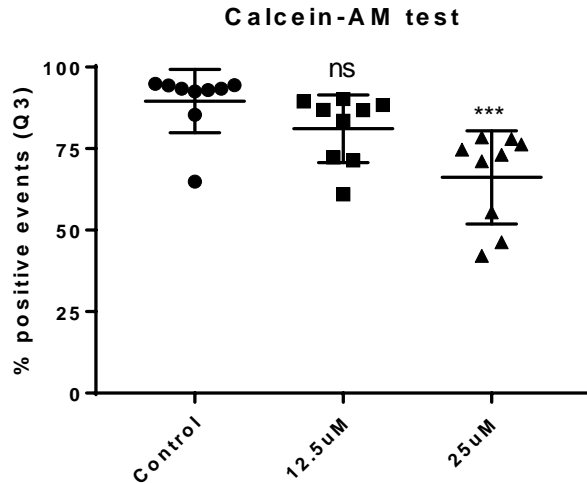


Figure 14. F1113-0067 does not affect platelet viability at 12.5 μ M, but higher concentrations reduce viability. Washed platelets were preincubated with 12.5 or 25 μ M of F1113-0067 for 10 minutes and then incubated with calcein-AM. Analyses were by flow cytometry, gating platelets by their size and MFI values on FL-1. (n.s. = not significant differences; *** $p < 0.0001$; data analysis using one-way ANOVA [Kruskal Wallis] in GraphPad Prism; N = 9).

4.3.1.4. Effect of F1113-0067 on tyrosine phosphorylation mediated by ITAM receptors

To explore in more detail the effects of F1113-0067 on platelet activation, we evaluated the role of F1113-0067 in preventing platelet phosphorylation on platelets treated with rhodocytin 100nM, or CRP 3 μ g/mL.

In concordance with the data observed in platelet aggregation, we found that 12.5 μ M of F1113-0067 significantly decreases the protein tyrosine

phosphorylation profile in platelets treated with rhodocytin, in a similar way to platelets treated with the vehicle control (DMSO 0.1%). A similar decrease was also observed on Syk and PLC γ phosphorylation levels (**Figure 15**)

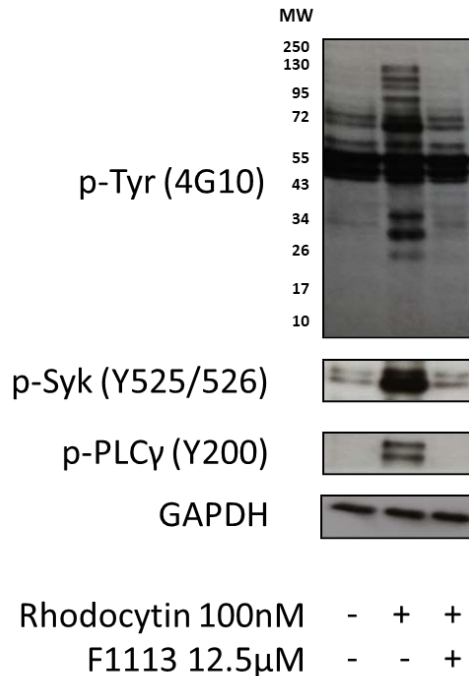


Figure 15. Effect of F1113-0067 on platelet signalling induced by rhodocytin. Human washed platelets at 4×10^8 cells/ml were pre-treated with F1113-0067 (12.5 μ M) and stimulated with rhodocytin (100nM). The first lane shows resting platelets treated with DMSO 0.1%, the second lane shows platelets preincubated with DMSO 0.1% and stimulated with 100nM rhodocytin, the third lane shows platelet preincubated with F1113-0067 and 100nM rhodocytin. This figure shows a representative western blot of four different experiments. p-Tyr; phosphorylated tyrosine profile; p-Syk (Y525/526): phosphorylated Syk in the tyrosine residues 525 and 526; pPLC γ (Y200): phosphorylated PLC γ in the tyrosine 200; GAPDH: Loading control.

Conversely, platelets treated with F1113-0067 at 12.5 μ M and stimulated with CRP did not show a significant decrease in the global tyrosine, Syk or PLC- γ phosphorylation levels (**Figure 16**).

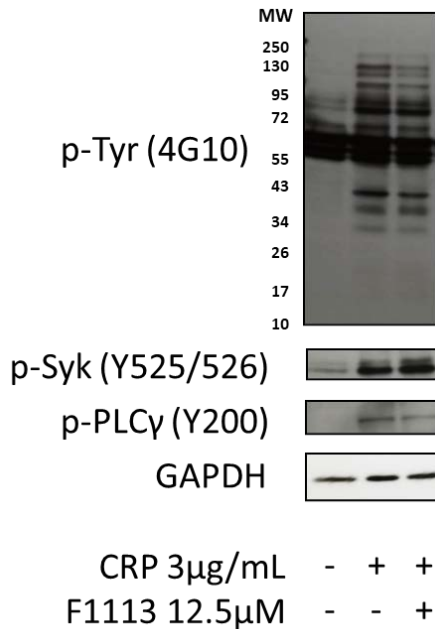


Figure 16. Effect of F1113-0067 on platelet signalling induced by CRP. Washed platelets at 4x10⁸ cells/ml under non-aggregating conditions (9 μ M of Eptifibatide) were pre-treated with F1113-0067 (12.5 μ M) and stimulated with CRP (3 μ g/mL). The first lane shows resting platelets treated with 0.1% DMSO, the second lane shows platelets preincubated with the 0.1% DMSO and treated with CRP, the third lane shows platelet preincubated with F1113-0067 and stimulated with CRP. This figure shows a representative western blot of four different experiments. p-Tyr: phosphorylated tyrosine profile; p-Syk (Y525/526): phosphorylated Syk in the tyrosine residues 525 and 526; pPLC γ (Y200): phosphorylated PLC γ in the tyrosine 200; GAPDH: Loading control.

4.4. Discussion

In this chapter it was observed that F1113-0067 prevents platelet aggregation mediated by CLEC-2 and GPVI. We predicted that the effect of F1113-0067 on platelet aggregation induced by ITAM receptor activation may be mediated by the inhibition of common signalling pathways, between both CLEC-2 and GPVI receptors, due to the lack of selectivity between the receptors.

F1113-0067 prevents platelet aggregation more effectively when induced by rhodocytin, compared to induction by CRP. This trend could be mediated by an effect on the release of secondary mediators (ADP and thromboxane A₂). It has been well established that the CLEC-2 signalling pathway is more dependent on secondary mediators than GPVI; therefore, any inhibitor impacting secondary mediators may have a stronger effect on platelet aggregation mediated by CLEC-2. Further research is needed to fully understand where F1113-0067 is playing a role and its biological impact on human platelets.

F1113-0067 is a benzosulphonamide which obeys the Lipinski's rule of having a molecular weight inferior of 500Da (482.517 g/mol), and a logP of 5.625. Meaning that this molecule is likely to cross membrane and have an intracellular effect rather than preventing the ligand and receptor interaction. Despite of our early observations using the virtual screening, where was suggested that F1113-0067 was likely to bind to the CLEC-2 surface based on the in silico docking assay.

The biological role of F1113-0067 is unknown, however, another benzosulfonamide, namely F1113-0789 has been reported to target the signal transducer and activator of transcription 3 (STAT3) (Redell, Ruiz et al. 2011), which is phosphorylated on platelets activated with collagen (Zhou, Gushiken et al. 2010) or rhodocytin (Izquierdo, Barrachina et al. 2020). However, it is unknown if F1113-0067 is also able to target STAT3. Besides of the lack of selectivity of F1113-0067, the low affinity and potential toxicity in higher doses may indicate that this molecule may not be a suitable choice for a future drug candidate. It was also observed that 3 kinase inhibitors also prevent calcium release however further was not carried out, since they were not commercially available. Furthermore, low selectivity is expected.

This chapter reflects the challenges on the development of potent and selective inhibitors of PPI such as CLEC-2 using a cell-based assay and a drug-like compounds-based chemical library, suggesting the need to explore chemical libraries with higher molecular diversity and the use of biochemical assays rather than cell-based models, in order to identify more selective compounds. To address the above challenges, we decided to follow a different approach based on an inhibition of the interaction amongst the endogenous ligand, podoplanin, and the human CLEC-2 receptor to identify a more promising small molecule ligand.

CHAPTER 5

RESULTS

5. Chapter 5: Biochemical-based HTS for the identification of a novel CLEC-2 ligand

5.1. Introduction

CLEC-2 is the receptor for the glycopeptide podoplanin and is activated by multivalent protein interactions. For decades, protein-protein interactions (PPIs) were considered undruggable targets using traditional drug discovery approaches, based on small molecules. Nowadays, PPIs remain as one of the most challenging interactions to be disrupted using small molecule inhibitors (SMI)(Lu, Zhou et al. 2020). The challenging of targeting PPIs is because the binding interface of the receptor are large and planar surfaces, which allows the multiple interactions. Therefore, it is difficult for a small molecule to match and fit in such a unique and large surface (Buchwald 2010).

However, targeting a PPI is still possible but the small molecule must follow one of the next mechanisms:

- 1) Binding to a hot-spot on the receptor binding surface: these are regions of several amino acid on the binding surface that play a critical role on the PPI (Moreira, Fernandes et al. 2007).
- 2) Binding to an allosteric pocket: These are regions outside of the ligand binding site of the receptor, that could induce conformational changes and prevent agonist binding (Cossins and Lawson 2015).

The development of SMI could be overcome using HTS approaches by carefully considering the inhibitor design process and performing large library screens. For instances, the first criterion to be considered for the investigation of new inhibitors against protein-receptor interaction is to select a proper chemical library with larger compounds (>500 Da) and hydrophobic properties, as is the case of molecules derived from natural compounds, or libraries with higher chemical complexity (Pagliaro, Felding et al. 2004), including substances such as macrocycles, or coordination compounds (Damaskinaki, Moran et al. 2021).

To identify novel molecules able to interrupt podoplanin-CLEC-2 interaction, we needed to set up a robust biochemical assay suitable for further miniaturisation. In this case, the amplified luminescent proximity homogeneous assay (ALPHA) screen technology was chosen. A schematic representation of the assay is shown in **Figure 17**.

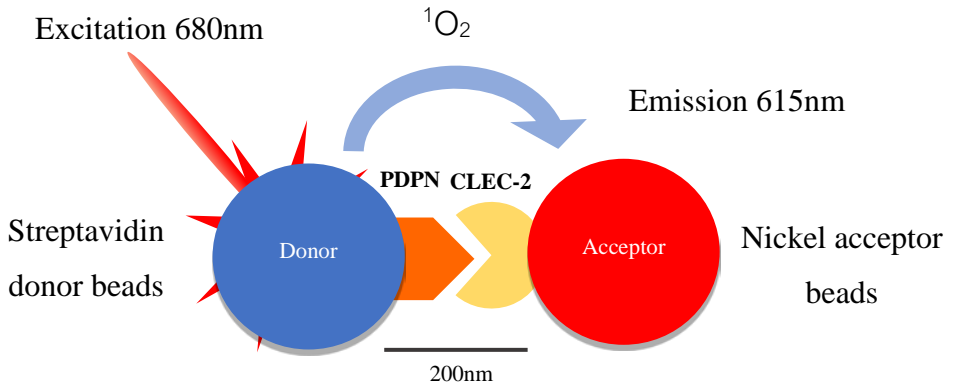


Figure 17. Schematic representation of an ALPHA screen assay based on podoplanin and CLEC-2 interaction. ALPHA screen assay is based on the proximity of the donor and acceptor beads mediated by protein-protein interactions (PPIs). After laser excitation, podoplanin-conjugated donor beads transform ambient oxygen into singlet oxygen, which is absorbed by CLEC-2-conjugated nickel acceptor beads. Then an ALPHA signal is emitted and detected by the plate reader.

ALPHA screen technology is a biochemical assay based on the donor and acceptor beads' proximity, around 200nm, which is mediated by ligand-receptor interaction (Eglen, Reisine et al. 2008). The main advantage of this assay compared with other biochemical assays, such as an Enzyme Linked Immunoassay (ELISA), is that it is homogenous and does not require any additional washing steps with the risk of losing material. It is relatively straightforward to optimise; however, its optimisation still has some intrinsic challenges. For instance, ALPHA screen assays are known for showing a hook effect. Therefore, an

inappropriate concentration of ligand and receptor would result in a reduction of the signal, affecting the signal-to-noise ratio, and the robustness of the assay would not be suitable for a miniaturised single-spot assay.

The first step is to identify the type of donor and acceptor beads' coating combination required for the assay. The coating of the beads is based on affinity properties, and the coating required is based on the tags of the recombinant proteins to be used

The identification of small-molecule ligands of CLEC-2 may lead to a better understanding of its mechanism of activation. It may also uncover potential allosteric binding sites for CLEC-2 and act as an intermediate for the development of further antagonists with higher potency.

5.2. Aim

The aim of this chapter was to identify potential new small molecule ligands for human CLEC-2.

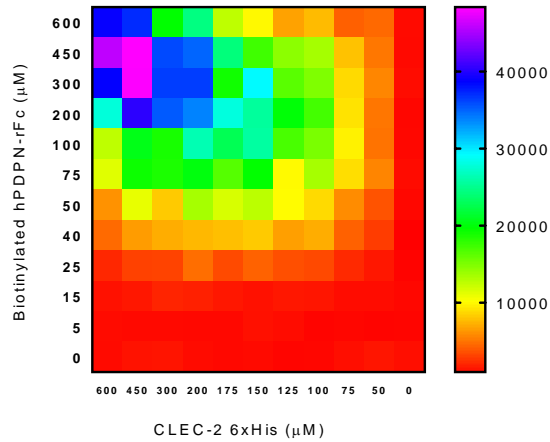
5.3. Results

5.3.1. Setting-up a podoplanin-CLEC-2 interaction assay based on ALPHA screen

To identify the appropriate podoplanin and CLEC-2 concentration for the assay, we evaluated different concentrations in the nanomolar range for each protein, as showed in the heat map (**Figure 18**), where red colour indicates low or background signal and blue and purple shows higher signal. An initial matrix with a wide range of concentrations was used to evaluate the optimal concentration range (**Figure 18A**), and second and smaller matrix was used to define the optimal concentration for the screening (**Figure 18B**). The optimal signal-to-noise ratio was observed using 100nM of h-podoplanin and 125nM of CLEC-2.

We also demonstrated that rhodocytin at 100nM is a potent disruptor of the podoplanin-CLEC-2 interaction, and it was used as a positive control of the assay (Appendix I).

A



B

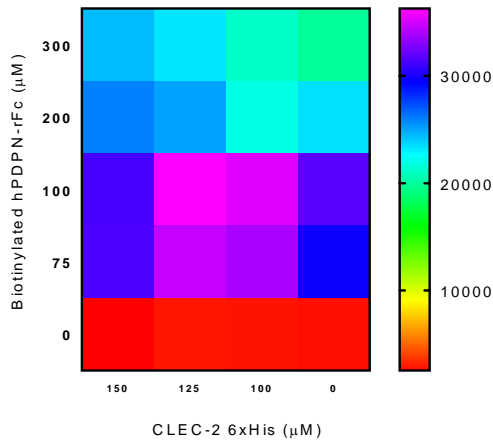


Figure 18. Matrix of different CLEC-2 and podoplanin concentrations. We tested different concentrations of CLEC-2 and podoplanin to identify a range with higher signals for the screening. Heatmap shows arbitrary units of ALPHA signal, purple colour represents maximal binding, and red low or no protein binding A) represents an initial matrix with a broad range of concentration for both proteins; B) represents a second and more defined range of concentrations. The set of concentrations with higher ALPHA signals was used for further optimisation of the screen.

5.3.1.1. HTS based on ALPHA screen assay

5016 compounds were tested in the ALPHA screen assay. A high signal indicates an interaction between podoplanin and CLEC-2. Agents able to significantly decrease the ALPHA signal, based on the equation $(X - 2SD)$, were considered as a potential disruptor.

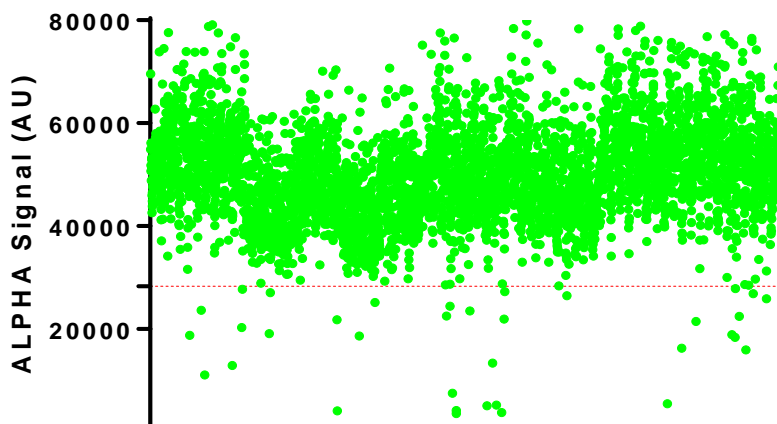


Figure 19. Scatter plot showing the effect of each compound on the ALPHA signal values emitted by a CLEC-2-podoplanin interaction. Dots below the cut off (red line) represent compounds that significantly decreased the signal, these are considered potential hits. The scatter plot shows data from a single point HTS.

In this assay, we identified 40 compounds from the EU open-screen chemical library which were able to interrupt the interaction between podoplanin and CLEC-2 in the first screening (**Figure 19**). However, biochemical assays, such as ALPHA screen, can be altered by false positive agents which can be detected using the TruHits Kit® designed by Perkin Elmer. Using the TruHits assay, we identified 17 potential hits, as it is shown in the **Figure 20** (blue dots).

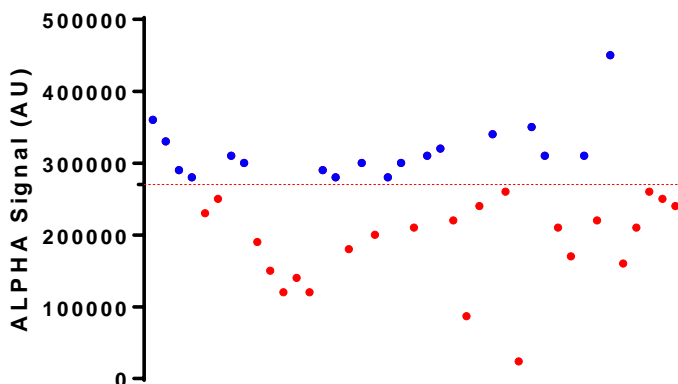


Figure 20. Scatter plot showing TruHits® assay to identify potential false positive compounds on the screening. Blue dots over the cut-off indicate potential hits and red dots below indicate false positive compounds. The scatter plot was shows data from a single point assay.

We continued to categorise the possible candidate compounds by their potency after identifying the false positive compounds. To do so, we assessed different concentrations of the compounds on our ALPHA screen platform. The two most powerful compounds, sennoside A (IC₅₀ 1.3 μ M; **Figure 21i**) and katacine (IC₅₀ 2.7 μ M; **Figure 21ii**), were chosen for functional tests utilising light transmission aggregometry (LTA). The remaining, less powerful chemicals (**Figure 21iii–vi**) were not tested. The list of compounds and IC₅₀ is shown in Table 66. The dose responses corresponding to the other 11 compounds are found in the appendix II.

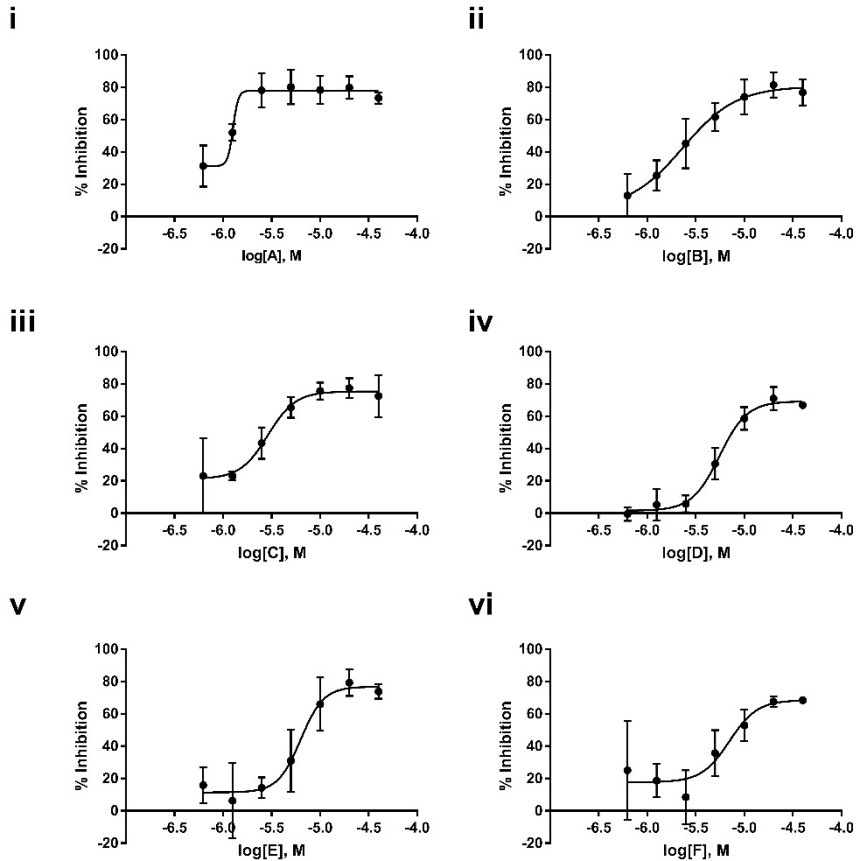


Figure 21. Dose-response curves of potential hits and IC50 of six potential compounds. Graphs show the percentage inhibition of the ALPHA screen signal by incubation with six different compounds tested (A-F). The graphs represent the mean value and SD of three different experiments (n=3). Concentration is represented in log scale.

Table 6. List of potential hits identified on ALPHA screen. Detailed information of top compounds identified during ALPHA screening as a disruptor of CLEC-2- podoplanin interaction and ranked according to their potency showed on the concentration-response curves. Molecular weight (MW), half maximal inhibitory concentration (IC50) and Simplified Molecular Input Line Entry System (SMILE) identifier are shown for each compound.

Label	Name	MW	IC50 (μM)	SMILE CODE
A	Sennoside A	862.74	1.3	<chem>OC[C@H]([C@H]([C@@H]([C@H]1O)O)O)O[C@@H]1Oc1cccc([C@@H]([C@@H](c2cccc(O[C@H]([C@@H]([C@H]3O)O)O[C@H](CO)[C@H]3O)c22)c3cc(C(O)=O)cc(O)c3C2=O)c2c3c(O)cc(C(O)=O)c2)c1C3=O</chem>
B	Katacine	914.77	2.7	<chem>O[C@H]1[C@@H](c(cc2O)cc(O)c2O)Oc2c([C@H]([C@H]3O)c(c(O)cc(O)c4[C@H]([C@H]5O)c(c(O)cc(O)c6)c6O[C@@H]5c(cc5O)c(O)c5O)c4O[C@@H]3c(cc3O)cc(O)c3O)c(O)cc(O)c2C1</chem>

C	4-[[4-(pyridin-2-yl)-1,3-thiazol-2-yl]aminophenol	269.32	2.9	<chem>Oc(cc1)ccc1Nc1nc(-c2ncccc2)cs1</chem>
D	6-dipyridin-2-ylpyrimidin-4-amine	357.41	5.3	<chem>C(CNc1cc(-c2ncccc2)nc(-c2ncccc2)n1)Cn1cncc1</chem>
E	N-allyl-6-phenyl-2-pyridin-2-ylpyrimidin-4-amine	288.35	6.3	<chem>C=CCNc1cc(-c2cccc2)nc(-c2ncccc2)n1</chem>
F	N'-[(E)-(3-ethoxy-2-hydroxyphenyl)methylidene]pyridine-2-carbohydrazide	285.30	6.7	<chem>CCOc1cccc(/C=N/NC(=O)c1O</chem>

5.3.1.2. Identification of katechin as a CLEC-2 ligand by HTS

Based on the above results, we proceeded to test the two most promising compounds based on their IC₅₀ on the ALPHA screen. First, we started testing the most potent compound identified, sennoside A (a well-known herbal laxative), at concentrations of 10 and 30 μ M. Results indicated that it has no effect on platelet aggregation or preventing platelet aggregation induced by rhodocytin 100 nM (data not shown). However, when we tested katechin at 30 or 10 μ M, we found that it induced a quick and full platelet aggregation response (Figure 22). At lower concentrations of katechin tested (5, 1, and 0.1 μ M) no platelet response was observed. Therefore, platelet aggregation induced by katechin followed an all-or-none response mechanism.

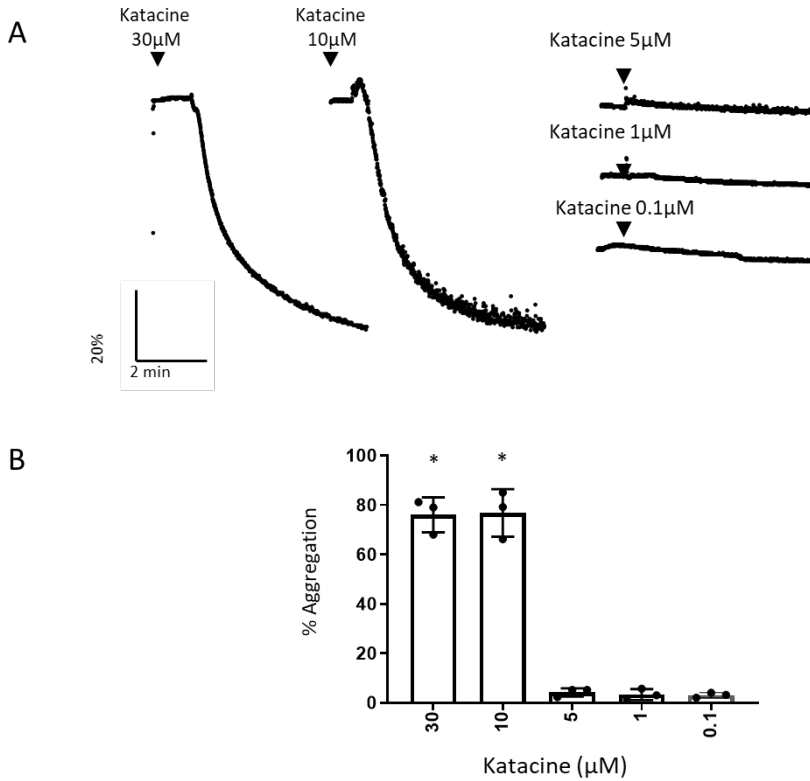


Figure 22. Katakine can induce platelet aggregation in an all-or none response mechanism. A) Representative traces of washed platelets (2×10^8 platelets/mL) stimulated by different doses of katakine (0.1-10 μ M) and B) The mean \pm SD of three independent experiments. Kruskal-Wallis One-Way ANOVA test was used to evaluate significant differences between the treatment in relation with the control, * represent significance differences ($p < 0.05$).

5.3.1.3. Platelet aggregation induced by katacine is Syk- and Src-dependent and mediated by CLEC-2 activation

CLEC-2, like other ITAM receptors, depends on Syk and Src phosphorylation to activate downstream signalling and further platelet aggregation; therefore, to investigate if these kinases were also required to induce platelet aggregation, we pre-treated platelets with the Syk inhibitor PRT-060318 (1 μ M) and Src inhibitor PP2 (20 μ M) before stimulated with 10 μ M katacine. Both inhibitors completely blocked platelet aggregation induced by katacine (**Figure 23**). These results clearly suggest that platelet aggregation induced by katacine is dependent on Syk and Src, indicating that this aggregation could be initiated by any receptor dependent on these kinases, such as CLEC-2 or GPVI.

To confirm that CLEC-2 is involved in platelet aggregation induced by katacine, we incubated platelets with the anti-CLEC-2 monoclonal antibody fragment, AYP1 F(ab)'₂ (10 μ g/ml), to block CLEC-2 with a high degree of selectivity. We observed that platelet aggregation was partially reduced to 28.3% \pm 2.6, demonstrating that activation is partially mediated by CLEC-2 (**Figure 23**).

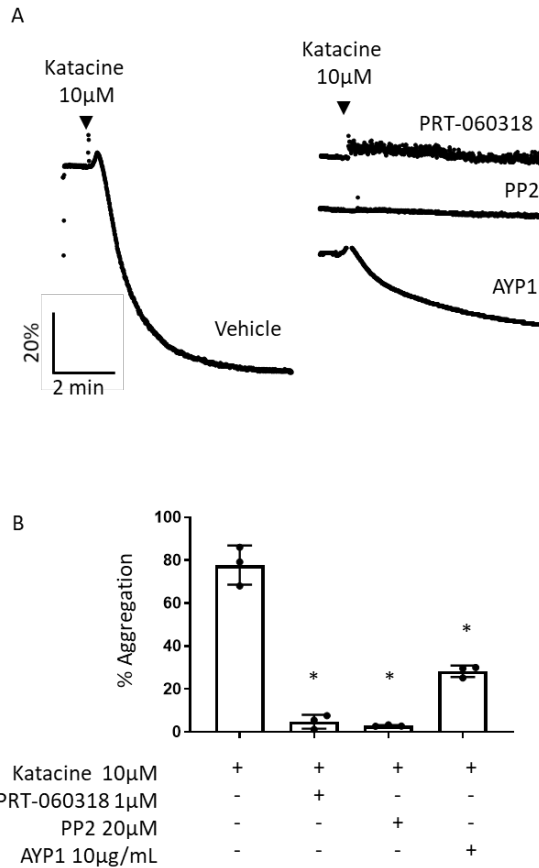


Figure 23. Platelet aggregation induced by katasine is Syk- and Src-dependent and mediated by CLEC-2 receptor. A) Representative traces of washed platelets (2×10^8 platelets/mL) stimulated with $10 \mu\text{M}$ of katasine and pre-treated with 0.1 % DMSO, the Syk inhibitor, PRT-060318 ($1 \mu\text{M}$); The Src inhibitor, PP2 ($20 \mu\text{M}$), or the anti-CLEC-2 antibody AYP1 F(ab)'2 ($10 \mu\text{g/mL}$). B) The mean and standard deviation (SD) of three independent experiments. Kruskal-Wallis One-Way ANOVA test was used to evaluate significant differences between the treatment in relation with the control, * represent significance differences where $p < 0.05$.

5.3.1.4. **Katacine induces phosphorylation of CLEC-2 and key signalling proteins in the CLEC-2 signalling pathway**

To assess the effect of katacine on CLEC-2 signalling activation, we evaluated its impact on the global protein tyrosine phosphorylation profile. We observed that platelets activated with katacine showed a comparable profile to platelets stimulated with rhodocytin at 100nM, as shown in **Figure 24A**.

Moreover, we used phospho-specific antibodies against tyrosine phosphorylated Syk on the residues Y525/526 and observed an increase in phosphorylation levels (4.5 ± 0.9 fold), compared to platelets treated with the vehicle. This result is comparable to the phosphorylation levels observed in platelets activated with rhodocytin at 100nM (4.5 ± 1.0 fold; **Figure 24B**). In addition, we evaluated the effect of katacine on the tyrosine phosphorylation levels on LAT (Y200) and observed an increase of 18.8 ± 5.9 fold when treated with katacine at 10 μ M, compared to the vehicle condition. Platelets treated with rhodocytin also showed an increase in LAT Y200 phosphorylation (41.5 ± 4.5 fold).

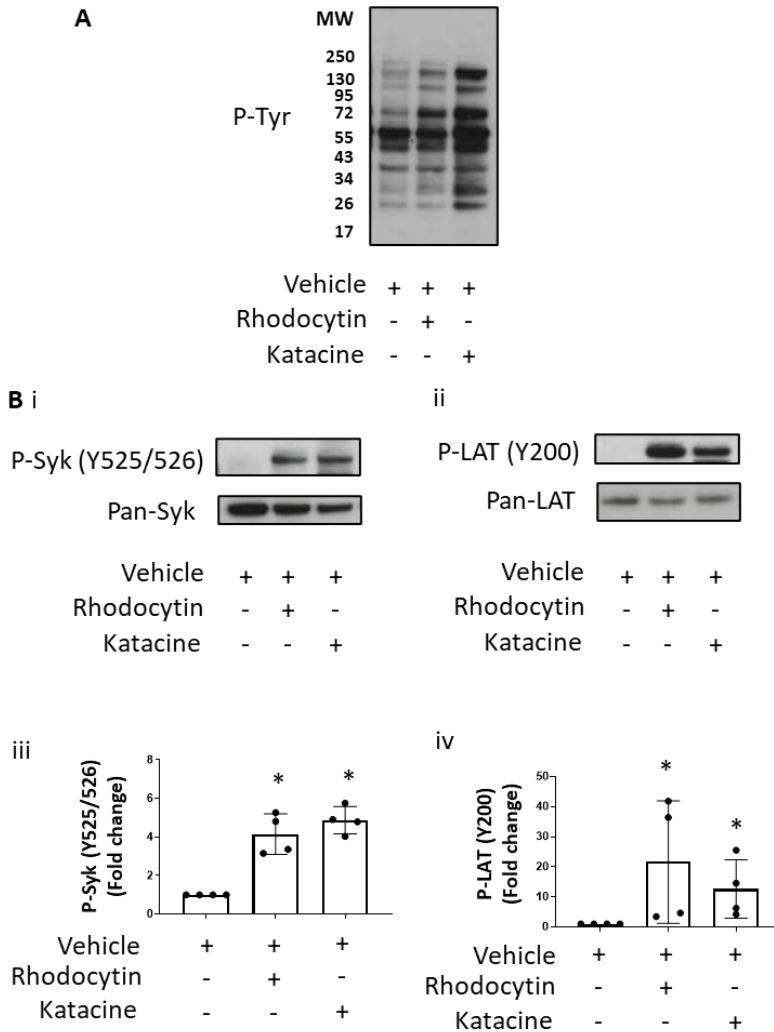


Figure 24. Katakine increases tyrosine phosphorylation levels of Syk, LAT, and global protein tyrosine phosphorylation profiles. A) Representative western blot against 4G10 antibody. B) representative blot against p-Syk/Syk (i) and p-LAT/LAT(ii). Mean and SD of three independent experiments quantitated using image J are represented in (iii) and (iv). Kruskal-Wallis One-Way ANOVA test was used to evaluate significant differences between the treatment in relation with the control, * represents significance difference where $p < 0.05$, as stated.

5.3.1.5. Katakine increased tyrosine phosphorylation levels of CLEC-2

As proof of a direct interaction between katakine and human platelets, we immunoprecipitated CLEC-2 and probed it against 4G10 to evaluate the impact of katakine on CLEC-2 phosphorylation levels. We demonstrated that katakine caused a marked increase in CLEC-2 tyrosine phosphorylation levels (6.6 ± 4.6 fold), relative to platelets treated with the vehicle. A similar result was observed in platelets treated with rhodocytin (6.1 ± 4.6 fold) (**Figure 25**).

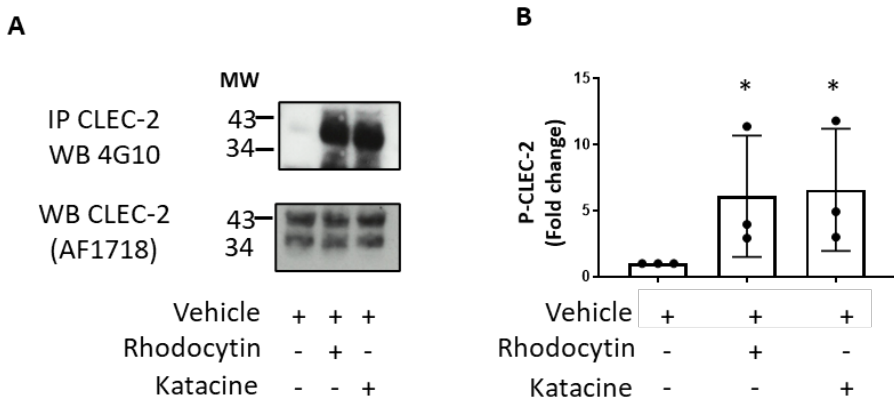


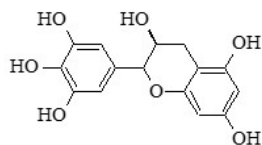
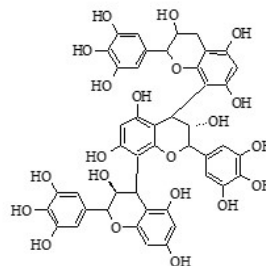
Figure 25. Katakine increases CLEC-2 tyrosine phosphorylation levels. A) CLEC-2 tyrosine phosphorylation levels in platelets stimulated with rhodocytin 100 nM or katakine 10 μ M compared with the DMSO 0.1% control. (B) shows the mean \pm SD values from three independent experiments. A Kruskal-Wallis one-way ANOVA test was used to evaluate significant differences between the treatment in relation to the control. (* represents significance difference where $p < 0.05$, as stated.)

5.3.1.6. Katakine structure

It is not fully understood how katakine induces platelet aggregation through CLEC-2, but it is known that clustering is required for CLEC-2 activation. Proanthocyanidins, such as katakine, are known to polymerise, which may explain why katakine is an agonist rather than an antagonist, as expected for a monomeric ligand.

Therefore, we decided to analyse katakine by mass spectrometry to confirm the polymeric nature of the ligand. First, we estimated the monomeric structure for a proanthocyanidin, which corresponds to flavan-3-ol ($C_{15}H_{14}O_7$) and has a mass of 306 Da. This was considered as the basic unit of katakine. Based on this criterion, we calculated the expected mass of oligomers of katakine, as shown in table 7.

Table 7. Molecular weight and size of the oligomer of katakine calculated based on flavan-3-ol. A) Molecular structures of i) the monomeric flavan-3-ol and ii) its trimer (katakine). B) Table to show different theoretical order of oligomerisation that can be formed from flavan-3-ol (monomer) and their calculated formula and molecular weight. Formula of each polymer was calculated using the equation showed in (A)

A i C₁₅ H₁₄ O₇ (X₁)ii C₄₅ H₃₈ O₂₁ (X₃)

Polymer is $X^*n - (2n-2)^*(H)$

B

Formula	Order of oligomerisation	Molecular weight (Da)
C ₁₅ H ₁₄ O ₇	X ₁	306.0739
C ₃₀ H ₂₆ O ₁₄	X ₂	610.1322
C ₄₅ H ₃₈ O ₂₁	X ₃	914.1905
C ₆₀ H ₅₀ O ₂₈	X ₄	1218.2488
C ₇₅ H ₆₂ O ₃₅	X ₅	1522.3070
C ₉₀ H ₇₄ O ₄₂	X ₆	1826.3654
C ₁₀₅ H ₈₆ O ₄₉	X ₇	2130.4236
C ₁₂₀ H ₉₈ O ₅₆	X ₈	2434.4819
C ₁₃₅ H ₁₁₀ O ₆₃	X ₉	2738.5400
C ₁₅₀ H ₁₂₂ O ₇₀	X ₁₀	3042.5984
C ₁₆₅ H ₁₃₄ O ₇₇	X ₁₁	3346.6567
C ₁₈₀ H ₁₅₆ O ₈₄	X ₁₂	3660.7932

Using mass spectrometry, we identified the minimum size of katacine as a trimer (~914 Da) (**Figure 26A**). We also identified the presence of tetramers (~1218Da), pentamers (~1522Da), hexamers (~1826Da), and a higher order of oligomerisation up to dodecamers (~3660 Da) (**Figure 26A**).

Furthermore, we discovered that katacine trimers and hexamers are sodiated and potassiated in mass spectra (**Figure 26B–E**), implying that medium-sized oligomeric entities are polar. This could indicate that the negative charge of katacine is essential for interaction with the positively charged extracellular CLEC-2 domain.

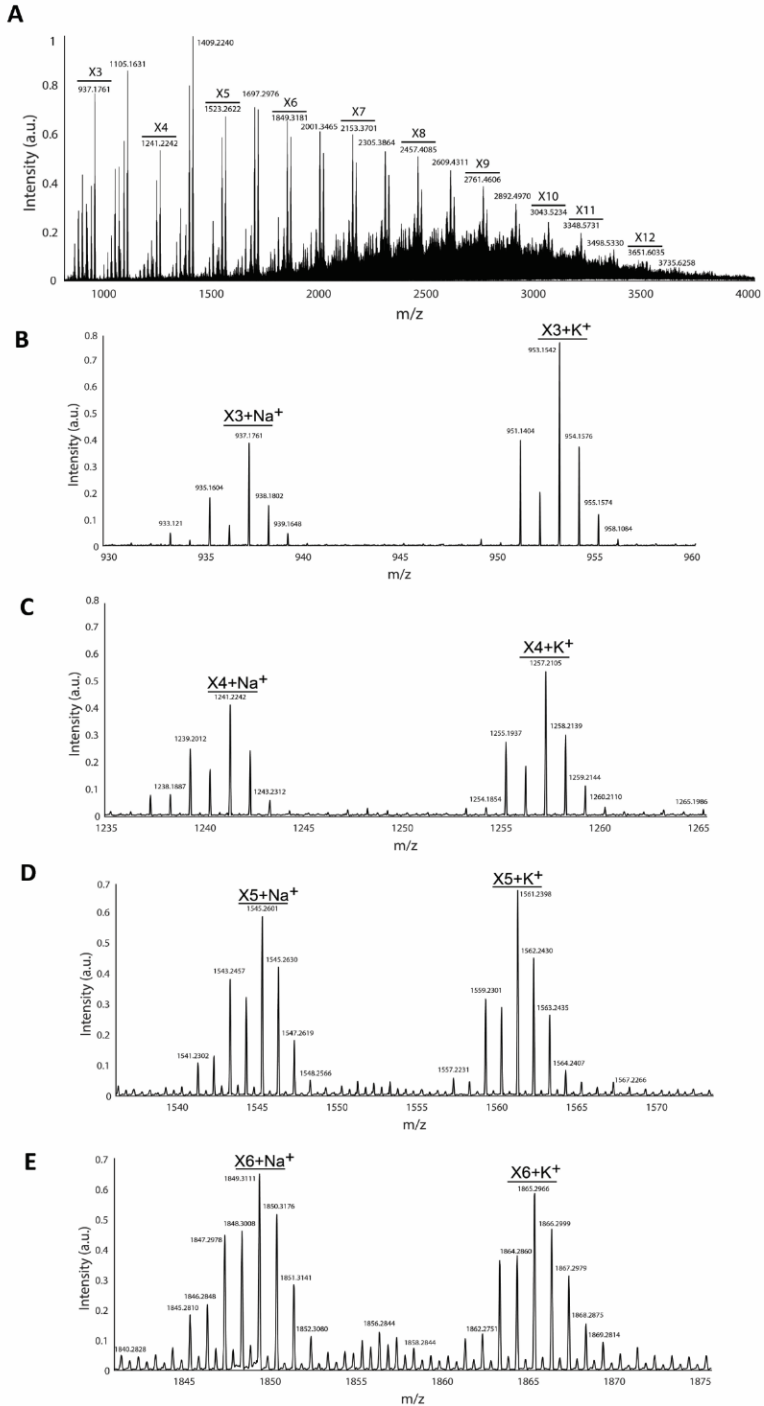


Figure 26. Mass spectra of katanine confirm that it is a mixture of oligomers with different sizes and has a polar nature, with possible implications on CLEC-2 binding. 10 μM of katanine resuspended in 200 mM ammonium acetate was injected into an HPLC for separation and electrosprayed into an Orbitrap mass spectrometer in Intact protein mode for mass spectrometry analysis. (A) represents the global mass spectra of katanine; X1-X12 indicates the size of the polymer of katanine. A decrease in the intensity of the signal is observed with the size of the polymer. The size of the oligomers was calculated based on the monomeric structure of flavan-3-ol. (B-E) represent the zoom in peaks belonging to trimers (B), tetramers (C), pentamers (D), and hexamers (E) in their sodiated and potassiated forms. m/z indicates the mass of the species. X(n) indicates the size of the oligomer (X3: Trimers; X4: Tetramers, X5: Pentamers, etc.); sodiated and potassiated oligomers are indicated by $+\text{Na}^+$ and $+\text{K}^+$, respectively.

5.3.1.7. Molecular docking studies predict katanine binds to the same CLEC-2 binding site as podoplanin

We applied the AutoDock Vina algorithm for the binding site prediction of katanine. Our in-silico analysis suggested that katanine may bind to Arg-117, Arg-118, Arg-152, and Arg-157 on the extracellular domain of CLEC-2, as is the case for rhodocytin and podoplanin with an affinity of -6.6Kcal/mol , according to the AutoDock Vina score (Figure 27).

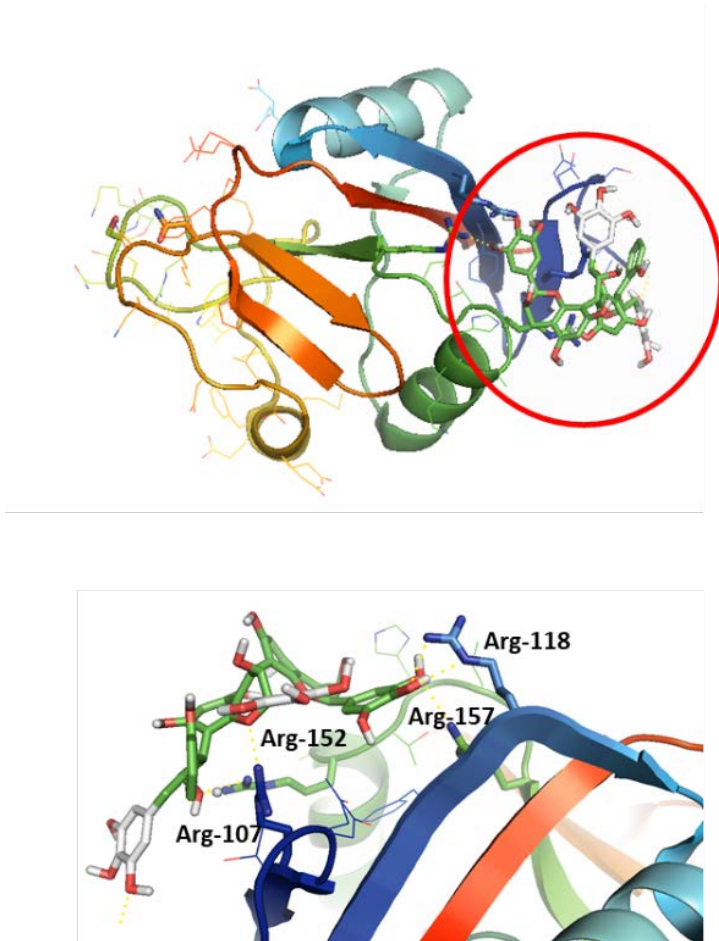


Figure 27. Molecular docking prediction of the katacine binding site for CLEC-2. Molecular docking has been conducted using AutoDock Vina and ADT for protein preparation. Grid boxes for the binding prediction covered the extracellular domain of CLEC-2, using the crystal structure of human CLEC-2 (PDB: 2C6U). A) Katacine can bind to a positive charge surface rich in arginine in the CLEC-2 extracellular domain (Arg-107, Arg-118, Arg-152, Arg-157). The binding site for podoplanin and rhodocytin is enclosed in the red circle.

We also extended our research to other sites of the extracellular domains of CLEC-2, and the algorithm suggests a possible allosteric binding site of CLEC-2 on the opposite face of the canonical CLEC-2 binding site with an estimated affinity of -6.9 kcal/mol (Figure 28).

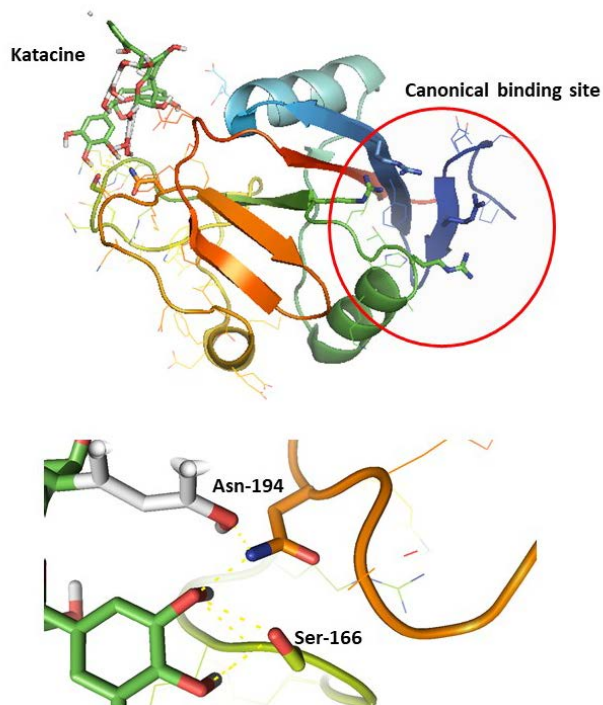


Figure 28. Katakine may bind to an allosteric binding site on CLEC-2. Molecular docking indicated an additional highly scored binding site on CLEC-2 for katacine interaction on the opposite site of the canonical binding site reported for other ligands (enclosed in a red circle). AutoDock Vina predicted a binding for katacine binding on Ser-166 and Asn-194.

5.4. Discussion

For the identification of small molecule ligands of CLEC-2, we used an ALPHA screening high-throughput assay, based on ligand-receptor interaction.

The main advantage of this technology is that it is a strong tool to identify agents with potential effects for interrupting podoplanin and CLEC-2 interaction. However, the probability of identifying false hits is high since many chemical agents can interrupt the ALPHA screen signal without having an interaction with the targeted receptor. Nevertheless, this limitation can be easily overcome using tools such as the AlphaScreen TruHits kit to identify potential false positives, such as singlet oxygen quenchers, as is the case with compounds containing transition metals such as Fe^{+3} , Fe^{+2} , Zn^{+2} , or Cu^{+2} . Biotin mimetics, colour quenchers (compounds absorbing energy at the wavelength as the donor or acceptor beads), and insoluble compounds (light scatterers) are also common false positives that can be identified by the AlphaScreen TruHits kit.

Another important limitation of the biochemical-based approach is that despite showing a direct interaction with the receptor, biochemical-based assays are unable to predict the effect of the potential ligand in functional assays. Therefore, it was crucial that potential hits were validated in platelet functional assays.

In line with the approaches described above, the experiments carried out in this thesis were designed to identify new ligands for CLEC-2. In our first set of experiments, we found a small molecule able to prevent platelet aggregation and calcium release induced by rhodocytin, but it also blocked platelet aggregation in platelets treated with the GPVI specific agonist, CRP. The compound F1113 potentially prevents platelet aggregation through an intracellular signalling event, common between both receptors. Nonetheless, global proteomic studies are needed to identify where F1113 is acting to block platelet aggregation induced by rhodocytin or CRP.

These experiments have shown that katechin induces platelet activation through Src- and Syk-mediated phosphorylation of CLEC-2 in a similar way to rhodocytin. We identified that platelet aggregation induced by katechin occurs as an all-or-none response mechanism (Shin & Morita, 1998) and that this activation can be partially inhibited by AYP1 F(ab)², a CLEC-2 antibody fragment.

Katechin is a proanthocyanidin derived from the knotweed family of flowering plants, which belongs to the polygonaceae family. These chemical structures are found in the plant kingdom as oligomers or polymers, and most of them have antioxidant characteristics and a high affinity for protein binding (Rue, Rush, & van Breemen, 2018). These polymers are of planar structure, and, predominantly, negatively charged. We believe that this characteristic allows the interaction with positively charged arginine residues, like those found in the canonical

rhodocytin and podoplanin (Martin et al., 2021; Nagae et al., 2014; Watson et al., 2008). In fact, katacine (trimer) can bind to the same location on CLEC-2 as podoplanin and rhodocytin, according to our molecular docking predictions. Furthermore, our in-silico studies revealed that Asn-194 and Ser-166 on the C-type lectin-like domain could bind to katacine, implying an allosteric binding site.

The recognition of this binding ligand pattern could help in the development of more powerful ligands. However, the katacine-CLEC-2 complex should be co-crystallised to map the binding site in detail and confirm the presence of an allosteric binding site. Furthermore, katacine binding to a non-canonical binding site on CLEC-2 may explain why AYP1 is not able to completely block platelet aggregation induced by katacine, considering that AYP1 may bind to the rhodocytin or podoplanin canonical binding site.

It has been demonstrated that CLEC-2 activation requires clustering of the receptor (A. Y. Pollitt et al., 2014). This mechanism is consistent with the fact that podoplanin is present as multiple copies on the cell surface, and rhodocytin is a tetrameric protein, allowing both proteins to stimulate platelet activation through the crosslinking of CLEC-2.

We have shown through mass spectrometry that katacine is a mixture of polymers, as has been reported for other proanthocyanidins (Rue et al., 2018). The relevance of this result is that it suggests a model in which katacine could promote oligomerisation of CLEC-2 by multiple

interactions between katacine oligomers and CLEC-2. We cannot exclude that katacine may also bind to other receptors on the platelet membrane, since we observed partial inhibition on platelet aggregation induced by katacine in the presence of AYP1, compared to the full inhibition observed in the presence of Syk and Src inhibitors. However, these results could also reflect the possibility that katacine may bind to two different sites on CLEC-2.

Recently, Montague et al. have found that the three platelet ITAM receptors behave as pattern recognition receptors (PRRs), since they are activated by a diverse range of polyvalent charged ligands (Montague et al., 2021). The charged nature of katacine that we observed is consistent with this mechanism. However, we did not see a clear increase in the phosphorylation of the FcR- γ chain, which may point to a degree of selectivity for CLEC-2.

Another interesting observation was the fact that katacine did not induce platelet aggregation in a murine model. We assume that this may be due to the lack of homology between human and mouse CLEC-2 (62%) (Martin, Zuidschewoude et al. 2021). This data may be in line with the hypothesis of katacine binding to an allosteric binding site, since the amino acid residues adjacent to S166 in this region are not conserved between human CLEC-2 (QKS¹⁶⁶NEV) and mouse CLEC-2 (QNS¹⁶⁶KKD).

We have highlighted potential challenges that should be considered for the development of new ligands against receptors in which activation is mediated by multivalent proteins, as is the case with CLEC-2 and rhodocytin/podoplanin. Nevertheless, we have identified katacine as a novel CLEC-2 ligand which activates platelets by a Syk- and Src-dependent mechanism. Nonpolymeric forms of proanthocyanidins may represent a novel scaffold for the development of subsequent CLEC-2 antagonists and we propose that this is an exciting avenue of further research.

CHAPTER 6

RESULTS

This work is associated to the follow publication: Morán LA, Di Y, Sowa MA, Hermida-Nogueira L, Barrachina MN, Martin E, Clark JC, Mize TH, Eble JH, Moreira D, Pollitt AY, Loza MI, Domínguez E, Watson SP, García A. Katakine is a new ligand of CLEC-2 that acts as a platelet agonist. *Thromb Haemost.* 2022 Feb 15. DOI: 10.1055/a-1772-1069.

6. Chapter 6: Development of Multimeric Ligands against Human CLEC-2

6.1. Introduction

CLEC-2 is a single transmembrane receptor, and clustering is required to induce downstream signalling and platelet aggregation after ligand engagement (Hughes, Pollitt et al. 2010, Pollitt, Grygielska et al. 2010, Martyanov, Balabin et al. 2020). CLEC-2 activation is mediated by proteins, or oligomeric ligands, that lead to multiple interactions between CLEC-2 and the ligand molecules. Divalent ligands, such as AYP1 F(ab)₂, are effective in blocking platelet aggregation mediated by CLEC-2 (Gitz, Pollitt et al. 2014), whereas tetrameric rhodocytin in snake venom induces platelet aggregation (Suzuki-Inoue, Fuller et al. 2006, Watson, Eble et al. 2008).

To our knowledge, it has not been systematically explored how the valency of the ligand affects CLEC-2 clustering, leading us to pose the following questions: (1) Is there a minimum size of the ligand required to initiate downstream signalling? (2) Does the valency of the ligand matter for the degree of oligomerisation?

To address these questions, this chapter focuses on the development of single-chain camelid nanobodies raised against CLEC-2 and their divalent and tetravalent forms, to investigate how different valences facilitate the crosslinking of a single transmembrane receptor and

induce platelet aggregation. The findings are expected to improve our knowledge of the CLEC-2 activation mechanism and provide novel insights for the development of therapeutical agents against CLEC-2.

6.2. Aim

The aim of this chapter is to determine, using novel multimeric nanobodies, the valency of the ligand required to cause platelet activation through CLEC-2.

6.3. Results

6.3.1. Initial Screening of Nanobodies Generated Against Human CLEC-2

To develop novel and potent ligands, nanobodies were raised against human CLEC-2 (residues 55–229) in collaboration with VIB Nanobody Core. In total, 48 clones inserted into a pMECS-GG vector backbone were received and were subsequently expressed in a bacterial system, followed by column affinity purification.

The purified nanobodies underwent an initial screening using flow cytometry to identify the interaction of the nanobodies with human platelets in whole blood. Platelets were incubated with each nanobody and then incubated with the anti-his tag antibody, which recognises the his-tag present in the nanobody. This screening suggested that 9 out of

48 nanobodies interacted with the platelet surface, suggesting they may potentially bind to CLEC-2 on human platelets (**Figure 29A**).

In another flow cytometry assay, samples were incubated in the presence of the CLEC-2 monoclonal antibody, AYP1 F(ab)2. The presence of AYP1 F(ab)2 prevented the binding of the 9 nanobodies tested (**Figure 29B**). This finding suggests that the nanobodies 4, 17, 18, 29, 30, 36, 37, 45, and 47 bind to the same binding site as that of AYP1.

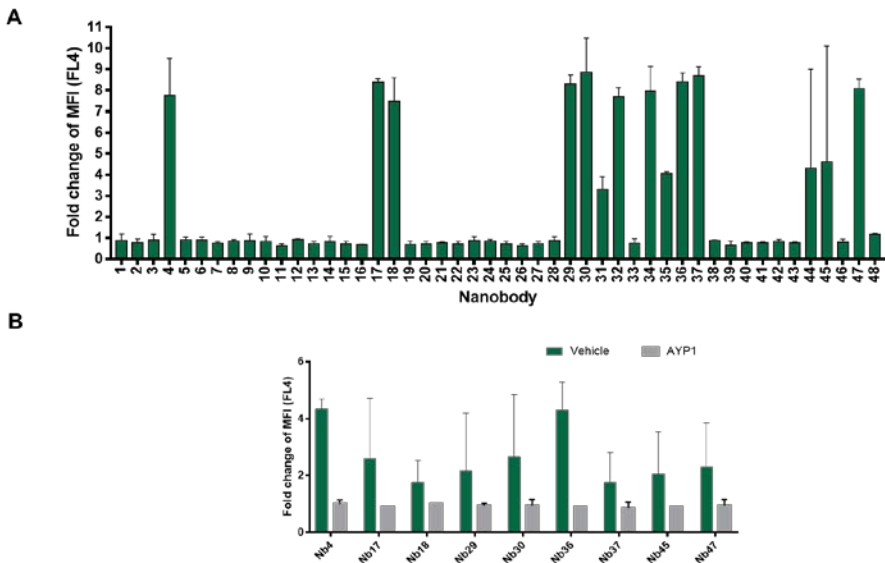


Figure 29. Screening of Nanobodies Against Human CLEC-2. Representative flow cytometry data of whole blood samples, presented as mean fluorescence intensity (MFI) normalised by MFI of secondary staining alone (a.u.) A) for all nanobodies raised against CLEC-2 and B) for 9 selected nanobodies, incubated in the presence of AYP1. Nb= nanobody. This screening was done by Ms Ying Di (Technician in the Birmingham platelet group).

Light transmission aggregometry revealed that only four nanobodies (Nb4, Nb32, Nb37, and Nb47) blocked platelet aggregation mediated by CLEC-2 in response to podoplanin on the surface of HEK293T cells (data not shown). Therefore, subsequent experiments focussed on Nb4, Nb32, Nb37, and Nb47.

To confirm binding and determine the affinity constant (K_D), the nanobodies were assessed using surface plasmon resonance (SPR; Biacore T200) in collaboration with Dr Eleya Martin (University of Birmingham). The SPR experiments were performed for Nb4, Nb36, Nb37, and Nb47.

The K_D value determined for the interaction of recombinant CLEC-2 with the nanobodies ranged from 144 nM to 218 nM, with Nb4 showing higher affinity for CLEC-2 than the other nanobodies, as shown in **Figure 30**.

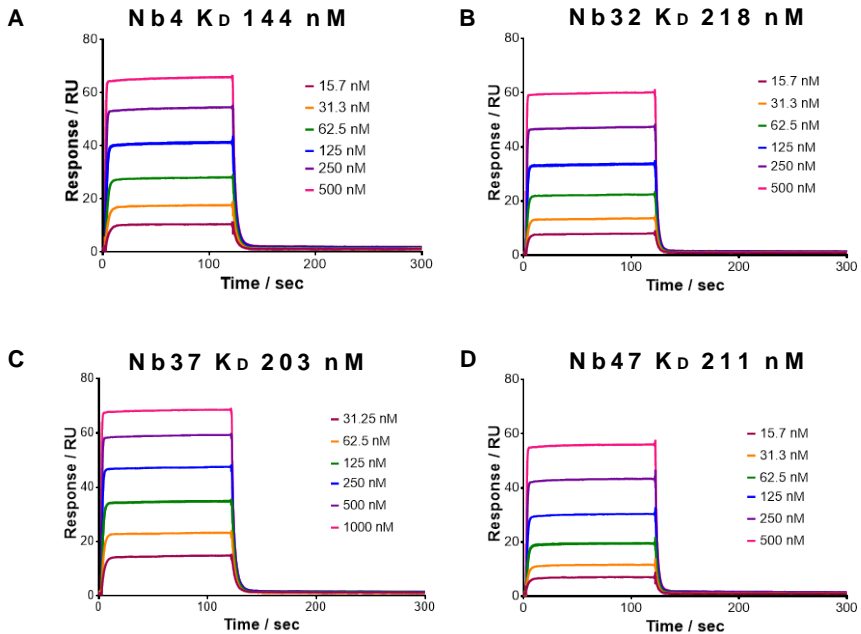


Figure 30. Surface Plasmon Resonance (SPR) Sensograms of Potential Nanobody Ligands for CLEC-2. A-D) Recombinant human CLEC-2-hisx6 was immobilised on a CM5 chip; different concentrations of nanobodies (A) Nb4, B) Nb32, C) Nb37, and D) Nb47) were flowed in the mobile phase over CLEC-2. Affinity constants (K_D) were calculated using steady-state analysis within Biacore T200 evaluation software. The experiments were performed by Dr Eleyna Martin (Postdoc in the Birmingham platelet group) in triplicate ($N = 3$).

It was also observed that the affinity of nanobodies was lower than that of the CLEC-2 monoclonal antibody, AYP1 F(ab)₂ ($K_D = 1.2$ nM; k_a [$1/M \times s$] was 2.681×10^6 , and the k_d (1/s) was 0.003138; **Figure 31**). Additionally, the SPR sensograms obtained for the nanobodies showed

an immediate association when the nanobodies were flowed over CLEC-2. However, a rapid dissociation was also observed after 120 s. This pattern differs from the pattern observed in the sensogram generated for the IgG fragment AYP1 (**Figure 31**).

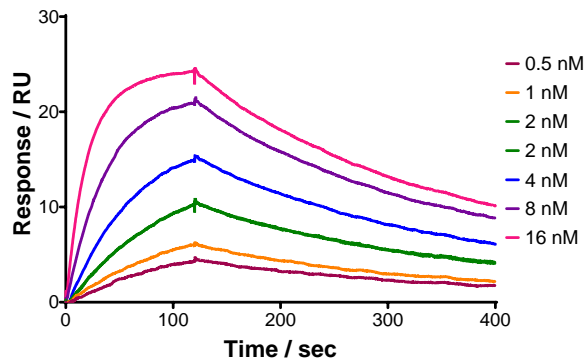


Figure 31. SPR Sensograms Showing AYP1 IgG Binding to an Immobilised Surface of a Recombinant CLEC-2-hisx6 Tag. An affinity constant (K_d) was calculated using kinetic analysis within Biacore T200 evaluation software. This experiment was performed by Eleya Martin (Postdoc in the Birmingham platelet group) in triplicate ($N = 3$).

6.3.2. Development of Multimeric Ligands of CLEC-2

To design multimeric ligands of CLEC-2, the sequence of the most potent nanobody identified by SPR—Nb4, later renamed as LUAS—was used. The first approach was to develop a homodimer of LUAS by

linking two copies of the LUAS DNA sequences (471 bp) by a flexible (Gly4Ser)₃ linker sequence. The first cloning strategy was the insertion of XmaI and SalI restriction sites sequences between the LUAS sequence and HA-His6 sequence (PelB-LUAS-XmaI-SalI-HA-His6) (namely, clone 1; 5Kb). The second clone consists in a copy of LUAS with the linker sequence (~500 bp)(PelB-XmaI-(GGGGS)₃-LUAS-SmaI-HA-His6; provided by Twist Biosciences).

After digestion, clones were visualised by gel electrophoresis (**Figure 33**). The first clone containing the vector and LUAS was observed around 5 kb, whereas the second digested clone showed two bands—a lower band around ~500 bp, which corresponded to the sequence containing LUAS and the linker (XmaI-(GGGGS)₃-LUAS-SalI) and an upper band, which was inferred to be the empty vector (**Figure 32**).

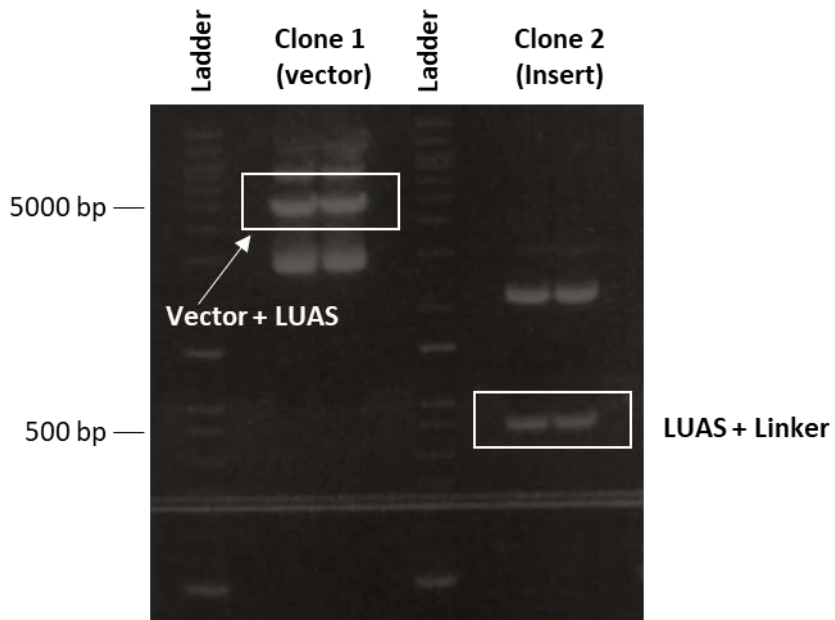


Figure 32. Agarose Gel Containing the Amplification Products of Clones 1 and 2. Both clones were digested with XmaI and Sall restriction enzymes and electrophoresed on a 4% agarose gel supplemented with SYBR™ Safe DNA Gel Stain. Fractions of the clones containing the open vector, including a copy of LUAS sequence (clone 1) and the LUAS+Linker insert (clone 2) DNA sequences are marked with a white rectangle.

6.3.2.1. Expression of LUAS-2 and LUAS-4

LUAS-2 and LUAS-4 (containing two or four copies of LUAS) were expressed using a *E. coli* expression system (WK6) and purified in two steps: firstly, using a gravity purification column packed with nickel-chelated beads, secondly the elutes were further purified by injecting

into a size exclusion column (SEC) coupled to an AKTA Pure system (gel filtration (GF)).

LUAS-2 was eluted from the GF column at 170 mL (**Figure 33Ai**), whereas LUAS-4 was eluted at 140 mL (**Figure 33 Aii**). The maximal absorbance values showed that LUAS-2 was highly expressed by the bacterial expression system (250 mAU UV), but the expression of LUAS-4 was markedly lower (4 mAU UV).

The theoretical molecular weight (MW) of LUAS-2 and LUAS-4 suggested that the mass of LUAS-2 and LUAS-4 was 29.7 kDa and 58.98 kDa, respectively.

Sodium dodecyl-sulfate polyacrylamide gel electrophoresis (SDS-PAGE) was used to characterise the LUAS-2 and LUAS-4 fractions obtained. In the case of LUAS-2, a single band per fraction was observed indicating high purity of the sample (**Figure 33Bi**); these fractions were combined and used for further characterisations. In the gel with LUAS-4, the first two fractions showed several bands, suggesting the presence of impurities. The intensity of the bands observed in fractions 7–10 was extremely low. Therefore, only the fractions 3–6 were combined for further experiments with LUAS-4.

The fact that the bands observed in the gels were below 34 kDa (**Figure 33 Bi**) and over 55 kDa (**Figure 33Figure 32 Bii**) indicates that the bands correspond to LUAS-2 and LUAS-4 (MW: 29.7 kDa and 58.98 kDa.), respectively.

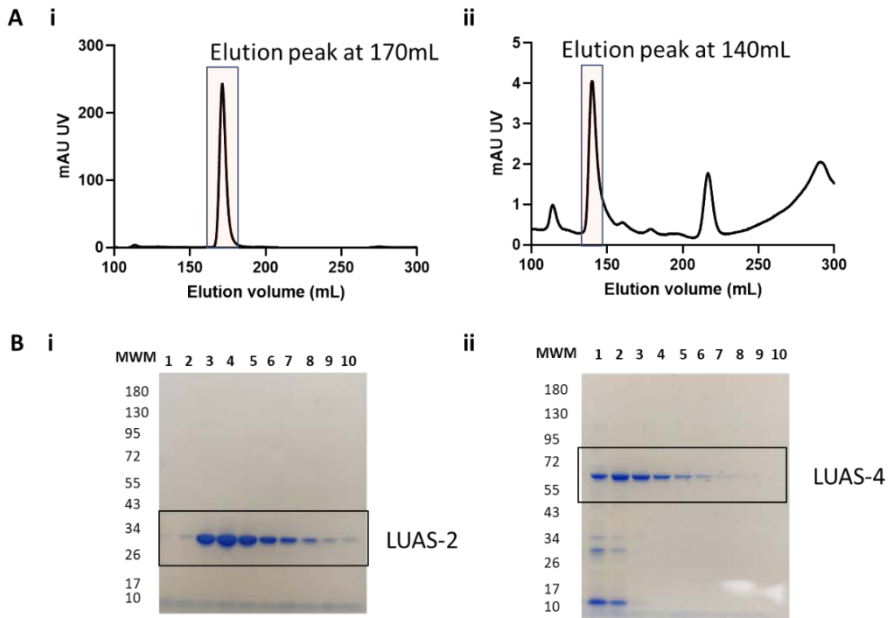


Figure 33. Chromatograms and SDS-Polyacrylamide Gels of LUAS-2 and LUAS-4. The chromatogram represents the arbitrary units of UV versus the elution volume of sample injected into an AKTA Pure system using a gel filtration column. (Ai) shows the LUAS-2 elution chromatogram and (Aii) shows the LUAS-4 elution chromatogram. (B) shows SDS-polyacrylamide gels of the elution fractions collected for LUAS-2 (Bi) and LUAS-4 (Bii).

6.3.3. Dimerisation of LUAS Significantly Improves Its Affinity for CLEC-2

To assess the effect of dimerisation on the affinity of the nanobody, surface plasmon resonance (SPR) technology (BIACORE T200) was performed, in collaboration with Dr Eleya Martin (University of Birmingham).

The affinity constant (K_D) for LUAS-2 was 0.5 nM (**Figure 34**), which was 200 times higher than the K_D (144 nM) of the original monovalent nanobody LUAS (**Figure 30**). The affinity of LUAS-2 (K_D : 0.5 nM; the on-rate [$1/M \times s$] was 3.094×10^9 , and the off-rate [$1/s$] was 1.416) is comparable with that of the CLEC-2 monoclonal antibody, AYP1 Fab2, (1.2 nM; k_a ($1/M \times s$) was 2.681×10^6 , and the K_D ($1/s$) was 0.003138; **Figure 30**).

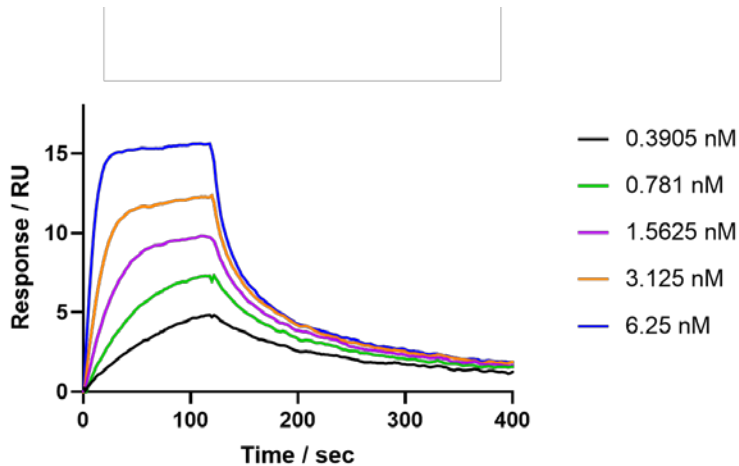


Figure 34. SPR sensograms showing LUAS-2 binding to recombinant CLEC-2-hisx6 tag immobilised on a surface. An affinity constant (K_D) was calculated using a kinetic analysis within Biacore T200 evaluation software. This experiment was performed by Eleya Martin (Postdoc in the Birmingham platelet group) N =3.

6.3.4. LUAS-2 Prevents Platelet Aggregation Induced by Rhodocytin

At 1 nM, LUAS-2 inhibits platelet aggregation induced by 100 nM rhodocytin ($2.08\% \pm 1.45\%$) compared with platelets treated with the vehicle control ($86\% \pm 2.3\%$; **Figure 35**). A similar result was observed for the divalent antibody fragment AYP1 Fab₂ ($3\% \pm 2\%$; **Figure 35**), whereas monovalent LUAS (200 nM) did not inhibit platelet aggregation induced by rhodocytin, likely owing to its lower affinity.

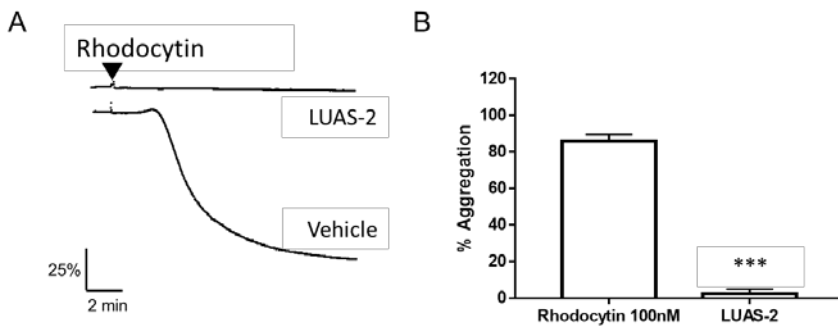


Figure 35. Divalent LUAS-2 and AYP1 F(ab)₂ Inhibits Platelet Aggregation Induced by Rhodocytin. (A) Representative platelet aggregation traces obtained from washed platelets stimulated with rhodocytin (100nM) and pre-treated with or without LUAS-2. PBS was used as a vehicle in the absent of LUAS-2 condition (B) Mean and standard deviation (SD) of three independent experiments (N = 3). Unpaired t-test with Welch's correction were used to determine significant differences ($p < 0.05$).

6.3.5. LUAS-4 Acts as Potent Agonist of CLEC-2

In contrast to LUAS and LUAS-2, the tetravalent ligand LUAS-4 induced strong platelet aggregation at a 10 nM dose (**Figure 36**).

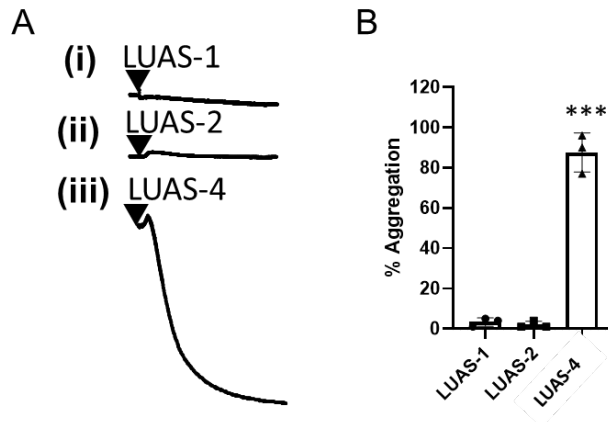


Figure 36. Comparison of the Effects of LUAS, LUAS-2, and LUAS-4 on Human Platelet Aggregation. (A) Representative platelet aggregation traces using washed platelets (2×10^8 cells/mL) treated with LUAS (i), LUAS-2 (ii) and LUAS-4 (iii) at 10 nM (B) Mean and standard deviation (SD) of three independent donors. Unpaired t-test with Welch's correction were used to determine significant differences ($p < 0.05$). (N = 3)

Platelet aggregation induced by LUAS-4 was fully inhibited by the Syk inhibitor PRT-060318 and the Src inhibitor PP2 (**Figure 37i-ii**). Additionally, the monoclonal antibody fragment AYP1 F(ab)2 also completely inhibited platelet aggregation induced by LUAS-4 (**Figure 37iii**).

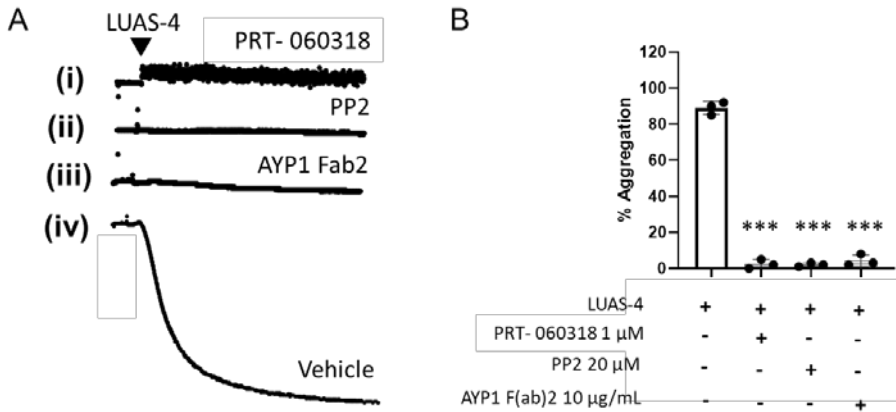


Figure 37. LUAS-4 Induces Platelet Aggregation Through CLEC-2. (A) Representative platelet aggregation traces of platelet stimulated with LUAS-4 (10 nM) and pre-treated with the Syk (PRT-060318 [1 μ M]) (i), the Src inhibitors (PP2 [20 μ M]) (ii), the monoclonal CLEC-2 antibody fragment AYP1 Fab2 (iii) or the vehicle (DMSO 0.1%) (iv). (B) Mean and SD of three independent experiments. Unpaired t-test with Welch's correction were used to determine significant differences ($p < 0.05$), (N = 3)

Additionally, LUAS-4 induced strong tyrosine phosphorylation in human platelets, to similar levels observed for rhodocytin (100 nM). There was an increase in the phosphorylation levels of Syk (Y525/526) and the adapter protein LAT (Y200; **Figure 38**). Tyrosine phosphorylation of platelets induced by LUAS-4 was inhibited by the Syk and Src inhibitors, PRT-06038 (1 μ M) and PP2 (20 μ M) respectively, and by 10 μ g/mL of AYP1 Fab2. In the latter cases, the

phosphorylation levels were comparable with the basal levels (**Figure 38**).

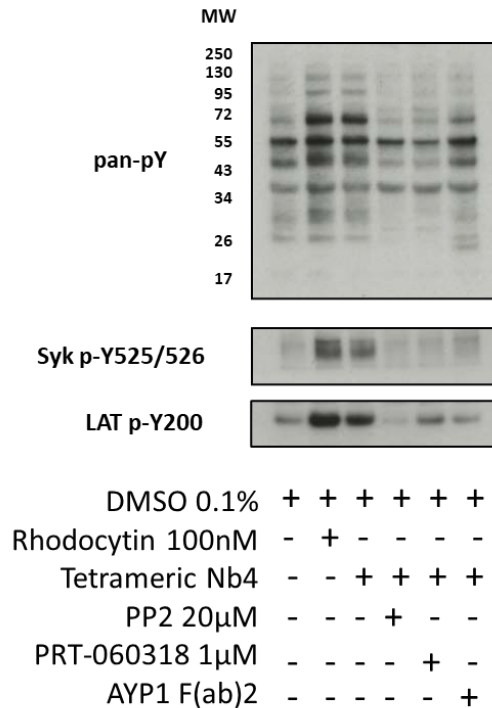


Figure 38. LUAS-4 Increases Protein Tyrosine Phosphorylation in Human Platelets, Reversed by Syk and Src Inhibitors or AYP1 F(ab)2. Washed platelets (4×10^8 /mL) under non-aggregating conditions were stimulated with LUAS-4 (10 nM). The role of Syk and Src was monitored preincubating platelets with PRT-060318 (1 μ M), PP2 (20 μ M), or the CLEC-2 monoclonal antibody AYP1 F(ab)₂ (10 μ g/mL). Rhodocytin (100 nM) was used as a positive control of protein tyrosine phosphorylation mediated by CLEC-2 activation. The blot shown is a representative figure of three independent experiments (N = 3).

The fact that tetrameric LUAS-4 induced tyrosine kinase phosphorylation and platelet aggregation mediated by CLEC-2, while the monomeric and dimeric forms did not, led us to systematically explore the effects of other CLEC-2 ligands according to their valency.

6.3.6. Dimeric and Monomeric Ligands Do Not Induce Human Platelet Aggregation

To assess whether other monomeric or dimeric CLEC-2 ligands could induce platelet aggregation, we first explored full-length, dimeric AYP1. AYP1 induced strong platelet aggregation in human washed platelets (**Figure 39i**), which was inhibited when platelets were incubated with the anti-Fc receptor fragment IV.3 Fab (**Figure 39ii**).

It was found that AYP1 Fab and F(ab)₂ failed to induce platelet aggregation (**Figure 39iii–iv**). These results are consistent with those previously observed with LUAS and LUAS-2, suggesting that monomeric or divalent ligands are unable to induce human platelet aggregation.

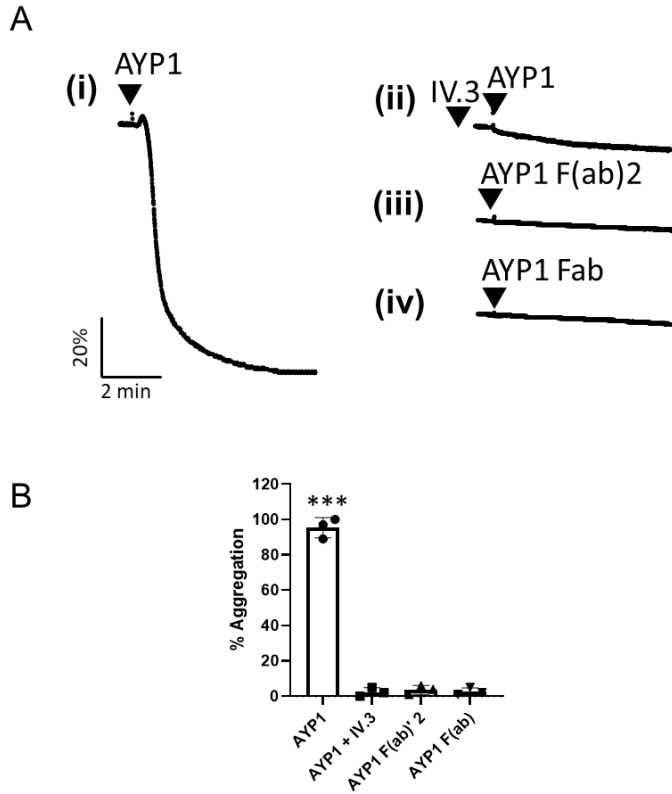


Figure 39. Monovalent or Divalent Forms of AYP1 Failed to Induce Human Platelet Aggregation. (A) Representative platelet aggregation traces obtained from washed platelets stimulated with (i) the IgG AYP1 (6.6nM) or (ii) pre-treated with the anti-Fc receptor (IV.3) at 30 $\mu\text{g}/\text{mL}$ and stimulated with the IgG AYP1 (6.6nM) (ii) or stimulated with AYP1 fragments Fab (iii) and Fab2 (iv). (B) Mean and standard deviation (SD) of three independent experiments ($N = 3$). Unpaired t-tests with Welch's correction were used to determine significant differences ($p < 0.05$).

Noting this pattern, the effect of the endogenous ligand of CLEC-2, podoplanin, was assessed using the recombinant human-podoplanin-rabbit Fc. It was observed that dimeric podoplanin failed to induce platelet aggregation (**Figure 40i**). However, when multiple copies of the ligand were immobilised on the cell membrane of HEK293T cells, podoplanin induced human platelet aggregation, whereas podoplanin-deficient HEK293T cells (*pdpn*^{-/-}) did not (**Figure 40ii-iii**).

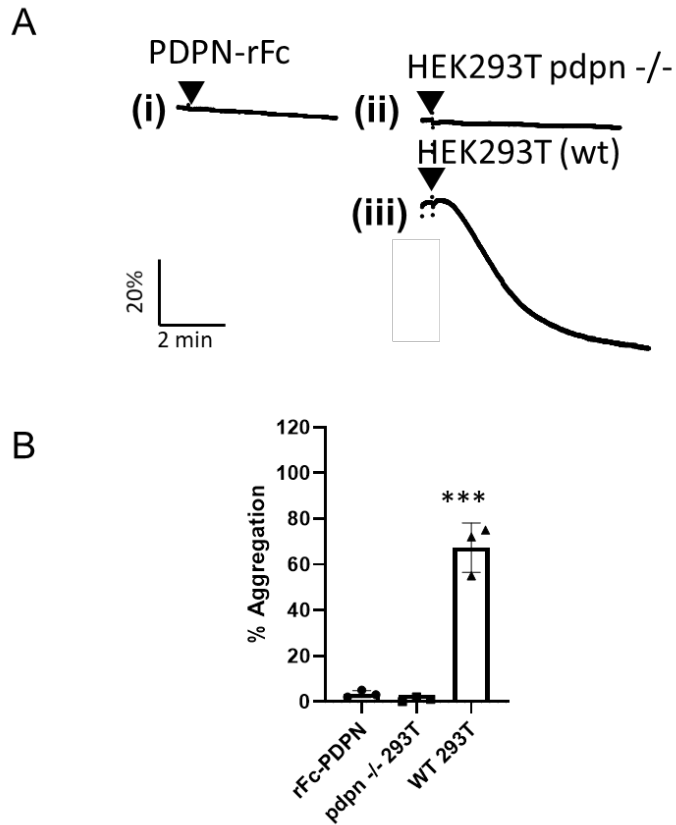


Figure 40. Dimeric Podoplanin Was Unable to Cause Platelet Aggregation in Human Platelets, Whereas Podoplanin-Expressing Cells Induced Platelet Aggregation. (A) Representative platelet aggregation traces obtained from washed platelets treated with (i) human podoplanin-rabbit Fc (330 nM), (ii) Podoplanin knockout HEK293T or (iii) wild-type HEK293T cells. (B) Mean and standard deviation (SD) of three independent experiments (N = 3). Unpaired t-tests with Welch's correction were used to determine significant differences ($p < 0.05$).

6.3.7. Effect of Monovalent, Divalent, and Tetravalent LUAS on CLEC-2 Clustering

The effect of the valency of the ligand in the clustering of CLEC-2 was assessed using fluorescence correlation spectroscopy (FCS), which allows the measurement of the molecular dynamics of a receptor on the membrane of living cells, through the observation of fluorescent molecules diffusing through a fixed and reduced observational confocal volume. FCS determines diffusion rates and molecular brightness (Kinjo, Sakata et al. 2011, Machan and Wohland 2014). Dr Joanne Clark performed FCS studies in CLEC-2-eGFP transfected HEK293T cells treated with the different valency nanobodies (LUAS, LUAS-2, and LUAS-4).

CLEC-2-eGFP transfected cells stimulated by the monovalent nanobody LUAS did not show significant differences in the diffusion rate or molecular brightness (**Figure 41**) when compared with untreated control. However, the addition of the multivalent forms of LUAS (LUAS-2 and LUAS-4) caused reduced diffusion rates of CLEC-2, showing only significant differences with LUAS-4 (**Figure 41**). The effect on the diffusion rate could be explained by the multivalent form of the ligand significantly increasing the size of the complex, slowing down the flux of the receptor through the confocal volume. LUAS-2 and LUAS-4 significantly increased the molecular brightness values of CLEC-2-eGFP (**Figure 41ii**), indicating oligomerisation of CLEC-2-

eGFP molecules in the membrane. These data together suggest receptor clustering by the multivalent nanobodies.

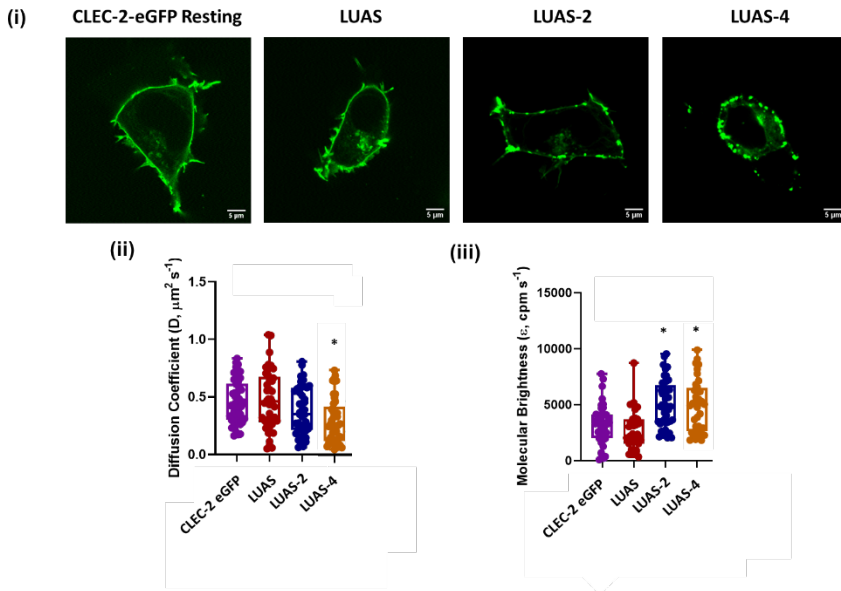


Figure 41. Membrane Dynamics and Molecular Brightness of CLEC-2-Transfected Cells Stimulated with LUAS, LUAS-2, and LUAS-4 Using fluorescence correlation spectroscopy (FCS). (i) Representative confocal microscopy images showing membrane localisation of CLEC-2-eGFP transfected HEK293T cells treated with LUAS (10 nM), LUAS-2 (10 nM), or LUAS-4 (10 nM). Box plots showing the effect of LUAS (10 nM), LUAS-2 (10 nM), or LUAS-4 (10 nM) on CLEC-2-eGFP (ii) diffusion coefficients, (iii) molecular brightness (cpm s⁻¹). For all box plots, the central line represents the median, whereas the box limits indicate the 25th and 75th percentiles, and whiskers extend to minimum and maximum points. Significance was determined with Kruskal-Wallis test with Dunn's post-hoc test, where $P \leq .05$. In (C), * = significance compared to CLEC-2 alone (no ligand). FCS measurements were taken in 39-65 cells (N = 3-6). scale bar = 5 μm. These experiments were performed by Dr Joanne Clark.

6.4. Discussion

Platelet activation mediated by CLEC-2 has been widely explored since its recognition as a rhodocytin receptor. Receptor dimerisation has been suggested as a potential mechanism of activation of CLEC-2. It is recognised that Syk plays an important role in bridging CLEC-2 on the platelet membrane from its SH2 domains (Hughes, Pollitt et al. 2010). Thus, Syk has a role as an intracellular linker. However, it is well known that for CLEC-2 activation an extracellular ligand (or linker) is also required to induce receptor mediated platelet activation.

Nonetheless, the mechanism by which an extracellular linker activates CLEC-2 had not been systematically explored, raising the following questions: What is the minimum ligand size needed to activate CLEC-2-mediated platelet aggregation? Could ligand multimerisation be used as a tool to generate more potent ligands for CLEC-2? Does the ligand regulate the size of the cluster?

To address some of these questions, molecular biology technologies were used to generate novel nanobody-based ligands for human CLEC-2. The present findings demonstrate that dimerisation of the most potent nanobody identified by SPR (nanobody 4 or LUAS) potentially increases the affinity of the ligand, resulting in an ultra-potent antagonist of CLEC-2.

This is not the first time that this approach has been used for the generation of a potent antagonist against a platelet receptor. The most

successful approach resulted in caplacizumab, a divalent nanobody targeting von Willebrand factor, clinically approved for the treatment of acquired thrombotic thrombocytopenic purpura (Knoebl, Cataland et al. 2020, Logothetis, Patel et al. 2021, Palanques-Pastor, Megias-Vericat et al. 2021). Therefore, LUAS-2 may be considered a potential antagonist of CLEC-2 for clinical development. The inhibitory effect of divalent LUAS-2 is consistent with that observed for the antibody fragment AYP1 F(ab)₂ on human platelets.

However, because the divalent nanobody did not lead to human platelet aggregation, the question regarding the minimum size of the ligand (or external crosslinker) remained unanswered. Therefore, a tetrameric nanobody form (LUAS-4) was generated, which caused clustering of multiple CLEC-2 receptors and acted as a strong CLEC-2 agonist. The present findings are consistent with those observed with the tetrameric ligand rhodocytin (Shin and Morita 1998, Bergmeier, Bouvard et al. 2001). The findings indicate that tetrameric ligands such as rhodocytin and LUAS-4 are capable of clustering multiple CLEC-2 receptors, which is required to induce human platelet aggregation.

The results demonstrate that the divalent ligand AYP1 fab2 and LUAS-2 are not large enough to induce platelet aggregation in human platelets. However, they promote CLEC-2 clustering in CLEC-2 transfected HEK293T cells. Observations in mouse platelets (data not shown), have shown that AYP1 f(ab)₂ and LUAS-2 can induce platelet aggregation.

Taken together, these findings suggests that dimeric CLEC-2 ligands

can act as a partial agonist by inducing receptor clustering and this mechanism most likely depends on multiple factors such as receptor density. This has previously been observed with other platelet agonists, such as GPCR agonists, where the dual behaviour is mediated by the membrane receptor density (Cusack and Hourani 1981, Clark, Knoll et al. 1999, Michino, Boateng et al. 2017, Shukla 2019).

Data from transfected HEK293T cells showed that CLEC-2 was present as a mixture of monomers and dimers. However, this finding may vary when the protein expression level is lower, as may be the case in human platelets.

The activation of CLEC-2 is a complex and multifactorial process, where external ligands (oligomeric), internal ligands (such as Syk or SFK) and receptor density must be finely synchronised to initiate and propagate CLEC-2 activation. Thus, the absence of one of these factors can completely inhibit CLEC-2 activation. A model of a possible activation mechanism of CLEC-2 by divalent and tetravalent ligands is illustrated in **Figure 48**.

These findings may be extended to other ITAM receptors on the platelet membrane, such as FcγRIIA, which is also activated by a tetravalent ligand, PF4. This ligand has been shown to initiate activation in human platelets and can lead to complex clinical conditions such as heparin-induced-thrombocytopenia (HIT) and vaccine-induced immune thrombotic thrombocytopenia (VITT; **Figure 48**).

CHAPTER 7

RESULTS

This work has been done in equally contribution with Hilaire Cheung.

This work is associated to the follow publication:

Cheung HYF*, Morán LA*, Sickmann A, Heemskerk JWM, Garcia A, Watson SP. Inhibition of Src but not Syk causes weak reversal of GPVI-mediated platelet aggregation measured by light transmission aggregometry. *Platelets*. 2022 May 9:1-8. doi: 10.1080/09537104.2022.2069235 * Co-first author

7. Chapter 7: Tyrosine kinase signalling is not required for sustained platelet aggregation measured by light transmission aggregometry

7.1. Introduction

CLEC-2 and GPVI have important implications in thrombus stability. As mentioned in the general introduction, CLEC-2 and GPVI activation triggers platelet aggregation through Src and Syk tyrosine kinases, initially via an immunoreceptor tyrosine-based activation motif (ITAM) and hemITAM, and culminating with the activation of PLC- γ . However, the question remains, does the ITAM tyrosine kinase play a role in maintaining aggregate stability?

In 2011, Andre et al. demonstrated the critical role of Syk in aggregate stability when whole blood was flowed over a collagen surface. They also suggested that the inhibition of Syk kinase protects from arterial and venous thrombosis in murine models with marginal effects on bleeding time (Andre, Morooka et al. 2011).

Additionally, platelet disaggregation mediated by ITAM signalling was demonstrated by Ahmed et al. (2020). They showed that inhibition of GPVI signalling, by either directly blocking GPVI or through inhibiting Src and Syk kinases, enhances disaggregation of platelets on a collagen surface at arterial shear force in the presence of anticoagulants.

However, they also observed that GPVI-blocking Fab 9012 was unable to reverse aggregation measured by light transmission platelet aggregometry (LTA) (Ahmed, Kaneva et al. 2020). On the other hand, it has been observed that the role of CLEC-2 in stabilising thrombus formation is independent of signalling mediated by the hemITAM motif and has been suggested that its role is mediated by adhesive properties of the CLEC-2 extracellular domain (Haining, Cherpokova et al. 2017). Both studies were performed under flow and arterial shear rate conditions.

7.2. Aim

In this chapter, we aim to explore the role of tyrosine kinases in stabilising aggregates formed under low shear conditions, by measuring platelet disaggregation by LTA in platelet aggregates induced by CLEC-2 and GPVI agonists.

We also aim to demonstrate whether platelet aggregation can be reversed by the dephosphorylation of relevant tyrosine kinases in ITAM signalling.

7.3. Results

7.3.1. Platelet aggregation mediated by CLEC-2 and GPVI receptors is weakly reversed after addition of Src, Syk, and Btk inhibitors

Firstly, to determine the role of tyrosine kinases on ITAM signalling and the maintenance of platelet aggregates, we tested the effect of tyrosine kinases inhibitors (Syk, Src and Btk inhibitors) in aggregates formed by CLEC-2 and GPVI agonists, using LTA.

Platelets were stimulated with either the GPVI-specific ligand, CRP, or the CLEC-2 ligand rhodocytin. 150 seconds after agonist stimulation, kinase inhibitors were given, and platelet aggregation was monitored for an additional 20 minutes. The maximally effective concentration for each inhibitor was determined by blocking platelet aggregation induced by CRP or rhodocytin

Platelet disaggregation was estimated using the following equation:

$$\% \text{ disaggregation} = \text{maximum \% aggregation} - \% \text{ aggregation at 20 min}$$

In platelets stimulated with CRP, we observed a $1.5 \pm 2.8\%$ disaggregation in the presence of 0.1% DMSO (vehicle control) over 20 minutes (**Figure 42Ai-ii**). Similarly, platelets treated with the Syk and Btk inhibitors, PRT-060318 and ibrutinib, showed a small reversal (3 ± 3.4 and $0.4 \pm 0.5\%$ respectively), not indicating any significant differences compared to the control. However, this result was different

with platelets treated with the Src inhibitor, PP2, showing a small but significant percentage of disaggregation ($11.4 \pm 3.9\%$ and $12.1 \pm 6.8\%$ of disaggregation, respectively), over the same period ($p < 0.05$; **Figure 42Ai–ii**).

The addition of Btk kinase inhibitors to rhodocytin-stimulated platelets had no significant effect on aggregation over 20 minutes ($3.1 \pm 4.9\%$) compared to the vehicle ($0.58 \pm 0.5\%$). However, the Src inhibitors, PP2 and dasatinib, induced a slight but significant platelet disaggregation (10.8 ± 10.0 and $5.8 \pm 5.7\%$ respectively). Syk inhibition did not show significance differences compared to the vehicle control, but a tendency for disaggregation was observed in some donors ($6.86 \pm 7.7\%$) ($p < 0.05$; **Figure 42Bi–ii**).

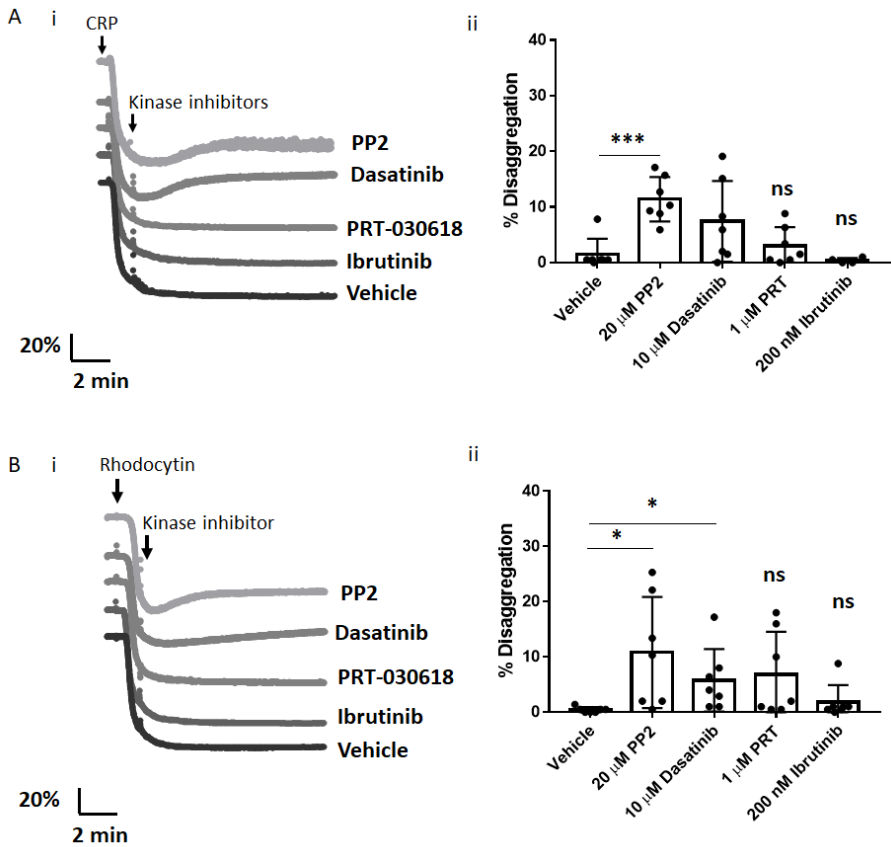


Figure 42. Kinase inhibitors cannot reverse GPVI and CLEC-2 mediated platelet aggregation. Washed platelets at 2×10^8 /ml were stimulated with (A) $10 \mu\text{g}/\text{mL}$ CRP or (B) 100 nM rhodocytin. Both conditions were then incubated with PP2 ($20 \mu\text{M}$), dasatinib ($10 \mu\text{M}$), PRT-060318 ($1 \mu\text{M}$), ibrutinib (200 nM), or vehicle after 150 seconds of agonist stimulation. LTA was monitored for 20 minutes. (i) Representative platelet aggregation traces. (ii) Mean \pm SD % disaggregation after 20 minutes of agonist stimulation from seven identical aggregation experiments. * ($P < 0.05$) and *** ($P < 0.001$) calculated using Welch's t-test to indicate statistically significant differences. ns = not significant. $N = 7$ separate donors.

7.3.2. Effect of tyrosine kinase inhibitors on phosphorylation

GPVI and CLEC-2 induce strong tyrosine phosphorylation once their ligands are engaged, but the effect of tyrosine kinases inhibitors once phosphorylation has been initiated is unknown. Therefore, our objective was to evaluate if tyrosine kinase-induced phosphorylation could be reversed once initiated by the ITAM receptors.

To do so, we monitored if protein tyrosine phosphorylation mediated by GPVI or CLEC-2 is maintained and at what time maximum phosphorylation levels are achieved. Tyrosine phosphorylation was monitored over a period between 0 to 3000 seconds on whole lysates, using a phospho-specific antibody (4G10 mAb) to follow the global tyrosine phosphorylation profile. This was also extended to specific kinases, such as tyrosine phosphorylation on Syk at Y525/526, LAT at Y200, Btk at Y551 and Y233, and PLC γ 2 at Y1217.

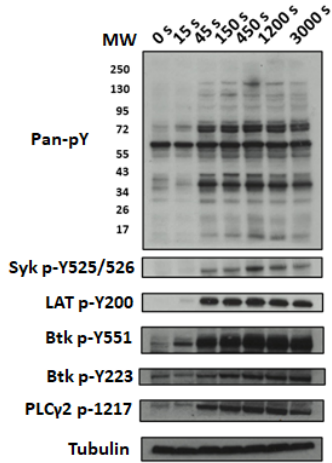
In the case of platelets stimulated with CRP 10 μ g/mL, we observed that tyrosine phosphorylation of Btk (Y223 and Y525/526) and LAT (Y200) were increased, with maximum phosphorylation levels after 150 seconds, which was maintained for up to 50 minutes (**Figure 43Ai–ii**). A similar response was observed for Syk (Y525/526) and PLC γ 2 (Y1217) but with a tendency for phosphorylation to start decreasing after 30 minutes; however, phosphorylation levels were still significantly higher than in the basal condition ($p < 0.05$; **Figure 43Ai–ii**). Similar patterns were found for Btk (Y223 and Y525/526), LAT (Y200) and PLC γ 2 (Y1217) when platelets were stimulated with

rhodocytin. In the case of Syk (Y525/526), we observed a rapid phosphorylation response, achieving maximal levels at 150 seconds, followed by a quick reversal of the phosphorylation after 450 seconds; however, the phosphorylation levels were significantly elevated even after 50 minutes. This result shows a transient phosphorylation of Syk, compared to the other kinases where phosphorylation was maintained (**Figure 43Bi-ii**).

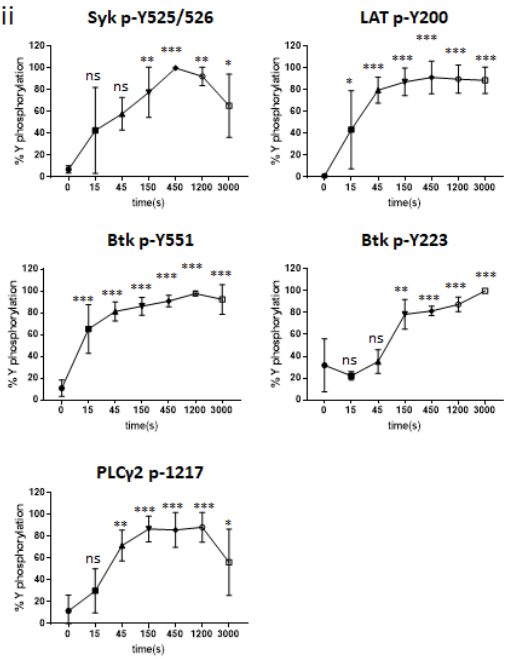
Since full phosphorylation was achieved after 150 seconds, we tested the effect of tyrosine kinase inhibitors added at this stage, in the same way as the LTA assays had been performed. When the Src kinase inhibitors PP2 and dasatinib were administered in platelets stimulated with CRP, they triggered fast dephosphorylation of Syk Y525/526, LAT Y200, Btk Y223, Btk Y551, and PLC2 Y1217, returning to baseline levels after 20 minutes. Whilst PRT-060318, a Syk inhibitor, suppressed tyrosine phosphorylation of proteins downstream of Syk, including LAT Y200, Btk Y223, Btk Y551, and PLC2 Y1217, it only partially reduced phosphorylation of Syk at Y525/526, which suggests Syk can be phosphorylated via Src kinases (**Figure 44Ai-ii**).

Similarly, ibrutinib only inhibited tyrosine phosphorylation of proteins which lie downstream of Btk, as observed by the autophosphorylation at Y223 and PLC□2 at Y1217 (**Figure 44Ai-ii**).

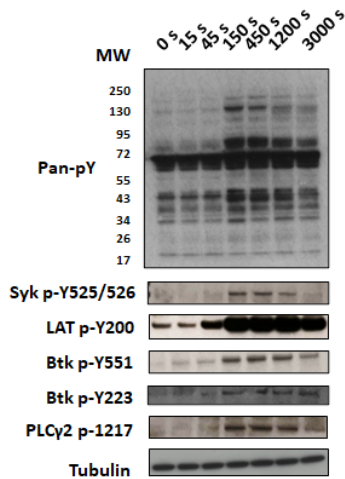
A i



ii



B i



ii

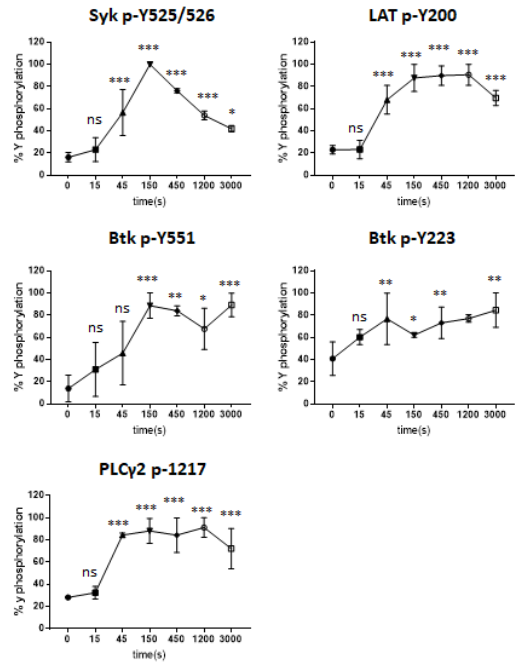


Figure 43. Tyrosine phosphorylation is sustained for 50 minutes in GPVI and CLEC-2 mediated protein phosphorylation. Washed platelets at 4×10^8 /ml were stimulated with (A) 10 $\mu\text{g}/\text{mL}$ CRP or (B) 100 nM rhodocytin in the presence of 9 μM eptifibatide. Platelets were lysed with 5x reducing sample buffer at the stated times after addition of agonist. Whole cell lysates were probed for whole cell phosphorylation or kinase phosphorylation with the stated antibodies. (i) Representative blot and (ii) bar charts to show the mean \pm SD % of tyrosine phosphorylation from three independent experiments. *($P < 0.05$), **($P < 0.01$), and ***($P < 0.001$) assessed by one-way ANOVA multiple comparison analysis indicate statistically significant differences. Ns = not significant. N = 3

We repeated the same set of experiments in platelets stimulated with rhodocytin, and the results showed a similar pattern of inhibition in the presence of inhibitors of Src, Syk, and Btk kinases (**Figure 44Bi-ii**). These were consistent with our observations in platelets stimulated with CRP since both share similar signalling pathways. Nevertheless, there were several minor differences compared to experiments based on GPVI activation. For example, PP2 did not inhibit LAT Y200 phosphorylation, and there was no significant difference on phosphorylation of Syk Y525/526 or PLC γ 2 Y1217 when treated with PRT-060318 and ibrutinib, respectively.

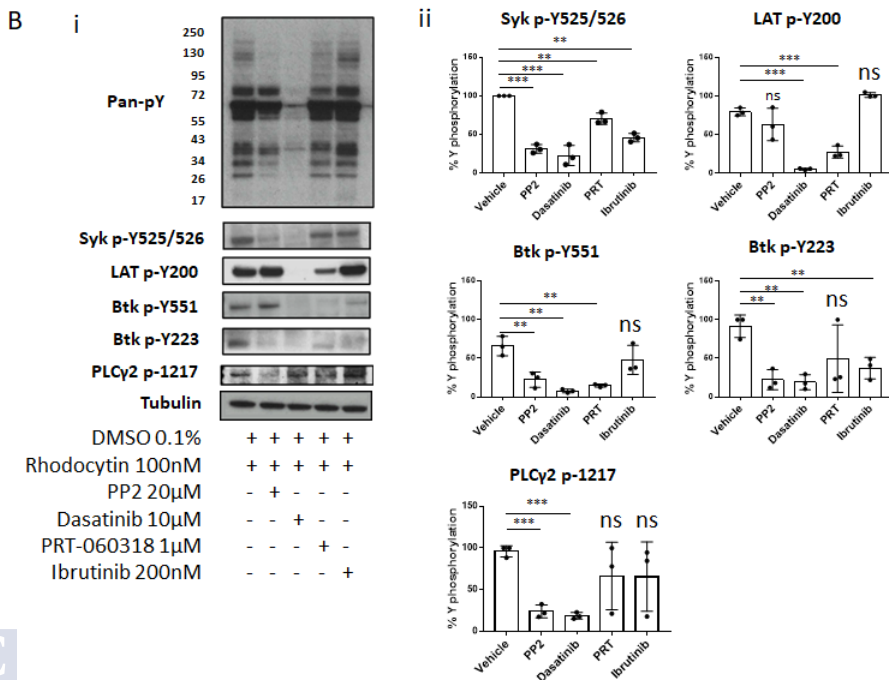
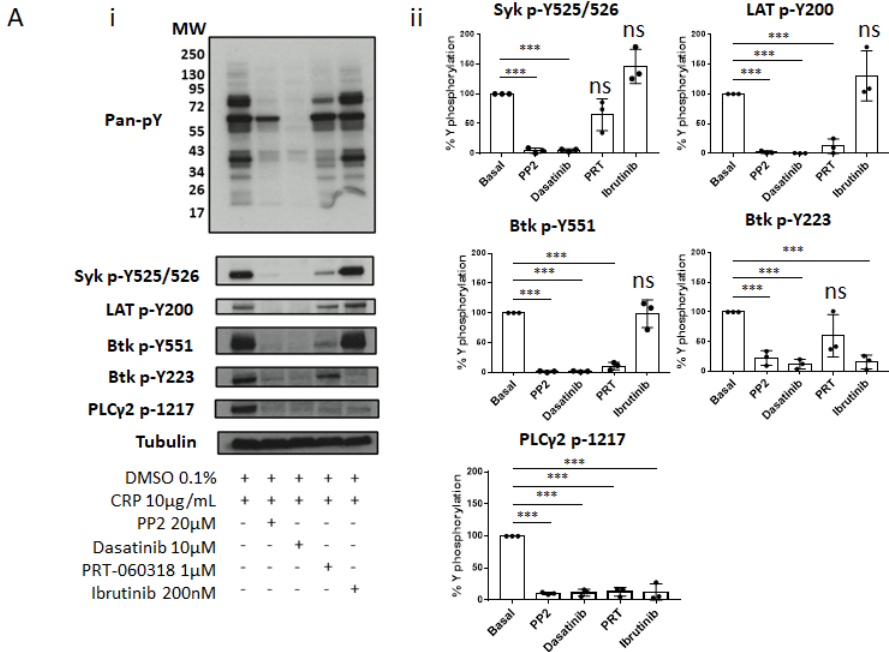


Figure 44. Kinase inhibitors reverse GPVI- and CLEC-2-mediated protein phosphorylation. Washed platelets at 4×10^8 /ml were stimulated with (A) 10 μ g/mL CRP or (B) 100 nM rhodocytin in the presence of 9 μ M eptifibatide. Platelets were incubated with PP2 (20 μ M), dasatinib (10 μ M), PRT-060318 (1 μ M), ibrutinib (200 nM), or vehicle after 150 seconds of agonist stimulation. Platelets were then lysed with 5X reducing sample buffer 20 minutes after addition of agonist. Whole cell lysates were probed for whole cell phosphorylation or kinase phosphorylation with the stated antibodies. (i) Representative blot and (ii) bar charts to show the mean \pm SD % of tyrosine phosphorylation from three experiments. *($P < 0.05$), **($P < 0.01$), and ***($P < 0.001$) calculated using Welch's t-test indicate statistically significant differences. Ns = not significant. N = 3.

7.3.3. Platelet aggregation was sustained in the presence of tyrosine kinase inhibitors combined with apyrase and indomethacin

To explore the role of the feedback messengers ADP and TxA₂, we combined tyrosine kinase inhibitors with the ADP/ATP scavenger, apyrase, and the cyclooxygenase inhibitor, indomethacin. Surprisingly, we observed that platelet aggregation was maintained when apyrase and indomethacin were given both in combination with tyrosine kinase inhibitors, and in combination with secondary mediator inhibitors (**Figure 45**).

Platelet aggregation mediated by GPVI showed a reversal (7.21 ± 3.43 % and 3.93 ± 1.44 % of disaggregation, respectively), when PP2 and dasatinib were given in combination with apyrase and indomethacin (**Figure 45Ai-ii**). These values are even lower than those observed for Src inhibitors given in the absence of apyrase and indomethacin

(**Figure 45A**). We did not observe differences in the percentage of disaggregation when PRT-060318 (1.47 ± 1.16 %), or ibrutinib (0.6 ± 0.25 %) were administrated in combination with apyrase and indomethacin (**Figure 45Ai-ii**).

In rhodocytin-stimulated platelets, a similar set of results was obtained (**Figure 45Bi-ii**). The maximal percentage of disaggregation was observed when platelets were treated with Src inhibitors, PP2 and dasatinib (6.22 ± 8.8 and 5.58 ± 6.97 % of disaggregation, respectively), but this was not significant. Similarly, PRT-060318 and ibrutinib did not significantly reverse platelet aggregation (4.7 ± 76.18 and 1.4 ± 1.9 % of disaggregation, respectively; **Figure 45Bi-ii**).

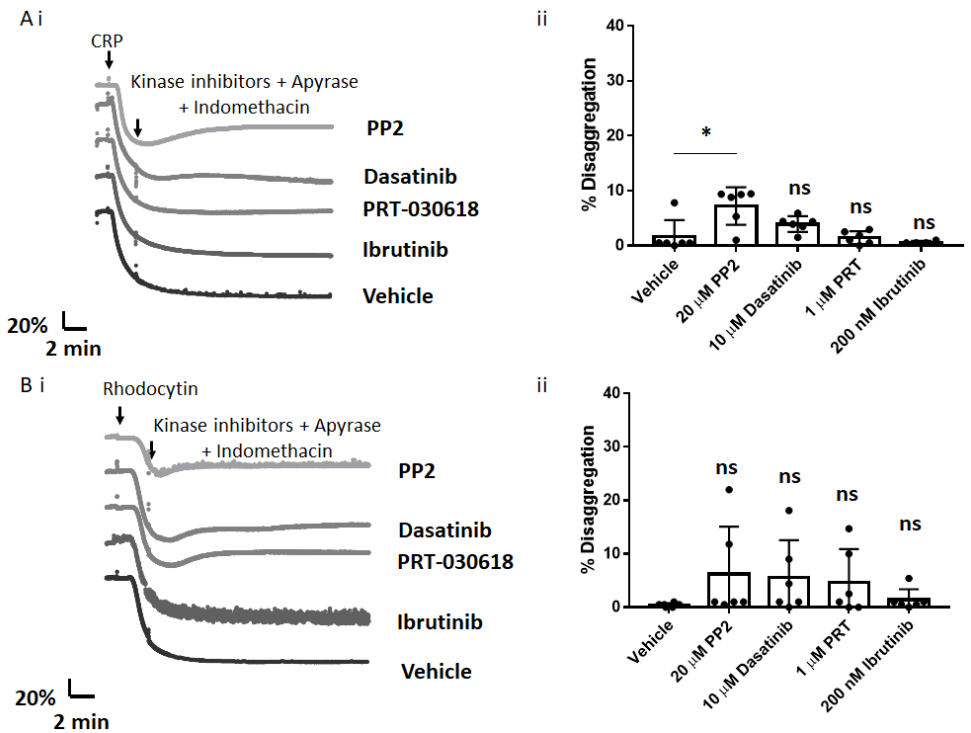


Figure 45. Kinase inhibitors together with secondary mediators antagonists cannot reverse GPVI- and CLEC-2-mediated platelet aggregation. Washed platelets at 2×10^8 /ml were stimulated with (A) 10 μ g/mL CRP or (B) 100 nM rhodocytin then incubated with PP2 (20 μ M), dasatinib (10 μ M), PRT-060318 (1 μ M), ibrutinib (200 nM), or vehicle together with 10 μ M indomethacin and 2.5 U/mL apyrase, after 150 seconds of agonist stimulation and monitored by LTA for 20 minutes. (ii) Bar charts show the mean \pm SD % of disaggregation after 20 minutes of agonist stimulation from seven identical experiments. *($P < 0.05$) calculated using Welch's t-test indicates statistically significant differences. Ns = not significant. N = 7.

7.3.4. Platelet α IIb β 3 activation is reversed by tyrosine kinase inhibitors, but platelet aggregation is sustained

We also administrated the α IIb β 3 antagonist, eptifibatide, alone or in combination with Src and Syk inhibitors after CRP stimulation. We observed that aggregation was still maintained, and the maximal reversal in the presence of eptifibatide in combination with Src and Syk inhibitors was increased (13.4 ± 11.6 , and 13.7 ± 7.4 %, respectively), compared to eptifibatide alone (4.5 ± 2.8 %) (**Figure 46Ai–ii**).

To further investigate the above data, we used flow cytometry to measure activation of the integrin α IIb β 3 using PAC-1-FITC in a diluted suspension of platelets to prevent aggregation. Src and Syk inhibitors PP2 and PRT-060318 were added 150 seconds after platelet activation with CRP, leading to a reversal of α IIb β 3 activation to basal level in 20 minutes (1.08 ± 0.31 and 1.07 ± 0.50 -fold change in MFI) compared to the sustained activation present in control platelets (12.8 ± 10.5 -fold) (**Figure 46Bi–ii**).

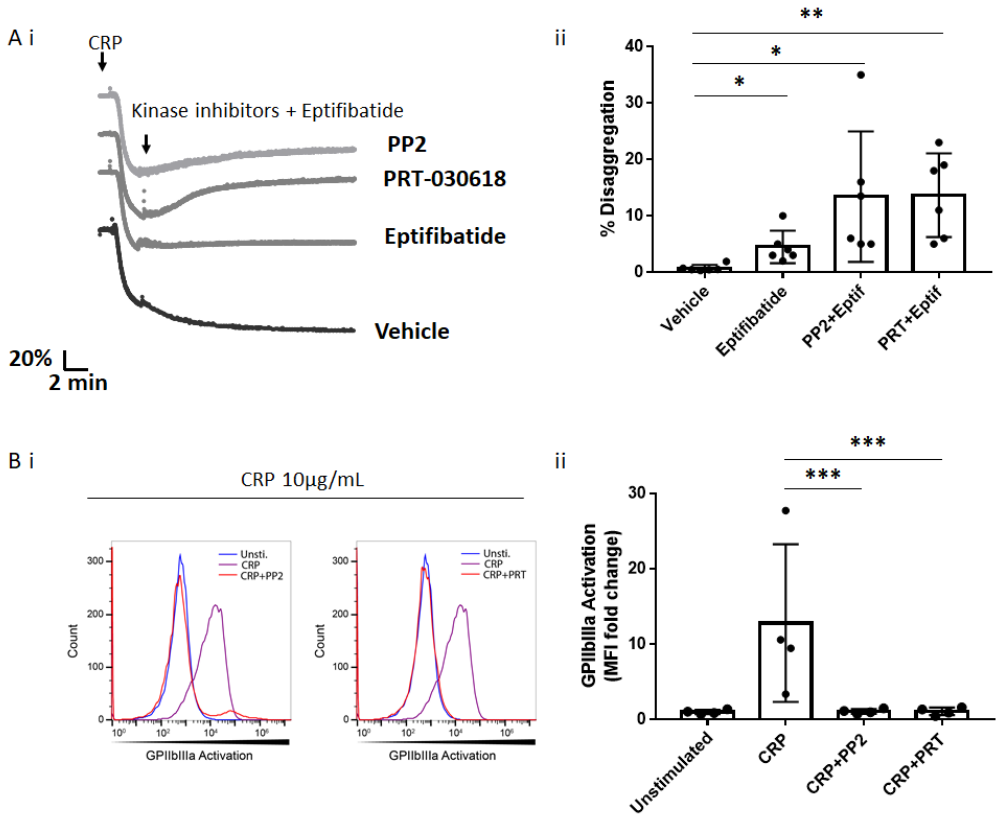


Figure 46. Role of the integrin $\alpha\text{IIb}\beta\text{3}$ activation on the reversal of platelet aggregation by tyrosine kinase inhibitors. A) Washed platelets ($2 \times 10^8/\text{ml}$) stimulated with $10 \mu\text{g}/\text{mL}$ CRP and then treated with eptifibatide $9 \mu\text{M}$ alone or together with PP2 ($20 \mu\text{M}$) or PRT-060318 ($1 \mu\text{M}$), after 150 seconds of agonist stimulation and monitored by LTA for 20 minutes. (i) Representative platelet aggregation traces (ii) bar chart to show mean \pm SD % of disaggregation after 20 minutes of agonist stimulation from six independent experiments ($N = 6$). $*$ ($P < 0.05$), $**$ ($P < 0.01$) and $***$ ($P < 0.001$) calculated using Welch's t-test indicates statistically significant differences. B) Reversal of $\alpha\text{IIb}\beta\text{3}$ activation by tyrosine kinase inhibitors. Washed platelets ($2 \times 10^7/\text{ml}$) were incubated with PAC-1-FITC, stimulated with CRP ($10 \mu\text{g}/\text{mL}$), and then treated with vehicle, PP2 ($20 \mu\text{M}$) or PRT-060318 ($1 \mu\text{M}$) 150 seconds after agonist stimulation. Flow cytometry measurements were done at 20 minutes after agonist stimulation. (i) Flow cytometry histograms depict activation of $\alpha\text{IIb}\beta\text{3}$ in platelets that were unstimulated (blue), treated with CRP ($10 \mu\text{g}/\text{mL}$) and followed with vehicle (purple), PP2 or PRT-060318 (red). (ii) Bar charts show MFI fold change \pm SD of four independent and identical experiments, $N=4$.

We also evaluated if these results are consistent when platelets are activated by another family of receptors, such as the thrombin GPCR. Therefore, we induced platelet aggregation using the PAR-1 agonist TRAP6. We observed that only the Src inhibitors administered led to a reversal of platelet aggregation mediated by PAR-1 (PP2: 9.99 ± 3.08 %, $p < 0.05$; Dasatinib: 5.95 ± 4.95 %, ns) while not significance differences were observed by addition of the Syk inhibitor (2.09 ± 0.867 %) (Figure 47).

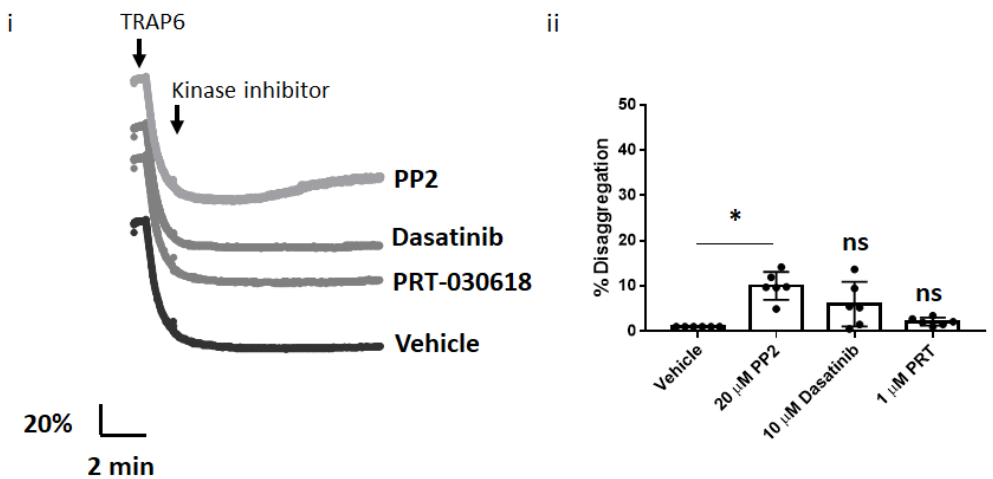


Figure 47. Kinase inhibitors cannot reverse TRAP6-mediated platelet aggregation. Washed platelets at 2×10^8 /ml were stimulated with 15μ M TRAP6 and incubated with PP2 (20μ M), dasatinib (10μ M), PRT-060318 (1μ M), or vehicle, after 150 seconds of agonist stimulation. LTA was monitored for 20 minutes. (i) Representative platelet aggregation traces (ii) bar chart to show mean \pm SD % disaggregation after 20 minutes of agonist stimulation calculated from six independent experiments. *($P < 0.05$) calculated using Welch's t-test indicates statistically significant differences. ns = not significant, $N = 6$.

7.4. Discussion

The full explanation of the mechanism by which platelet aggregates are stabilised is lacking, leaving many questions open: Is thrombus stabilisation dependent on tyrosine kinase phosphorylation in the platelet cytosol, such as Syk or Src kinases in the ITAM signalling pathway? Is the integrin $\alpha\text{IIb}\beta\text{3}$ uniquely responsible for the maintenance of thrombus stability? Despite these questions not yet having been answered, some emergent research is providing new insights into the mechanisms of how platelet aggregates are sustained.

It was initially thought that the mechanism sustaining aggregates was purely mediated by $\alpha\text{IIb}\beta\text{3}$ (Jackson 2007). Recently, however, it has been recognised that more receptors are involved. Ahmed et al. (2020) have demonstrated that the GPVI/FcR γ complex has a supporting role in platelet stability under flow conditions and have suggested, for the first time, that this mechanism could be mediated by interaction with fibrinogen, which was recently discovered as a GPVI ligand (Mangin, Onselae et al. 2018), rather than collagen. The tyrosine kinase Syk has also been proposed as having a key part in thrombus stabilisation under flow conditions (Andre, Morooka et al. 2011) and a supporting role in both platelet activation on fibrinogen and platelet aggregation in thrombi formed under flow conditions.

In this chapter, we investigated the role of tyrosine kinases that participate in ITAM signalling (Src, Syk, and Btk) in sustaining platelet

aggregation, in platelets stimulated by CLEC-2 or GPVI. Despite not observing fully disaggregation by any of these kinases, we found that Src inhibitors led to a partial disaggregation on platelet aggregation induced by CRP, rhodocytin and by the PAR-1 ligand TRAP6. We also observed that tyrosine kinase phosphorylation can be rapidly inhibited by the addition of the kinase inhibitors used in this study.

The fact that Src kinases showed an effect in sustaining platelet aggregates, and Syk and Btk had no impact, suggests that our observations might be a consequence of α IIb β 3 outside-in signalling, rather than a GPVI or CLEC-2-dependent mechanism, reducing the contractibility mediated by α IIb β 3. This may be in line with the observation of Auger et al. suggesting the role of Src on platelet contractibility and stability (Auger and Watson 2008). In contrast to these findings, an enhanced rate of disaggregation has been described at arteriolar rates of shear in thrombi produced on a collagen surface with the addition of a GPVI-blocking Fab or inhibitors of Src and Syk kinases (Ahmed, Kaneva et al. 2020).

However, the fact that the findings of Ahmed *et al* were obtained under high shear conditions makes the loss of platelets at the periphery of the aggregates more likely, which may be less contracted than the aggregates formed under LTA conditions, where there is a lack of shear forces when compared with flow adhesion experiments. Perella et al recently described how GPVI provides a weakly activating signal which relies on the integrin α IIb β 3-dependent platelet adhesion and Syk

activation, for the formation of small thrombi (Perrella, Huang et al. 2021). Therefore, it is likely that the role of Src kinase in maintaining platelet aggregate stability is also mediated by a cooperative mechanism between GPVI and integrin $\alpha\text{IIb}\beta\text{3}$, since both receptors play an important role in platelet aggregates stability and has been recognised as fibrinogen receptors.

Interestingly, we observed in the flow cytometry assay, that the integrin $\alpha\text{IIb}\beta\text{3}$ activation could be reversed by Syk and Src inhibitors in platelets incubated with them, while the aggregation is maintained in the LTA assay. One potential explanation for this, is the higher platelet density used in the LTA assay compared with the 10 times diluted platelet preparation used for the flow cytometry experiment. This factor may release a larger amount of endogenous fibrinogen, leading to the integrin activation through an inside-out and inside out mechanism, while in the flow cytometry assay is expected that the activation of the integrin is solely mediated by the inside-out mechanism. It is unknown if the outside-in mechanism could be entirely reversed by the inhibitors of tyrosine kinase Src or Syk. We also hypothesise the involvement of additional interactions through membrane proteins in supporting aggregation.

Additionally, we have also observed that platelet aggregation mediated by the ITAM receptors, GPVI and CLEC-2 are independent of the role of the positive feedback mediated by ADP and TxA₂ under low shear conditions.

Finally, the observation that tyrosine kinase inhibitors such as Src inhibitors could promote partial disaggregation under low shear conditions, and stronger disaggregation under flow, may have clinical implications on the detachment of thrombi. Further investigating the ability to cause thrombus destabilisation could provide possible targets for antithrombotic therapeutics.

CHAPTER 8

DISCUSSION

8. General discussion

CLEC-2 is considered a potential target for the development of a novel class of inhibitors with a promising antithrombotic effect and prevention of bleeding, which is the main side effect of current antiplatelet therapies. The role of CLEC-2 in thromboinflammatory syndromes also makes this receptor a promising alternative for the treatment of multiple thromboinflammation-associated diseases, including cancer or sepsis. However, to achieve this, significant research is required to understand the molecular and structural basis of CLEC-2 activation in human platelets.

To improve our understanding of CLEC-2 activation mechanisms, novel CLEC-2 ligands were developed based on small-molecule compounds (Chapter 4) and the recombinant sequence of a nanobody raised against CLEC-2 (Chapter 5). Owing to the implications of CLEC-2 in thrombus formation and stability, the role of tyrosine kinases present in the ITAM signalling pathway, in maintaining thrombus formation, was explored (Chapter 6).

Thus, the overall aim of this dissertation was the development of different tools to provide further insights into the mechanisms of activation of CLEC-2 and explore the role of kinases in the maintenance of the thrombus formed after CLEC-2 activation.

Chapter 4 of this dissertation focused on the identification of potential CLEC-2 antagonist based on small molecules; however, the most relevant finding was the unexpected identification of a novel agonist of CLEC-2, called katacine. This small molecule induces strong platelet aggregation, which is dependent on Src and Syk, and cause phosphorylation of CLEC-2, providing evidence of direct binding to the receptor. The identification of a CLEC-2 agonist from a small-molecule chemical library was difficult to explain initially because it has been reported in the literature that CLEC-2 requires clustering to induce platelet aggregation. Thus, it seemed unlikely that a small molecule could cause crosslinking of a single transmembrane receptor. However, further investigation by mass spectrometry allowed us to confirm that katacine is in fact a mixture of polymers with different sizes, suggesting that its polymeric nature allows it to induce platelet aggregation mediated by CLEC-2, probably by enabling CLEC-2 clustering.

In this section, it was proposed that monomeric forms of katacine may provide a scaffold for the generation of potential inhibitors of CLEC-2 to prevent the oligomerisation of CLEC-2 by endogenous ligands. Nevertheless, there are notable practical limitations. 1) It is speculated that the affinity of monomeric forms of katacine will be considerably low compared to protein-based ligands. 2) The generation of monomeric forms of katacine may be considerably challenging since this is a spontaneous process; therefore, substantial chemical modifications would be required to prevent the oligomerisation of this

ligand. However, identifying other proanthocyanins less prone to polymerisation may be an interesting approach to uncover novel antagonists of CLEC-2.

Is it Possible to Identify Small-Molecule Inhibitors for the Prevention of CLEC-2 and Podoplanin Interaction?

Our study did not identify a selective inhibitor of CLEC-2 using the small-molecule library. F1113 was identified as an antagonist of platelet aggregation mediated by CLEC-2 and GPVI, this is probably by inhibiting a common kinase in their signalling pathway when dose in micromolar range. However, this was not an unexpected outcome because of the intrinsic challenges in identifying small molecules able to prevent PPI, owing to their low affinity compared to the protein ligand, in this case, rhodocytin. To increase the likelihood of identifying potential small-molecule inhibitors of CLEC-2, it is necessary to screen compounds with higher chemical diversity; for instance, natural compounds, or larger molecules, based on the criteria specified in the Lipinski's rule of five (Lipinski, Lombardo et al. 2001).

Does the Generation of Biologics Represent an Alternative to Targeting CLEC-2?

Chapter 5 focuses on the generation of novel ligands of CLEC-2 using recombinant nanobodies, the smallest antibody-based proteins known to date. Nanobodies generated against CLEC-2 are superior to small molecules because their activity is in the nanomolar range, and thus

they are 1000 times more potent than small molecules. Therefore, they overcome the low affinity challenges observed for small molecules. Furthermore, they are suitable for the engineering process because they can be dimerised using amino acid linkers, which greatly increases the affinity between the ligand and the receptor, maintaining their blocking effect.

This study also highlights the relevance of oligomeric external linkers to induce platelet aggregation because they promote CLEC-2 clustering. This was evidenced by the fact that rhodocytin (tetramer), katacine (mix of oligomers), and LUAS-4 (tetramer) induced strong platelet aggregation, whereas monomeric and dimeric ligands, such as AYP1 F(ab)₂ and LUAS-2, were unable to. These findings provide a new insight into the minimum size of the ligand (likely a tetramer) to crosslink CLEC-2 and induce platelet aggregation.

A model depicting the possible activation mechanism of CLEC-2 by divalent or tetravalent ligands is illustrated in **Figure 48A-B**. However, multiple combinations may be involved based on the hypothesis that CLEC-2 is present in the membrane as a mixture of monomers and dimers, suggested on the basis of FCS findings (performed by Dr Clark). This is relevant to understand the stoichiometry of CLEC-2 and their ligands.

A few potential mechanisms of CLEC-2 activation by a divalent ligand are as follows:

- 1) A dimeric ligand binds to two single CLEC-2.
- 2) A dimeric ligand binds to two dimeric CLEC-2, probably formed by an intracellular linker, such as Syk.
- 3) A dimeric ligand binds to a monomeric CLEC-2 and one dimeric CLEC-2 in the membrane.

None of the presented models would lead to platelet aggregation as suggested by the present experimental data. The potential mechanisms of platelet aggregation mediated in the presence of a tetrameric ligand are as follows:

- 1) A tetrameric ligand binds to four monomeric CLEC-2.
- 2) A tetrameric ligand binds to four dimeric CLEC-2, thus clustering at least eight receptors.
- 3) A tetrameric ligand binds to a combination of monomeric and dimeric CLEC-2.

These models are entirely stochastic, and the reality *in vivo* would depend on a number of factors, including the proximity of the initial CLEC-2 that the ligand binds, receptor density in the platelet membrane, and how many of them are previously conjugated by an intracellular linker (e.g.: tyrosine kinases, as Syk bridging two single receptors). The models proposed here are based on a single ligand, as a fixed condition, to ensure simplicity and to provide an insight into the stoichiometry between the ligands and the CLEC-2 receptor. Furthermore, stoichiometric studies may also contribute to the study of the

other ITAM receptors on the platelet membrane, such as Fc γ RIIA, which is also activated by the tetravalent ligand PF4. This promotes activation of human platelets and leads to complex clinical conditions such as heparin-induced thrombocytopenia (HIT) and vaccine-induced immune thrombotic thrombocytopenia (VITT; **Figure 48C**).

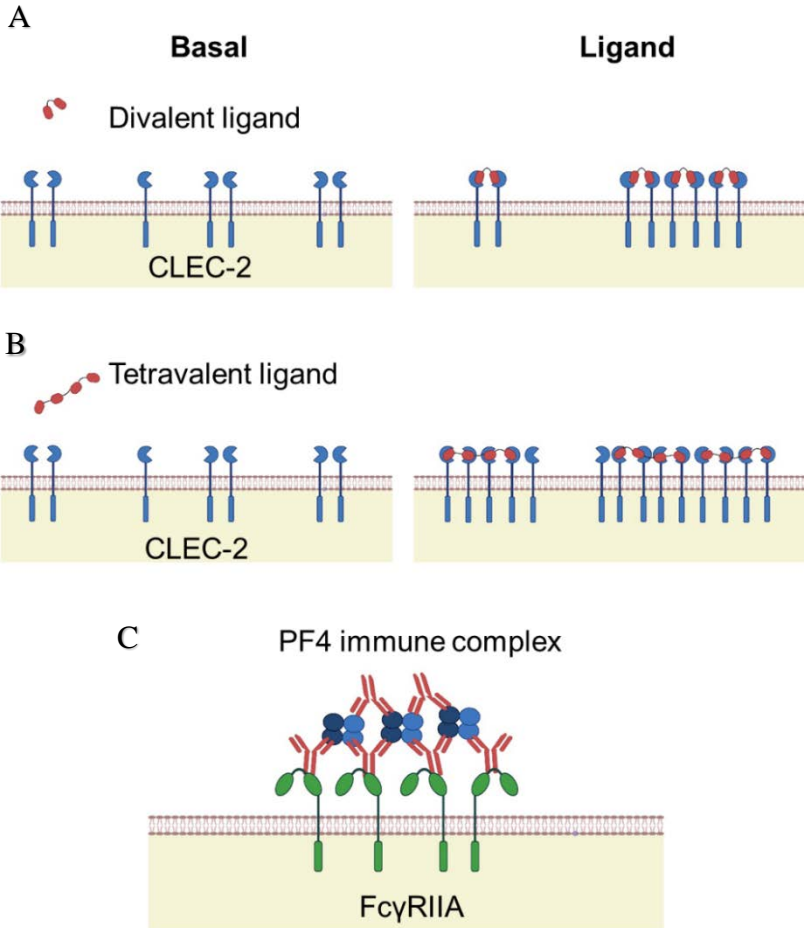


Figure 48. Schematic representation of a potential mechanism of activation caused by divalent ligands, tetravalent ligands, or the tetrameric complex PF4/FcγRIIA in vaccine-induced immune thrombotic thrombocytopenia (VITT).

In addition to investigating the role of external linkers in CLEC-2, an exploration of the role of intracellular linkers such as Syk or Src in the formation of CLEC-2 clusters would be interesting. However, it was not included in the present study. Clustering of CLEC-2 is likely a finely orchestrated event between extracellular and intracellular linkers. Further research into this dynamic interplay may inform the development of antagonists of CLEC-2 in the future.

Platelet Aggregate Stability: Is This Property Dependent on ITAM Tyrosine Kinases?

Chapter 6 focused on investigating whether the tyrosine kinases involved in the hemITAM signalling pathway play a role in maintaining aggregate stability by stimulating the CLEC-2 signalling pathway. These experiments were extended to also include other related receptors, including the collagen receptor GPVI and the non-ITAM thrombin receptor PAR-1.

LTA showed that Src plays a minor role in the stability of platelet aggregates formed by CLEC-2, GPVI, and PAR-1 in the absence of shear force. This role of Src may be mediated by a mechanism independent of CLEC-2 or GPVI and may be associated with a lack of outside-in signalling by the integrin $\alpha\text{IIb}\beta\text{III}$, which serves to consolidate the aggregates through an Src kinase-dependent process as proposed by Auger and Watson (Auger and Watson 2008). However, it was also observed that $\alpha\text{IIb}\beta\text{III}$ activation was completely reversed by

Src and Syk inhibitors in diluted platelets, suggesting the presence of additional interactions in supporting aggregation. Brass et al. have suggested that a number of proteins on the cell membrane participate in thrombus growth and stability (Brass, Zhu et al. 2008); CLEC-2 has also been suggested to promote platelet stability by a mechanism independent of the ITAM motif. These findings may explain why the thrombi remain stable when the tyrosine kinases are blocked.

However, the present finding is contrary to the findings reported in the literature, where complete disaggregation is observed under arterial shear conditions using flow adhesion assays. This may be a consequence of the fact that platelets are spread on a flat surface on the adhesion assay and the higher shear contributes to the disruption of the thrombus. Shear forces are nearly absent in the LTA conditions used in our assay.

The main limitation of the present study is the fact that the disaggregation experiment was only monitored in the absence of shear force, which may not entirely represent the physiological conditions; however, this model may better represent a phenomenon that occurs in venous thrombosis, in which shear force is considerably lower than that in arterial thrombosis. This is noteworthy because CLEC-2 has been observed to play a major role in venous thrombosis; therefore, we speculate that venous thrombi are characterised by higher stability, which highlights the importance of incorporating a destabilisation approach to target this type of thrombotic complication.

In conclusion, CLEC-2, which is associated with thrombus stability, is a noteworthy target for the treatment of thromboinflammatory conditions. The development of novel ligands may further our understanding of the activation mechanisms of the receptor, which is critical for the systematic development of novel, efficient inhibitors.

CHAPTER 9

CONCLUSIONS

9. Conclusions

9.1. Generation of new CLEC-2 ligands, based on calcium release or an ALPHA Screen assay in HTS format, using a small molecule based chemical library

- The generation of small molecule inhibitors against CLEC-2 and podoplanin is challenging due to the predicted low affinity and avidity of small molecules to prevent the multiple interactions between a protein ligand and CLEC-2.
- We have identified a small molecule inhibitor, F1113, able to prevent CLEC-2 and GPVI signalling. Small molecule ligands have the potential to inhibit kinase involved in downstream signalling, rather than preventing direct ligand and receptor binding.
- We have identified katacine, a new CLEC-2 agonist derived from natural products, with an oligomeric nature and a potential non-canonical binding site on CLEC-2.

9.2. Evaluation of the activation mode of CLEC-2 using novel multimeric nanobodies

- We have generated three new reagents for the study of CLEC-2 function, with different degrees of oligomerisation, based on the nanobody sequence of LUAS.

- Dimeric ligands of CLEC-2, such as AYP1 Fab2 and LUAS-2 are potent inhibitors of CLEC-2 in human platelets; however, in systems with highly expressed copies of CLEC-2 a potential activation of the receptor may be observed.
- Tetrameric ligands can induce enough clustering of CLEC-2 to induce human platelet aggregation through CLEC-2.

9.3. The role of tyrosine kinases in thrombus stability.

- Tyrosine kinase phosphorylation can be reversed in human platelets by tyrosine kinase inhibitors.
- Platelet aggregation is an irreversible process under low shear conditions used in a platelet aggregation assay, in contrast with platelet aggregation reversal observed by other researchers under high shear flow conditions.
- Src kinase inhibitors contribute to platelet stability, but most likely due to an effect independent of the ITAM signalling.

10. References

Ahmed, M. U., V. Kaneva, S. Loyau, D. Nechipurenko, N. Receveur, M. Le Bris, E. Janus-Bell, M. Didelot, A. Rauch and S. Susen (2020). "Pharmacological blockade of glycoprotein VI promotes thrombus disaggregation in the absence of thrombin." Arteriosclerosis, Thrombosis, and Vascular Biology **40**(9): 2127-2142.

Ahmed, M. U., V. Kaneva, S. Loyau, D. Nechipurenko, N. Receveur, M. Le Bris, E. Janus-Bell, M. Didelot, A. Rauch, S. Susen, N. Chakfe, F. Lanza, E. E. Gardiner, R. K. Andrews, M. Panteleev, C. Gachet, M. Jandrot-Perrus and P. H. Mangin (2020). "Pharmacological Blockade of Glycoprotein VI Promotes Thrombus Disaggregation in the Absence of Thrombin." Arterioscler Thromb Vasc Biol **40**(9): 2127-2142.

Andre, P., T. Morooka, D. Sim, K. Abe, C. Lowell, N. Nanda, S. Delaney, G. Siu, Y. Yan and S. Hollenbach (2011). "Critical role for Syk in responses to vascular injury." Blood, The Journal of the American Society of Hematology **118**(18): 5000-5010.

Arkin, M. R., Y. Tang and J. A. Wells (2014). "Small-molecule inhibitors of protein-protein interactions: progressing toward the reality." Chem Biol **21**(9): 1102-1114.

Asaadi, Y., F. F. Jouneghani, S. Janani and F. Rahbarizadeh (2021). "A comprehensive comparison between camelid nanobodies and single chain variable fragments." Biomarker Research **9**(1).

Auger, J. M. and S. P. Watson (2008). "Dynamic tyrosine kinase-regulated signaling and actin polymerisation mediate aggregate stability under shear." Arterioscler Thromb Vasc Biol **28**(8): 1499-1504.

Behnke, O. (1967). "Electron microscopic observations on the membrane systems of the rat blood platelet." Anat Rec **158**(2): 121-137.

Bender, M., F. May, V. Lorenz, I. Thielmann, I. Hagedorn, B. A. Finney, T. Vogtle, K. Remer, A. Braun, M. Bosl, S. P. Watson and B. Nieswandt (2013). "Combined in vivo depletion of glycoprotein VI and C-type lectin-like receptor 2 severely compromises hemostasis and abrogates arterial thrombosis in mice." Arterioscler Thromb Vasc Biol **33**(5): 926-934.

Bennett, J. S. (2005). "Structure and function of the platelet integrin alphaIIb beta3." J Clin Invest **115**(12): 3363-3369.

Bergmeier, W., D. Bouvard, J. A. Eble, R. Mokhtari-Nejad, V. Schulte, H. Zirngibl, C. Brakebusch, R. Fassler and B. Nieswandt (2001). "Rhodocytin (aggrexin) activates platelets lacking alpha(2)beta(1) integrin, glycoprotein VI, and the ligand-binding domain of glycoprotein Ibalpha." J Biol Chem **276**(27): 25121-25126.

Bernard, J. and J. P. Soulier (1948). "On a new variety of congenital thrombocytary hemo-ragiparous dystrophy." Sem Hop **24**(Spec. No.): 3217-3223.

Boulaftali, Y., P. R. Hess, T. M. Getz, A. Cholka, M. Stolla, N. Mackman, A. P. Owens, 3rd, J. Ware, M. L. Kahn and W. Bergmeier (2013). "Platelet ITAM signaling is critical for vascular integrity in inflammation." J Clin Invest **123**(2): 908-916.

Boulaftali, Y., P. R. Hess, M. L. Kahn and W. Bergmeier (2014). "Platelet immunoreceptor tyrosine-based activation motif (ITAM) signaling and vascular integrity." Circ Res **114**(7): 1174-1184.

Bourne, J. H., M. Colicchia, Y. Di, E. Martin, A. Slater, L. T. Roumenina, J. D. Dimitrov, S. P. Watson and J. Rayes (2021). "Heme induces human and mouse platelet activation through C-type-lectin-like receptor-2." Haematologica **106**(2): 626-629.

Brass, L. F., L. Zhu and T. J. Stalker (2008). "Novel therapeutic targets at the platelet vascular interface." Arteriosclerosis, thrombosis, and vascular biology **28**(3): s43-s50.

- Buchwald, P. (2010). "Small-molecule protein-protein interaction inhibitors: therapeutic potential in light of molecular size, chemical space, and ligand binding efficiency considerations." IUBMB Life **62**(10): 724-731.
- Bult, H. and I. L. Bonta (1977). "Comparison of the mediator release from platelets and the development of acute inflammation in rats which lack prostaglandin precursors." Agents Actions Suppl **2**: 47-59.
- Burkhart, J. M., M. Vaudel, S. Gambaryan, S. Radau, U. Walter, L. Martens, J. Geiger, A. Sickmann and R. P. Zahedi (2012). "The first comprehensive and quantitative analysis of human platelet protein composition allows the comparative analysis of structural and functional pathways." Blood **120**(15): e73-82.
- Chang, Y. W., P. W. Hsieh, Y. T. Chang, M. H. Lu, T. F. Huang, K. Y. Chong, H. R. Liao, J. C. Cheng and C. P. Tseng (2015). "Identification of a novel platelet antagonist that binds to CLEC-2 and suppresses podoplanin-induced platelet aggregation and cancer metastasis." Oncotarget **6**(40): 42733-42748.
- Chen, Y., Z. M. Ruggeri and X. Du (2018). "14-3-3 proteins in platelet biology and glycoprotein Ib-IX signaling." Blood **131**(22): 2436-2448.
- Clark, R. B., B. J. Knoll and R. Barber (1999). "Partial agonists and G protein-coupled receptor desensitization." Trends Pharmacol Sci **20**(7): 279-286.
- Clemetson, K. J. and J. M. Clemetson (1995). "Platelet GPIb-V-IX complex. Structure, function, physiology, and pathology." Semin Thromb Hemost **21**(2): 130-136.
- Cossins, B. P. and A. D. G. Lawson (2015). "Small Molecule Targeting of Protein-Protein Interactions through Allosteric Modulation of Dynamics." Molecules **20**(9): 16435-16445.

Cusack, N. J. and S. M. Hourani (1981). "Partial agonist behaviour of adenosine 5'-O-(2-thiodiphosphate) on human platelets." Br J Pharmacol **73**(2): 405-408.

Damaskinaki, F. N., L. A. Moran, A. Garcia, B. Kellam and S. P. Watson (2021). "Overcoming challenges in developing small molecule inhibitors for GPVI and CLEC-2." Platelets **32**(6): 744-752.

De Luca, L., F. E. Agharbaoui, R. Gitto, M. R. Buemi, F. Christ, Z. Debyser and S. Ferro (2016). "Rational Design, Synthesis and Evaluation of Coumarin Derivatives as Protein-protein Interaction Inhibitors." Mol Inform **35**(8-9): 460-473.

Dowal, L. and R. Flaumenhaft (2010). "Targeting platelet G-protein coupled receptors (GPCRs): looking beyond conventional GPCR antagonism." Curr Vasc Pharmacol **8**(2): 140-154.

Duchemin, A. M., L. K. Ernst and C. L. Anderson (1994). "Clustering of the high affinity Fc receptor for immunoglobulin G (Fc gamma RI) results in phosphorylation of its associated gamma-chain." J Biol Chem **269**(16): 12111-12117.

Eglen, R. M., T. Reisine, P. Roby, N. Rouleau, C. Illy, R. Bosse and M. Bielefeld (2008). "The use of AlphaScreen technology in HTS: current status." Curr Chem Genomics **1**: 2-10.

Engelmann, B. and S. Massberg (2013). "Thrombosis as an intravascular effector of innate immunity." Nat Rev Immunol **13**(1): 34-45.

Escolar, G., E. Leistikow and J. G. White (1989). "The fate of the open canalicular system in surface and suspension-activated platelets." Blood **74**(6): 1983-1988.

Escolar, G., I. Lopez-Vilchez, M. Diaz-Ricart, J. G. White and A. M. Galan (2008). "Internalization of tissue factor by platelets." Thromb Res **122 Suppl 1**: S37-41.

- Fan, Y., M. Jiang, D. Gong and C. Zou (2016). "Efficacy and safety of low-molecular-weight heparin in patients with sepsis: a meta-analysis of randomized controlled trials." Sci Rep **6**: 25984.
- Feng, W., M. Valiyaveetil, T. Dudiki, G. H. Mahabeleshwar, P. Andre, E. A. Podrez and T. V. Byzova (2017). "beta3 phosphorylation of platelet alphaIIb beta3 is crucial for stability of arterial thrombus and microparticle formation in vivo." Thromb J **15**: 22.
- Ferreira, S. H., F. B. Ubatuba and J. R. Vane (1976). "Platelets, acute inflammation and inflammatory mediators." Agents Actions **6**(1-3): 313-317.
- Fitch-Tewfik, J. L. and R. Flaumenhaft (2013). "Platelet granule exocytosis: a comparison with chromaffin cells." Front Endocrinol (Lausanne) **4**: 77.
- Gachet, C., B. Hechler, C. Leon, C. Vial, C. Leray, P. Ohlmann and J. P. Cazenave (1997). "Activation of ADP receptors and platelet function." Thromb Haemost **78**(1): 271-275.
- Garcia Rodriguez, L. A., M. Martin-Perez, C. H. Hennekens, P. M. Rothwell and A. Lanus (2016). "Bleeding Risk with Long-Term Low-Dose Aspirin: A Systematic Review of Observational Studies." PLoS One **11**(8): e0160046.
- Gitz, E., A. Y. Pollitt, J. J. Gitz-Francois, O. Alshehri, J. Mori, S. Montague, G. B. Nash, M. R. Douglas, E. E. Gardiner, R. K. Andrews, C. D. Buckley, P. Harrison and S. P. Watson (2014). "CLEC-2 expression is maintained on activated platelets and on platelet microparticles." Blood **124**(14): 2262-2270.
- Gorog, D. A. (2018). "Potentiation of thrombus instability: a contributory mechanism to the effectiveness of antithrombotic medications." J Thromb Thrombolysis **45**(4): 593-602.

Gorog, D. A., Z. A. Fayad and V. Fuster (2017). "Arterial Thrombus Stability: Does It Matter and Can We Detect It?" J Am Coll Cardiol **70**(16): 2036-2047.

Gremmel, T., A. L. Frelinger, 3rd and A. D. Michelson (2016). "Platelet Physiology." Semin Thromb Hemost **42**(3): 191-204.

Guha, S., S. Mookerjee, P. Guha, P. Sardar, S. Deb, P. D. Roy, R. Karmakar, S. Mani, M. B. Hema, S. Pyne, P. Chakraborti, P. K. Deb, P. Lahiri and U. Chaudhuri (2009). "Antiplatelet drug resistance in patients with recurrent acute coronary syndrome undergoing conservative management." Indian Heart J **61**(4): 348-352.

Haining, E. J., D. Cherpokova, K. Wolf, I. C. Becker, S. Beck, J. A. Eble, D. Stegner, S. P. Watson and B. Nieswandt (2017). "CLEC-2 contributes to hemostasis independently of classical hemITAM signaling in mice." Blood **130**(20): 2224-2228.

Hamers-Casterman, C., T. Atarhouch, S. Muyldermans, G. Robinson, C. Hamers, E. B. Songa, N. Bendahman and R. Hamers (1993). "Naturally occurring antibodies devoid of light chains." Nature **363**(6428): 446-448.

Harrison, P., B. Wilbourn, N. Debili, W. Vainchenker, J. Breton-Gorius, A. S. Lawrie, J. M. Masse, G. F. Savidge and E. M. Cramer (1989). "Uptake of plasma fibrinogen into the alpha granules of human megakaryocytes and platelets." Journal of Clinical Investigation **84**(4): 1320-1324.

Hughes, C. E., A. Y. Pollitt, J. Mori, J. A. Eble, M. G. Tomlinson, J. H. Hartwig, C. A. O'Callaghan, K. Futterer and S. P. Watson (2010). "CLEC-2 activates Syk through dimerization." Blood **115**(14): 2947-2955.

Hughes, C. E., A. Y. Pollitt, J. Mori, J. A. Eble, M. G. Tomlinson, J. H. Hartwig, C. A. O'Callaghan, K. Fütterer and S. P. Watson (2010).

- "CLEC-2 activates Syk through dimerization." Blood **115**(14): 2947-2955.
- Iba, T., M. Arakawa, J. H. Levy, K. Yamakawa, H. Koami, T. Hifumi and K. Sato (2018). "Sepsis-Induced Coagulopathy and Japanese Association for Acute Medicine DIC in Coagulopathic Patients with Decreased Antithrombin and Treated by Antithrombin." Clin Appl Thromb Hemost **24**(7): 1020-1026.
- Izquierdo, I., M. N. Barrachina, L. Hermida-Nogueira, V. Casas, L. A. Moran, S. Lacerenza, R. Pinto-Llorente, J. A. Eble, V. de Los Rios, E. Dominguez, M. I. Loza, J. I. Casal, M. Carrascal, J. Abian and A. Garcia (2020). "A Comprehensive Tyrosine Phosphoproteomic Analysis Reveals Novel Components of the Platelet CLEC-2 Signaling Cascade." Thromb Haemost **120**(2): 262-276.
- Jackson, S. P. (2007). "The growing complexity of platelet aggregation." Blood **109**(12): 5087-5095.
- Jandrot-Perrus, M., A. H. Lagrue, M. Okuma and C. Bon (1997). "Adhesion and activation of human platelets induced by convulxin involve glycoprotein VI and integrin alpha2beta1." J Biol Chem **272**(43): 27035-27041.
- Jones, S. and J. M. Thornton (1996). "Principles of protein-protein interactions." Proc Natl Acad Sci U S A **93**(1): 13-20.
- Kanaji, S., T. Kanaji, K. Furihata, K. Kato, J. L. Ware and T. J. Kunicki (2003). "Convulxin binds to native, human glycoprotein Ib alpha." J Biol Chem **278**(41): 39452-39460.
- Kinjo, M., H. Sakata and S. Mikuni (2011). "First steps for fluorescence correlation spectroscopy of living cells." Cold Spring Harb Protoc **2011**(10): 1185-1189.
- Klinger, M. H. (1997). "Platelets and inflammation." Anat Embryol (Berl) **196**(1): 1-11.

Knight, C. G., L. F. Morton, D. J. Onley, A. R. Peachey, T. Ichinohe, M. Okuma, R. W. Farndale and M. J. Barnes (1999). "Collagen-platelet interaction: Gly-Pro-Hyp is uniquely specific for platelet Gp VI and mediates platelet activation by collagen." Cardiovasc Res **41**(2): 450-457.

Knoebl, P., S. Cataland, F. Peyvandi, P. Coppo, M. Scully, J. A. Kremer Hovinga, A. Metjian, J. de la Rubia, K. Pavenski, J. Minkue Mi Edou, H. De Winter and F. Callewaert (2020). "Efficacy and safety of open-label caplacizumab in patients with exacerbations of acquired thrombotic thrombocytopenic purpura in the HERCULES study." J Thromb Haemost **18**(2): 479-484.

Kunita, A., T. G. Kashima, A. Ohazama, A. E. Grigoriadis and M. Fukayama (2011). "Podoplanin is regulated by AP-1 and promotes platelet aggregation and cell migration in osteosarcoma." Am J Pathol **179**(2): 1041-1049.

Lee, R. H. and W. Bergmeier (2016). "Platelet immunoreceptor tyrosine-based activation motif (ITAM) and hemITAM signaling and vascular integrity in inflammation and development." J Thromb Haemost **14**(4): 645-654.

Lin, C., Y. Zhang, X. Zhu, S. Cui, Y. Cao, R. Li and L. Wang (2020). "The study of killing effect and inducing apoptosis of 630-nm laser on lung adenocarcinoma A549 cells mediated by hematoporphyrin derivatives in vitro." Lasers Med Sci **35**(1): 71-78.

Logothetis, C. N., A. Patel, J. Eatrises, M. Jaglal, M. Haider, N. Visweshwar and D. A. Laber (2021). "Post Approval Experience with Caplacizumab for Acquired Thrombotic Thrombocytopenic Purpura at a Single Institution." J Clin Med **10**(15).

Lu, H. Y., Q. D. Zhou, J. He, Z. L. Jiang, C. Peng, R. S. Tong and J. Y. Shi (2020). "Recent advances in the development of protein-protein interactions modulators: mechanisms and clinical trials." Signal Transduction and Targeted Therapy **5**(1).

Machan, R. and T. Wohland (2014). "Recent applications of fluorescence correlation spectroscopy in live systems." *FEBS Lett* **588**(19): 3571-3584.

Maiese, A., G. Passaro, A. Matteis, V. Fazio, R. Raffaele and M. D. Paolo (2020). "Thromboinflammatory response in SARS-CoV-2 sepsis." *Med Leg J* **88**(2): 78-80.

Mangin, P. H., M.-B. Onselaer, N. Receveur, N. Le Lay, A. T. Hardy, C. Wilson, X. Sanchez, S. Loyau, A. Dupuis and A. K. Babar (2018). "Immobilized fibrinogen activates human platelets through glycoprotein VI." *haematologica* **103**(5): 898.

Martin, E. M., M. Zuidscherwoude, L. A. Moran, Y. Di, A. Garcia and S. P. Watson (2021). "The structure of CLEC-2: mechanisms of dimerization and higher-order clustering." *Platelets* **32**(6): 733-743.

Martin, E. M., M. Zuidscherwoude, L. A. Moran, Y. Di, A. Garcia and S. P. Watson (2021). "The structure of CLEC-2: mechanisms of dimerization and higher-order clustering." *Platelets*: 1-11.

Martinez, J. T., G. Fernandez and H. Vazquez-Leon (1966). "Clinical evaluation of new therapeutic concepts in septic shock." *Obstet Gynecol* **27**(2): 296-301.

Martyanov, A. A., F. A. Balabin, J. L. Dunster, M. A. Pantelev, J. M. Gibbins and A. N. Sveshnikova (2020). "Control of Platelet CLEC-2-Mediated Activation by Receptor Clustering and Tyrosine Kinase Signaling." *Biophys J* **118**(11): 2641-2655.

May, F., I. Hagedorn, I. Pleines, M. Bender, T. Vogtle, J. Eble, M. Elvers and B. Nieswandt (2009). "CLEC-2 is an essential platelet-activating receptor in hemostasis and thrombosis." *Blood* **114**(16): 3464-3472.

McNeil, J. J., R. Wolfe, R. L. Woods, A. M. Tonkin, G. A. Donnan, M. R. Nelson, C. M. Reid, J. E. Lockery, B. Kirpach, E. Storey, R. C. Shah, J. D. Williamson, K. L. Margolis, M. E. Ernst, W. P. Abhayaratna, N.

Stocks, S. M. Fitzgerald, S. G. Orchard, R. E. Trevaks, L. J. Beilin, C. I. Johnston, J. Ryan, B. Radziszewska, M. Jelinek, M. Malik, C. B. Eaton, D. Brauer, G. Cloud, E. M. Wood, S. E. Mahady, S. Satterfield, R. Grimm, A. M. Murray and A. I. Group (2018). "Effect of Aspirin on Cardiovascular Events and Bleeding in the Healthy Elderly." N Engl J Med **379**(16): 1509-1518.

Meade, T. W., P. J. Roderick, P. J. Brennan, H. C. Wilkes and C. C. Kelleher (1992). "Extra-cranial bleeding and other symptoms due to low dose aspirin and low intensity oral anticoagulation." Thromb Haemost **68**(1): 1-6.

Merten, M. and P. Thiagarajan (2000). "P-selectin expression on platelets determines size and stability of platelet aggregates." Circulation **102**(16): 1931-1936.

Michino, M., C. A. Boateng, P. Donthamsetti, H. Yano, O. M. Bakare, A. Bonifazi, M. P. Ellenberger, T. M. Keck, V. Kumar, C. Zhu, R. Verma, J. R. Deschamps, J. A. Javitch, A. H. Newman and L. Shi (2017). "Toward Understanding the Structural Basis of Partial Agonism at the Dopamine D3 Receptor." J Med Chem **60**(2): 580-593.

Moreira, I. S., P. A. Fernandes and M. J. Ramos (2007). "Hot spots-A review of the protein-protein interface determinant amino-acid residues." Proteins-Structure Function and Bioinformatics **68**(4): 803-812.

Nagae, M., K. Morita-Matsumoto, M. Kato, M. K. Kaneko, Y. Kato and Y. Yamaguchi (2014). "A platform of C-type lectin-like receptor CLEC-2 for binding O-glycosylated podoplanin and nonglycosylated rhodocytin." Structure **22**(12): 1711-1721.

Nelson, A. L. (2010). "Antibody fragments: hope and hype." MAbs **2**(1): 77-83.

Nieswandt, B., M. Moser, I. Pleines, D. Varga-Szabo, S. Monkley, D. Critchley and R. Fassler (2007). "Loss of talin1 in platelets abrogates

integrin activation, platelet aggregation, and thrombus formation in vitro and in vivo." J Exp Med **204**(13): 3113-3118.

Offermanns, S. (2006). "Activation of platelet function through G protein-coupled receptors." Circ Res **99**(12): 1293-1304.

Oishi, S., N. Tsukiji, S. Otake, N. Oishi, T. Sasaki, T. Shirai, Y. Yoshikawa, K. Takano, H. Shinmori, T. Inukai, T. Kondo and K. Suzuki-Inoue (2021). "Heme activates platelets and exacerbates rhabdomyolysis-induced acute kidney injury via CLEC-2 and GPVI/FcRgamma." Blood Adv **5**(7): 2017-2026.

Ozaki, Y., N. Asazuma, K. Suzuki-Inoue and M. C. Berndt (2005). "Platelet GPIb-IX-V-dependent signaling." J Thromb Haemost **3**(8): 1745-1751.

Page, C. P. (1989). "Platelets as Inflammatory Cells." Immunopharmacology **17**(1): 51-59.

Pagliari, L., J. Felding, K. Audouze, S. J. Nielsen, R. B. Terry, C. Krogh-Jensen and S. Butcher (2004). "Emerging classes of protein-protein interaction inhibitors and new tools for their development." Curr Opin Chem Biol **8**(4): 442-449.

Palacios-Acedo, A. L., D. Mege, L. Crescence, F. Dignat-George, C. Dubois and L. Panicot-Dubois (2019). "Platelets, Thrombo-Inflammation, and Cancer: Collaborating With the Enemy." Front Immunol **10**: 1805.

Palanques-Pastor, T., J. E. Megias-Vericat, V. Boso Ribelles, I. Gomez Seguí and J. L. Poveda Andres (2021). "Effectiveness of Caplacizumab Nanobody in Acquired Thrombotic Thrombocytopenic Purpura Refractory to Conventional Treatment." Acta Haematol: 1-5.

Parguñña, A. F., J. Alonso, I. Rosa, P. Velez, M. J. Gonzalez-Lopez, E. Guitian, J. A. Eble, M. I. Loza and A. Garcia (2012). "A detailed proteomic analysis of rhodocytin-activated platelets reveals novel clues

on the CLEC-2 signalosome: implications for CLEC-2 signaling regulation." Blood **120**(26): e117-126.

Payne, H., T. Ponomaryov, S. P. Watson and A. Brill (2017). "Mice with a deficiency in CLEC-2 are protected against deep vein thrombosis." Blood **129**(14): 2013-2020.

Perrella, G., J. Huang, I. Provenzale, F. Swieringa, F. Heubel-Moenen, R. W. Farndale, M. Roest, P. E. J. van der Meijden, M. Thomas, R. A. S. Ariens, M. Jandrot-Perrus, S. P. Watson and J. W. M. Heemskerk (2021). "Nonredundant Roles of Platelet Glycoprotein VI and Integrin α IIb β 3 in Fibrin-Mediated Microthrombus Formation." Arterioscler Thromb Vasc Biol **41**(2): e97-e111.

Perrella, G., S. J. Montague, H. C. Brown, L. Garcia Quintanilla, A. Slater, D. Stegner, M. Thomas, J. W. M. Heemskerk and S. P. Watson (2022). "Role of Tyrosine Kinase Syk in Thrombus Stabilisation at High Shear." Int J Mol Sci **23**(1).

Pollitt, A. Y., B. Grygielska, B. Leblond, L. Désiré, J. A. Eble and S. P. Watson (2010). "Phosphorylation of CLEC-2 is dependent on lipid rafts, actin polymerization, secondary mediators, and Rac." Blood **115**(14): 2938-2946.

Pollitt, A. Y., N. S. Poulter, E. Gitz, L. Navarro-Nunez, Y. J. Wang, C. E. Hughes, S. G. Thomas, B. Nieswandt, M. R. Douglas, D. M. Owen, D. G. Jackson, M. L. Dustin and S. P. Watson (2014). "Syk and Src family kinases regulate C-type lectin receptor 2 (CLEC-2)-mediated clustering of podoplanin and platelet adhesion to lymphatic endothelial cells." J Biol Chem **289**(52): 35695-35710.

Poulter, N. S., A. Y. Pollitt, D. M. Owen, E. E. Gardiner, R. K. Andrews, H. Shimizu, D. Ishikawa, D. Bihan, R. W. Farndale, M. Moroi, S. P. Watson and S. M. Jung (2017). "Clustering of glycoprotein VI (GPVI) dimers upon adhesion to collagen as a mechanism to regulate GPVI signaling in platelets." J Thromb Haemost **15**(3): 549-564.

- Rayes, J., S. Lax, S. Wichaiyo, S. K. Watson, Y. Di, S. Lombard, B. Grygielska, S. W. Smith, K. Skordilis and S. P. Watson (2017). "The podoplanin-CLEC-2 axis inhibits inflammation in sepsis." Nat Commun **8**(1): 2239.
- Rayes, J., S. P. Watson and B. Nieswandt (2019). "Functional significance of the platelet immune receptors GPVI and CLEC-2." J Clin Invest **129**(1): 12-23.
- Redell, M. S., M. J. Ruiz, T. A. Alonzo, R. B. Gerbing and D. J. Tweardy (2011). "Stat3 signaling in acute myeloid leukemia: ligand-dependent and -independent activation and induction of apoptosis by a novel small-molecule Stat3 inhibitor." Blood **117**(21): 5701-5709.
- Ribatti, D. and E. Crivellato (2007). "Giulio Bizzozero and the discovery of platelets." Leuk Res **31**(10): 1339-1341.
- Rivera, J., M. L. Lozano, L. Navarro-Nunez and V. Vicente (2009). "Platelet receptors and signaling in the dynamics of thrombus formation." Haematologica **94**(5): 700-711.
- Schattner, M., C. N. Jenne, S. Negrotto and B. Ho-Tin-Noe (2020). "Editorial: Platelets and Immune Responses During Thromboinflammation." Front Immunol **11**: 1079.
- Scully, M., S. R. Cataland, F. Peyvandi, P. Coppo, P. Knobl, J. A. K. Hovinga, A. Metjian, J. de la Rubia, K. Pavenski, F. Callewaert, D. Biswas, H. De Winter, R. K. Zeldin and H. Investigators (2019). "Caplacizumab Treatment for Acquired Thrombotic Thrombocytopenic Purpura." New England Journal of Medicine **380**(4): 335-346.
- Semeraro, N., C. T. Ammollo, F. Semeraro and M. Colucci (2015). "Coagulopathy of Acute Sepsis." Semin Thromb Hemost **41**(6): 650-658.
- Severin, S., A. Y. Pollitt, L. Navarro-Nunez, C. A. Nash, D. Mourao-Sa, J. A. Eble, Y. A. Senis and S. P. Watson (2011). "Syk-dependent

phosphorylation of CLEC-2: a novel mechanism of hem-immunoreceptor tyrosine-based activation motif signaling." J Biol Chem **286**(6): 4107-4116.

Shin, Y. and T. Morita (1998). "Rhodocytin, a functional novel platelet agonist belonging to the heterodimeric C-type lectin family, induces platelet aggregation independently of glycoprotein Ib." Biochem Biophys Res Commun **245**(3): 741-745.

Shukla, A. K. (2019). "Structural Basis of Partial Agonism at the beta2-Adrenergic Receptor." Biochemistry **58**(3): 137-139.

Simmons, S. R., P. A. Sims and R. M. Albrecht (1997). "alpha IIb beta 3 redistribution triggered by receptor cross-linking." Arterioscler Thromb Vasc Biol **17**(11): 3311-3320.

Stalnikowicz-Darvasi, R. (1995). "Gastrointestinal bleeding during low-dose aspirin administration for prevention of arterial occlusive events. A critical analysis." J Clin Gastroenterol **21**(1): 13-16.

Suzuki-Inoue, K., G. L. Fuller, A. Garcia, J. A. Eble, S. Pohlmann, O. Inoue, T. K. Gartner, S. C. Hughan, A. C. Pearce, G. D. Laing, R. D. Theakston, E. Schweighoffer, N. Zitzmann, T. Morita, V. L. Tybulewicz, Y. Ozaki and S. P. Watson (2006). "A novel Syk-dependent mechanism of platelet activation by the C-type lectin receptor CLEC-2." Blood **107**(2): 542-549.

Suzuki-Inoue, K., O. Inoue, G. Ding, S. Nishimura, K. Hokamura, K. Eto, H. Kashiwagi, Y. Tomiyama, Y. Yatomi, K. Umemura, Y. Shin, M. Hirashima and Y. Ozaki (2010). "Essential in vivo roles of the C-type lectin receptor CLEC-2: embryonic/neonatal lethality of CLEC-2-deficient mice by blood/lymphatic misconnections and impaired thrombus formation of CLEC-2-deficient platelets." J Biol Chem **285**(32): 24494-24507.

Takagi, S., S. Sato, T. Oh-hara, M. Takami, S. Koike, Y. Mishima, K. Hatake and N. Fujita (2013). "Platelets promote tumor growth and

metastasis via direct interaction between Aggrus/podoplanin and CLEC-2." PLoS One **8**(8): e73609.

Taus, F., G. Salvagno, S. Cane, C. Fava, F. Mazzaferri, E. Carrara, V. Petrova, R. M. Barouni, F. Dima, A. Dalbeni, S. Romano, G. Poli, M. Benati, S. De Nitto, G. Mansueto, M. Iezzi, E. Tacconelli, G. Lippi, V. Bronte and P. Minuz (2020). "Platelets Promote Thromboinflammation in SARS-CoV-2 Pneumonia." Arterioscler Thromb Vasc Biol **40**(12): 2975-2989.

Trott, O. and A. J. Olson (2010). "AutoDock Vina: improving the speed and accuracy of docking with a new scoring function, efficient optimization, and multithreading." J Comput Chem **31**(2): 455-461.

Tsukiji, N., M. Osada, T. Sasaki, T. Shirai, K. Satoh, O. Inoue, N. Umetani, C. Mochizuki, T. Saito, S. Kojima, H. Shinmori, Y. Ozaki and K. Suzuki-Inoue (2018). "Cobalt hematoporphyrin inhibits CLEC-2-podoplanin interaction, tumor metastasis, and arterial/venous thrombosis in mice." Blood Adv **2**(17): 2214-2225.

Vogtle, T., D. Cherpokova, M. Bender and B. Nieswandt (2015). "Targeting platelet receptors in thrombotic and thrombo-inflammatory disorders." Hamostaseologie **35**(3): 235-243.

Vu, T. K., D. T. Hung, V. I. Wheaton and S. R. Coughlin (1991). "Molecular cloning of a functional thrombin receptor reveals a novel proteolytic mechanism of receptor activation." Cell **64**(6): 1057-1068.

Wang, Y., Y. Ouyang, B. Liu, X. Ma and R. Ding (2018). "Platelet activation and antiplatelet therapy in sepsis: A narrative review." Thromb Res **166**: 28-36.

Watson, A. A., C. M. Christou, J. R. James, A. E. Fenton-May, G. E. Moncayo, A. R. Mistry, S. J. Davis, R. J. Gilbert, A. Chakera and C. A. O'Callaghan (2009). "The platelet receptor CLEC-2 is active as a dimer." Biochemistry **48**(46): 10988-10996.

Watson, A. A., J. A. Eble and C. A. O'Callaghan (2008). "Crystal structure of rhodocytin, a ligand for the platelet-activating receptor CLEC-2." Protein Sci **17**(9): 1611-1616.

Weiss, H. J. and B. Lages (1997). "Platelet prothrombinase activity and intracellular calcium responses in patients with storage pool deficiency, glycoprotein IIb-IIIa deficiency, or impaired platelet coagulant activity- a comparison with Scott syndrome." Blood **89**(5): 1599-1611.

Wiviott, S. D., E. Braunwald, C. H. McCabe, G. Montalescot, W. Ruzyllo, S. Gottlieb, F. J. Neumann, D. Ardissino, S. De Servi, S. A. Murphy, J. Riesmeyer, G. Weerakkody, C. M. Gibson, E. M. Antman and T.-T. Investigators (2007). "Prasugrel versus clopidogrel in patients with acute coronary syndromes." N Engl J Med **357**(20): 2001-2015.

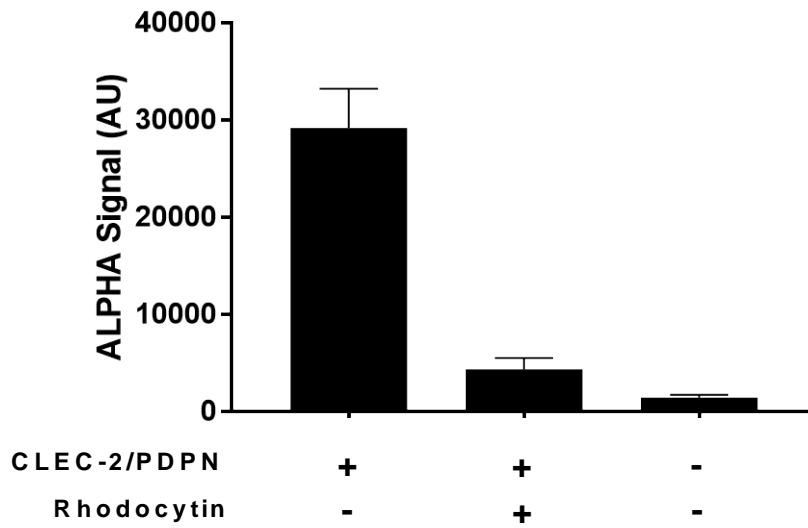
Woulfe, D. S. (2005). "Platelet G protein-coupled receptors in hemostasis and thrombosis." J Thromb Haemost **3**(10): 2193-2200.

Wu, Y., K. Suzuki-Inoue, K. Satoh, N. Asazuma, Y. Yatomi, M. C. Berndt and Y. Ozaki (2001). "Role of Fc receptor gamma-chain in platelet glycoprotein Ib-mediated signaling." Blood **97**(12): 3836-3845.

Zhou, Z., F. C. Gushiken, A. Bergeron, V. K. Vijayan, R. Rumbaut, J. A. Lopez and J. F. Dong (2010). "STAT3 Regulates Collagen-Induced Platelet Aggregation Independent of Its Transcription Factor Activity." Blood **116**(21): 73-73.

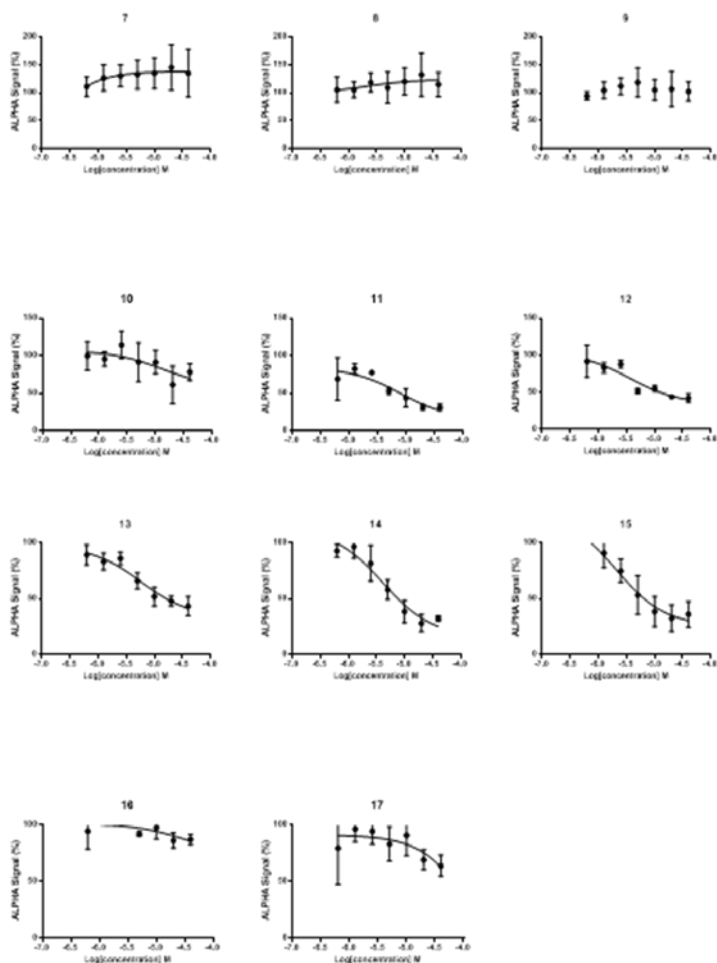
Zhu, X., M. Xu, X. Zhao, F. Shen, C. Ruan and Y. Zhao (2020). "The Detection of Plasma Soluble Podoplanin of Patients with Breast Cancer and Its Clinical Signification." Cancer Manag Res **12**: 13207-13214.

APPENDIX I



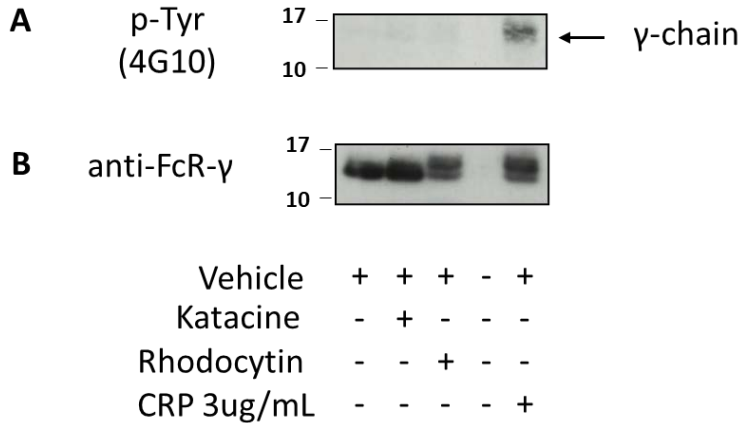
Rhodocytin prevents podoplanin-CLEC-2 interaction using ALPHA Screen assay. ALPHA Screen donor and acceptor beads were incubated with podoplanin and CLEC-2 and incubated with or without rhodocytin (100 nM), as an inhibition control. Donor and acceptor beads were also incubated without podoplanin and CLEC-2 to represent the background signal.

APPENDIX II



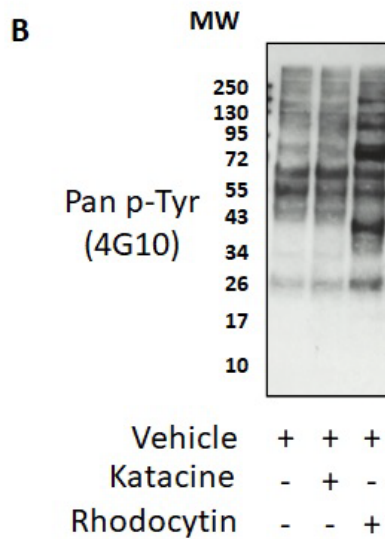
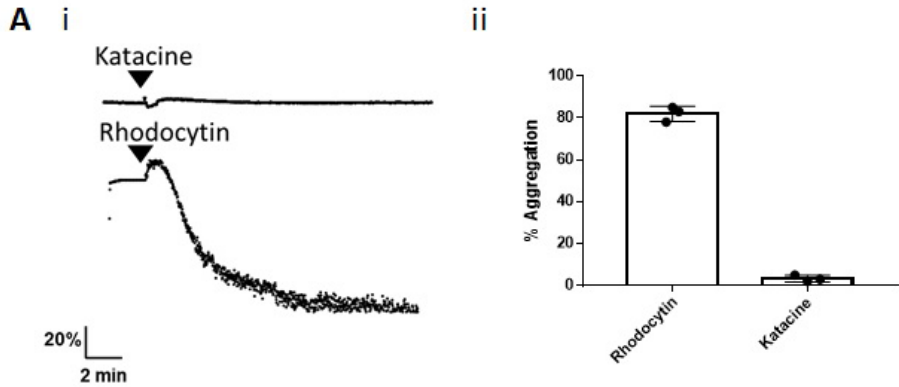
Dose response of compounds potential hits identified in the initial ALPHA screening. Concentration is represented in log scale. For most of these compounds IC50 was not calculated seems they don't fit to the dose response model used. Graphs were done using graphpad prism 7. Numbers from 7-17 were used as identifiers for each compound.

APPENDIX III



Katacine does not induce an increase in tyrosine phosphorylation levels of the FcR γ -chain in human platelets. A) Representative immunoblots of platelet lysates (4×10^8) stimulated with DMSO 0.1% (negative control), 100 nM rhodocytin, 10 μ M katacine, or 3 μ g/mL CRP (positive control). Lysates were run by SDS-PAGE and transferred to a PDVF membrane for western blotting against the anti-tyrosine antibody (4G10). B) The membrane was stripped and re-probed against the anti-FcR antibody (B).

APPENDIX IV



Katakine does not induce platelet aggregation or protein tyrosine phosphorylation in mouse platelets. A) Representative traces of mouse washed platelets (2×10^8 platelets/mL) stimulated with $10 \mu\text{M}$ katacine or 100nM rhodocytin. Aii) Column chart representing the mean aggregation \pm SD of three independent experiments. B) Representative immunoblots of mouse platelet lysates (4×10^8 platelets/mL) stimulated with 0.1% DMSO (negative control), 100 nM rhodocytin (positive control) or $10 \mu\text{M}$ katacine.

CLEC-2 Nb4 coding sequence (459 bp) (from 322-459 bp)

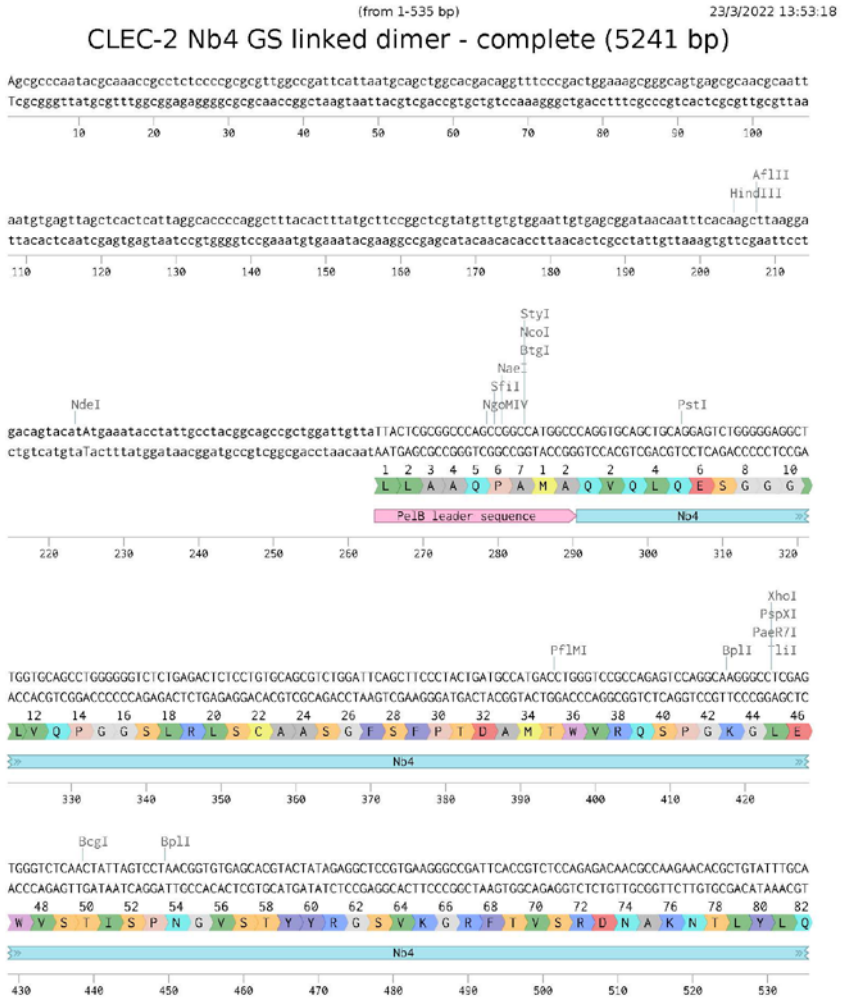
23/3/2022 13:52:37



https://benchling.com/eleyana/f/lib_8QFXPMYM-nanobodies/seq_9FBCXJ9L-clec-2-nb4-coding-sequence/edit

2/2

APPENDIX VI- dimeric Nb4 DNA sequence



https://benchling.com/veleyna/ff/lib_8QFXPFYM-nanobodies/seq_Dh8dyGR-clec-2-nb4-gs-linked-dimer-complete/edit

1/7

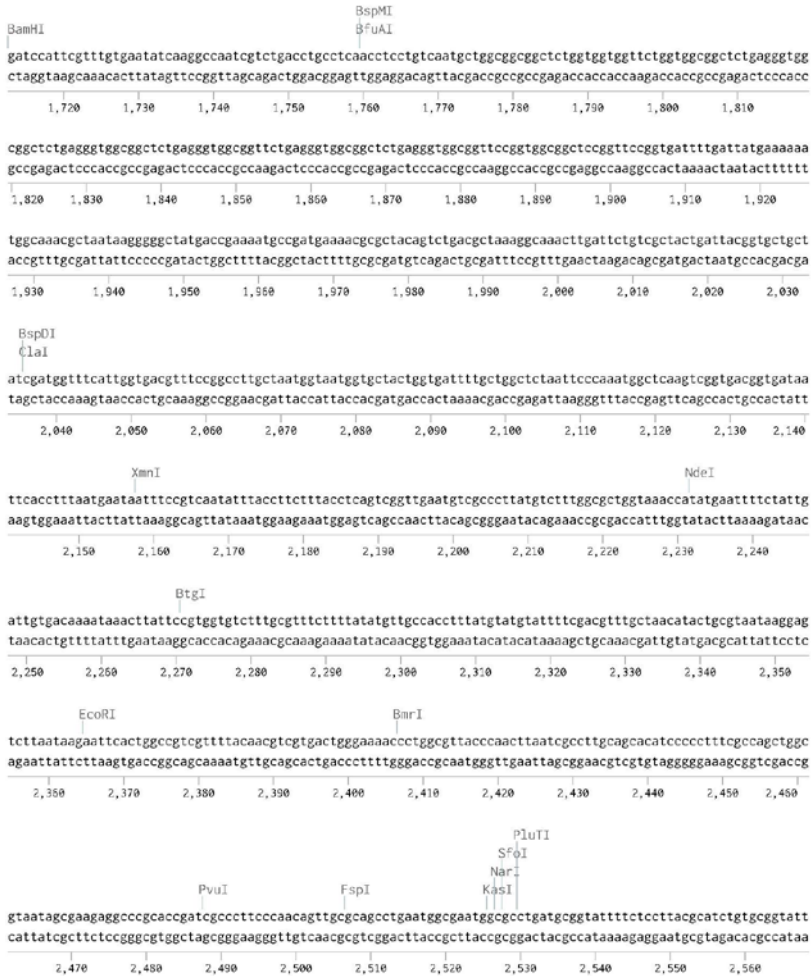


https://benchling.com/eleyyna/f/1ib_BQFXFMYM-nanobodies/seq_Oh8dy/GR-clec-2-nb4-gs-linked-dimer-complete/edit

2/7

CLEC-2 Nb4 GS linked dimer - complete (5241 bp) (from 1713-2568 bp)

23/3/2022 13:53:18

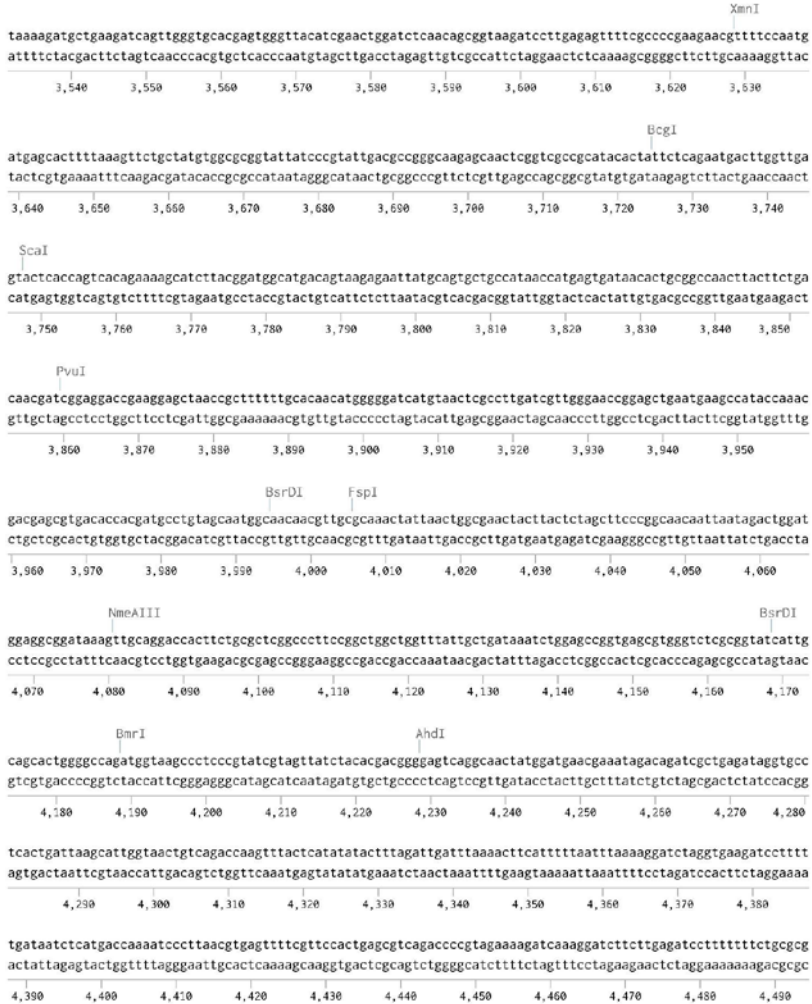


https://benchling.com/eleyana/f/1ib_BQFXFMYM-nanobodies/seq_Oh8dy/GR-clec-2-nb4-gs-linked-dimer-complete/edit

4/7

CLEC-2 Nb4 GS linked dimer - complete (5241 bp) (from 3532-4494 bp)

23/3/2022 13:53:18



https://benchling.com/eleyrna/f//lib_BQFXFMYM-nanobodies/seq_Oh8dy/GR-clec-2-nb4-gs-linked-dimer-complete/edit

6/7

CLEC-2 Nb4 GS linked dimer - complete (5241 bp) (from 4495-5241 bp)

23/3/2022 13:53:18

```

taatctgctgttgcacaacaaaccaccgctaccagcgggtttgtttgccggatcaagagctaccaactctttccgaaggtaactgcttcagcagagc
attagcgcgaacgtttgttttttgggtggcgtggtccaccaacaacggcctagtctcgtggttgagaaaaaggctccattgacgcaatgctcgc
4,500 4,510 4,520 4,530 4,540 4,550 4,560 4,570 4,580 4,590 4,600

cagataccaatactgtccttctagtgtagccgttagttagccaccactccaagaactctgtagcaccgccacatacctcgtctgtctaatcctgttaccagtgcc
4,610 4,620 4,630 4,640 4,650 4,660 4,670 4,680 4,690 4,700

tgctgccagtgccgataagctgtgtcttaccgggttggaactcaagcagatagttaccggataaggcgcagcggctgggctgaacggggggtctgtgcacacgccca
acgaggtcaccgctattcagcagaaatggcccaacctgagttctgctatacaatggcctattccgctcggcagccgacttgcccccaagcagctgtgtcgggt
4,710 4,720 4,730 4,740 4,750 4,760 4,770 4,780 4,790 4,800 4,810

gcttggagcgaacacacaccgaactgagatcacacagcgtgagctatgagaaagccacgcttcccgaaggagaaaaggcggacaggtatccgtaagcggc
cgaacctcgttctggtggtggtgactctatggatgctgactcgtatactcttccgggtgcgaaggcttccctcttccgctgtccatagccatcgcgc
4,820 4,830 4,840 4,850 4,860 4,870 4,880 4,890 4,900 4,910 4,920

agggtcggaaacaggagagcgcaggggagcttcaggggaaacgctggatctttatagtcctgtcgggttccgccactcgtacttgagcgtcgattttgtg
tcccagcctgtcctcgcgctcctcgaaggctcccccttggcgaccatagaaatcaggacgccaaagcgggtggagactgaactcgcagctaaaaaac
4,930 4,940 4,950 4,960 4,970 4,980 4,990 5,000 5,010 5,020

atgctcgcagggggcggacctatgaaaaacgcagcaacgcgaccttttacggttccctgaccttttgccttctgaccttgcctacatgttcttccgcgcttat
tagagcagtcccccgctcggataccttttgcggtcgttgcgcggaaaaaatgccaaggaccggaanaacgacgggaaacagagtgtaacaagaagacccaata
5,030 5,040 5,050 5,060 5,070 5,080 5,090 5,100 5,110 5,120 5,130

ccctgatctgtgataaccgtataccgctttagtgagctgataccgctcggcagcgaacgaccgagcgcagcagtcagtgagcaggaaagcggaaag
ggggactaaagacctattggcaataatggcgaactcaactcgaactatggcgaagcggcctcggttctgctgctcgcgtcagtcactcctctcgccttc
5,140 5,150 5,160 5,170 5,180 5,190 5,200 5,210 5,220 5,230 5,240

```

BciVI

NspI

AflIII

PciI

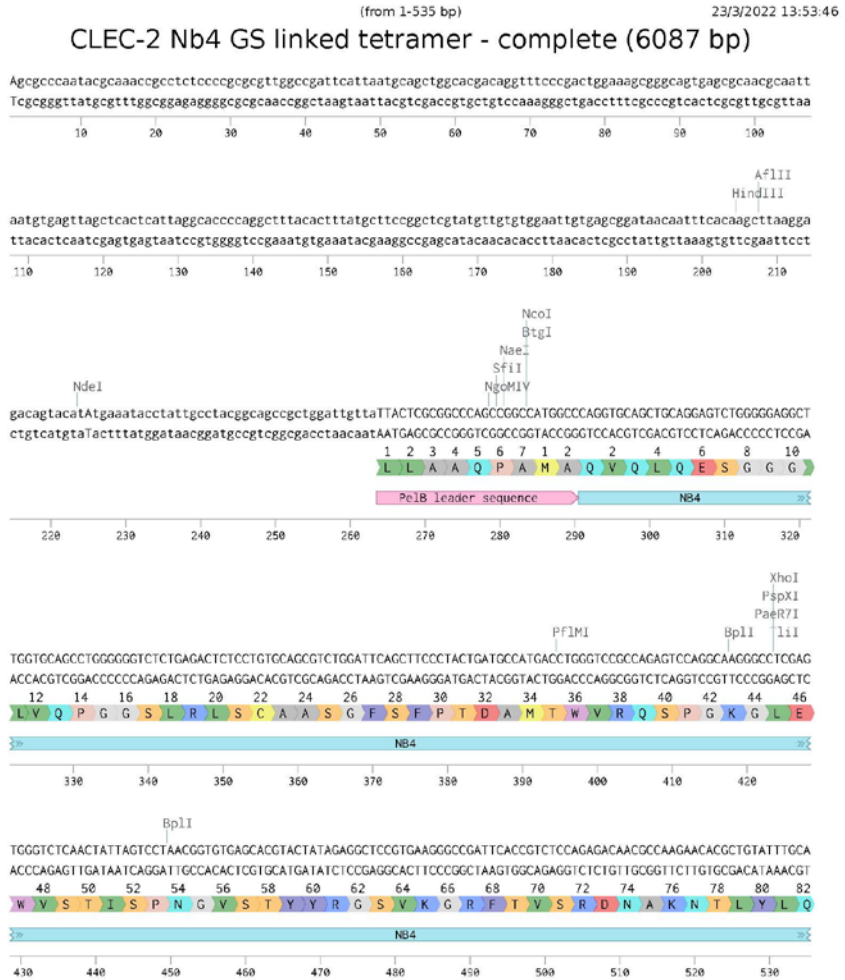
BspQI

SapI

https://benchling.com/eleyana/f//lib_BQFXPMYM-nanobodies/seq_Oh8dy/GR-clec-2-nb4-gs-linked-dimer-complete/edit

7/7

APPENDIX VII- tetrameric Nb4 DNA sequence



https://benchling.com/eleyrna/ff/lib_8QFXFMYM-nanobodies/seq_4hjbLbAu-clec-2-nb4-gs-linked-tetramer-complete/edit

1/8

CLEC-2 Nb4 GS linked tetramer - complete (6087 bp) (from 536-1070 bp)

23/3/2022 13:53:46



https://benchling.com/eleyana/f/1ib_BQFXPFMYM-nanobodies/seq_4hjbLbAu-clec-2-nb4-gs-linked-tetramer-complete/edit

2/8

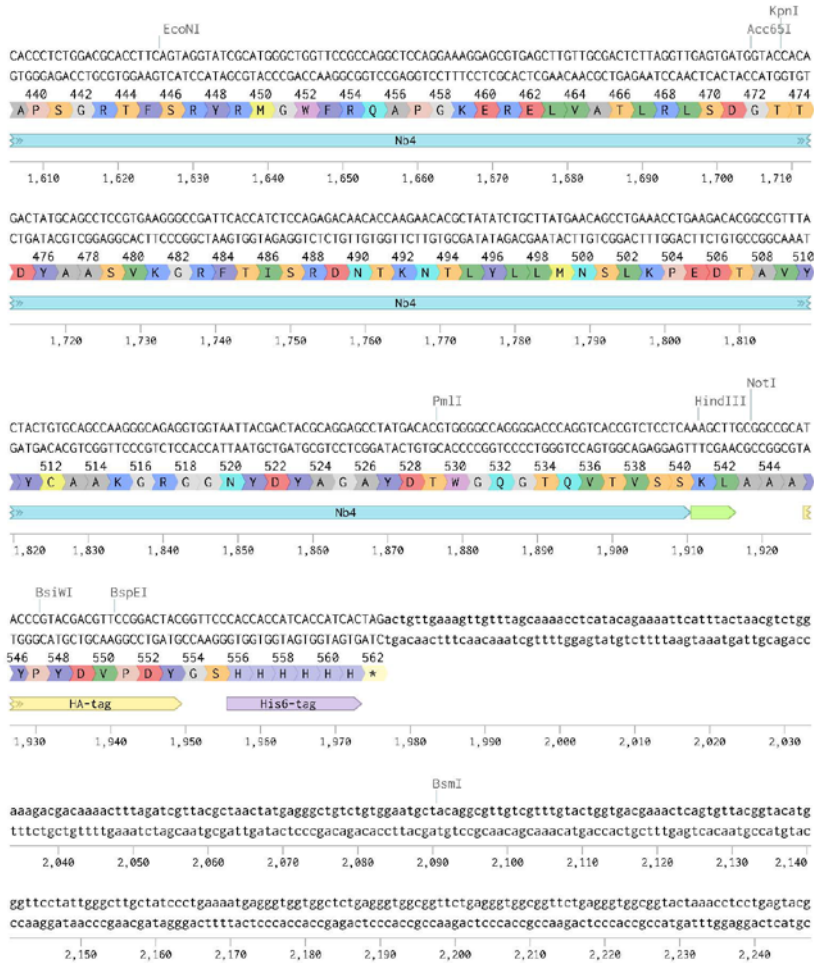


https://benchling.com/veleyna/f/1ib_BOQXFMYM-nanobodies/seq_4hjbLbAu-clec-2-nb4-gs-linked-tetramer-complete/edit

3/8

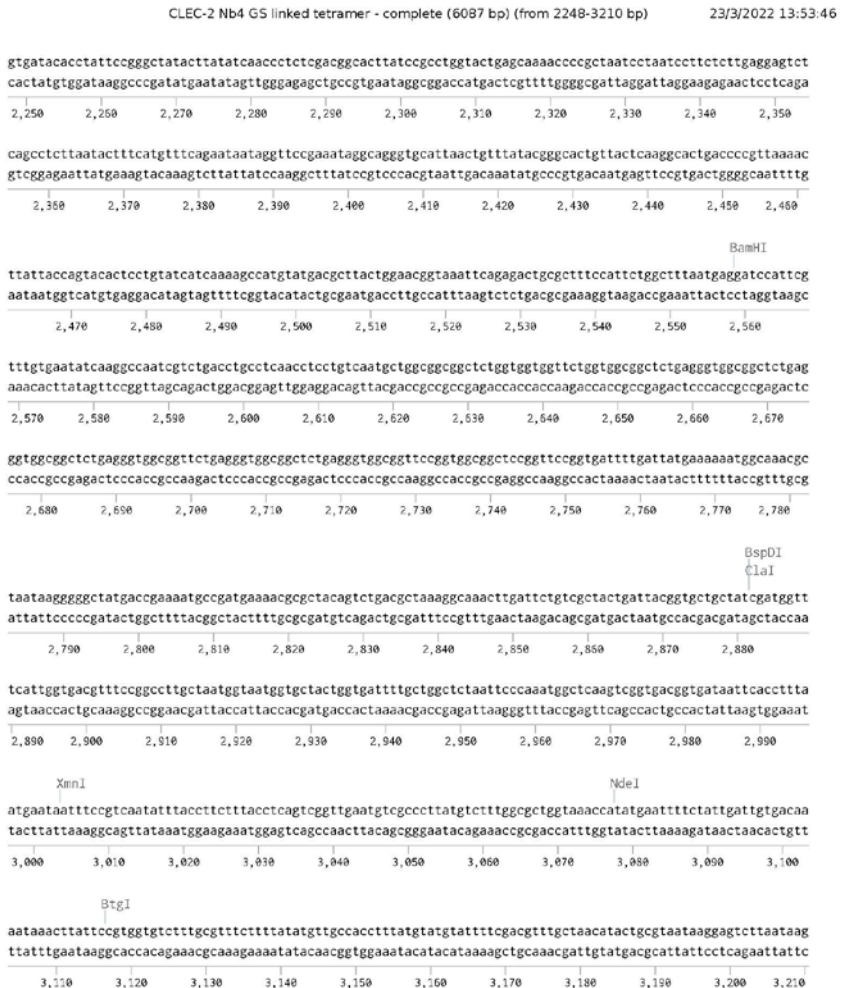
CLEC-2 Nb4 GS linked tetramer - complete (6087 bp) (from 1606-2247 bp)

23/3/2022 13:53:46



https://benchling.com/veleyna/f/1ib_BQFXFMYM-nanobodies/seq_4hjbLbAu-clec-2-nb4-gs-linked-tetramer-complete/edit

4/8

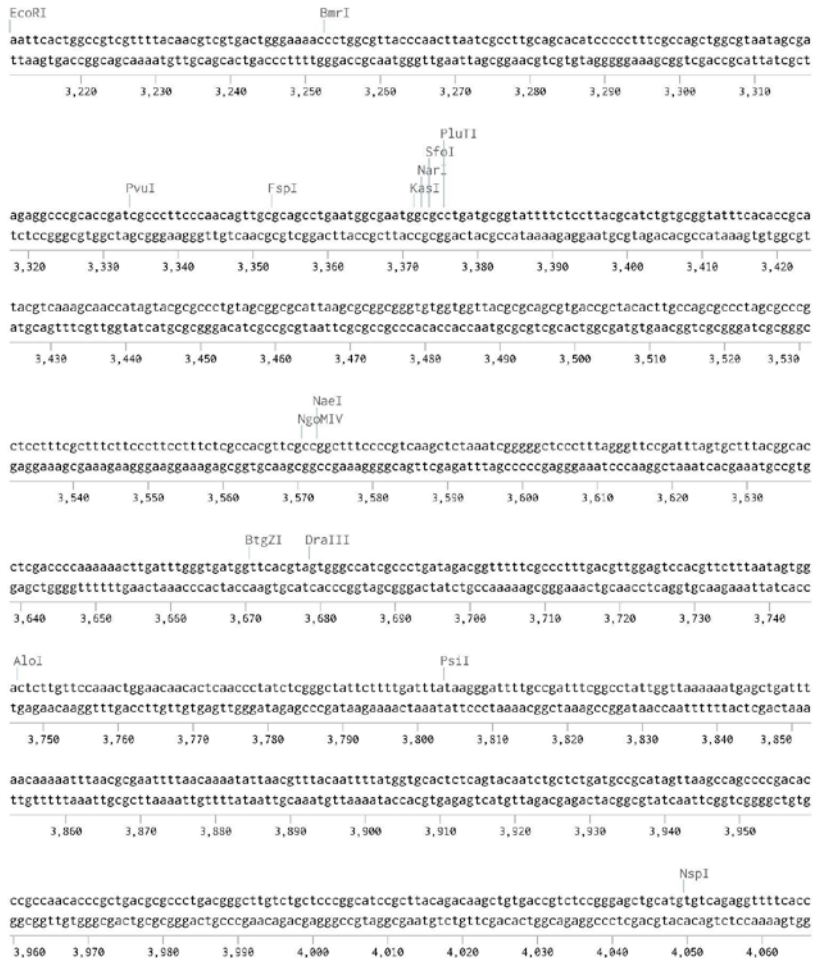


https://benchling.com/eleyana/f/1ib_BOQFXMYM-nanobodies/seq_4hjbLbAu-clec-2-nb4-gs-linked-tetramer-complete/edit

5/8

CLEC-2 Nb4 GS linked tetramer - complete (6087 bp) (from 3211-4066 bp)

23/3/2022 13:53:46

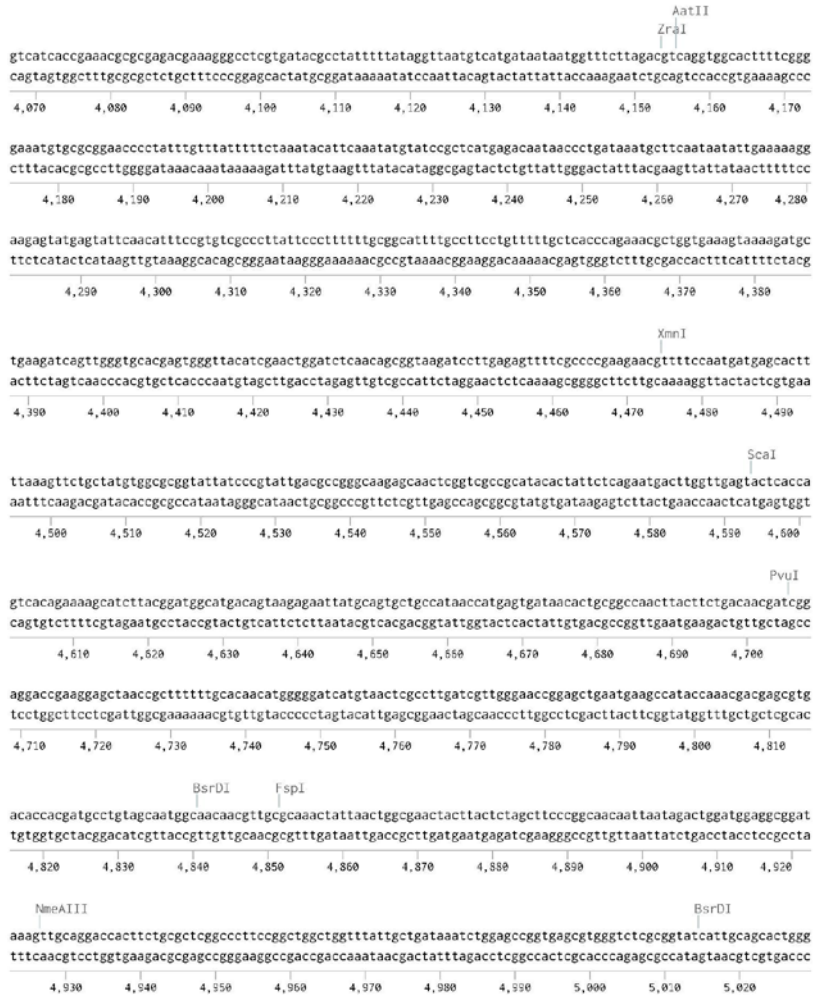


https://benchling.com/eleyana/f/llib_BOQXPMYM-nanobodies/seq_4hjbLbAu-clec-2-nb4-gs-linked-tetramer-complete/edit

6/8

CLEC-2 Nb4 GS linked tetramer - complete (6087 bp) (from 4067-5029 bp)

23/3/2022 13:53:46

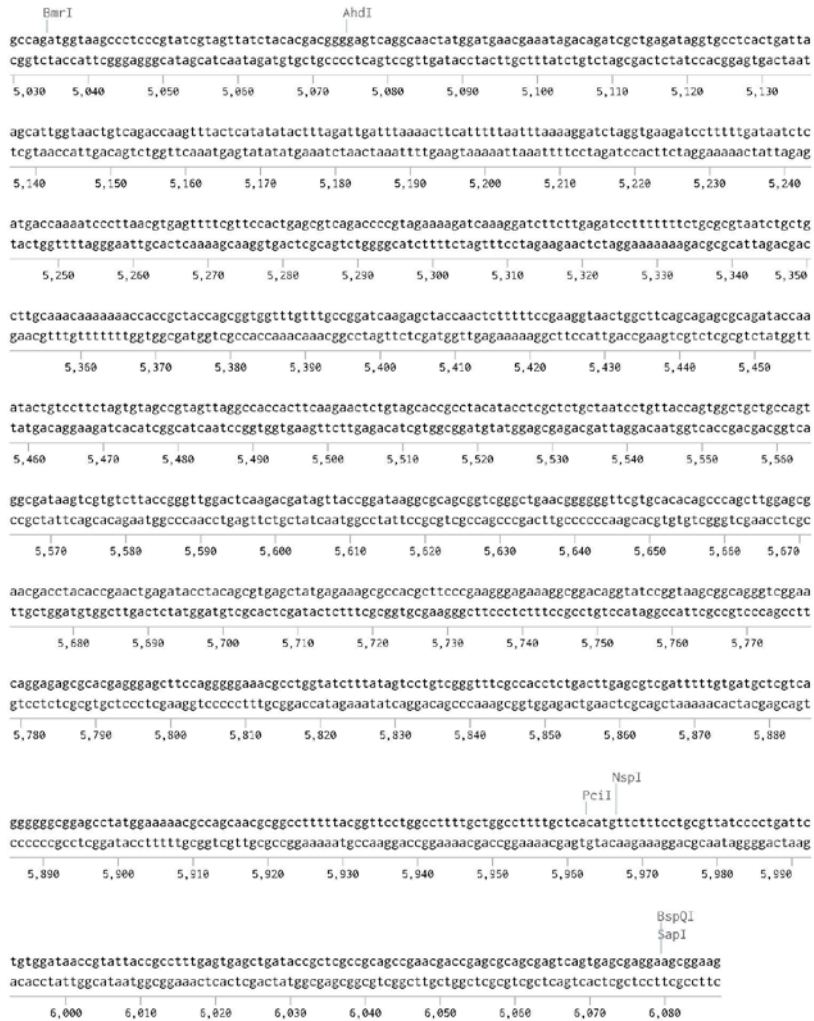


https://benchling.com/veleyna/f//lib_BOQFXMYM-nanobodies/seq_4hjbLbAu-clec-2-nb4-gs-linked-tetramer-complete/edit

7/8

CLEC-2 Nb4 GS linked tetramer - complete (6087 bp) (from 5030-6087 bp)

23/3/2022 13:53:46

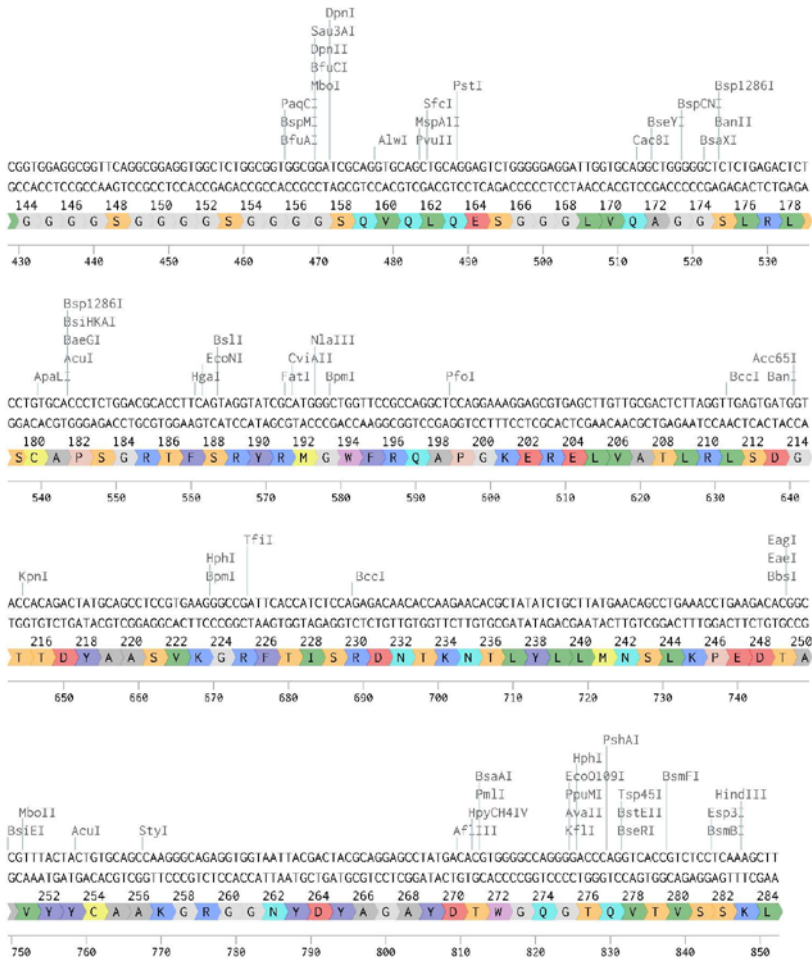


https://benchling.com/veleyna/f//lib_BOQXFMYM-nanobodies/seq_4hjbLbAu-clec-2-nb4-gs-linked-tetramer-complete/edit

8/8

Twist Bioscience - Nb4 dimer synthesized DNA (852 bp) (from 429-852 bp)

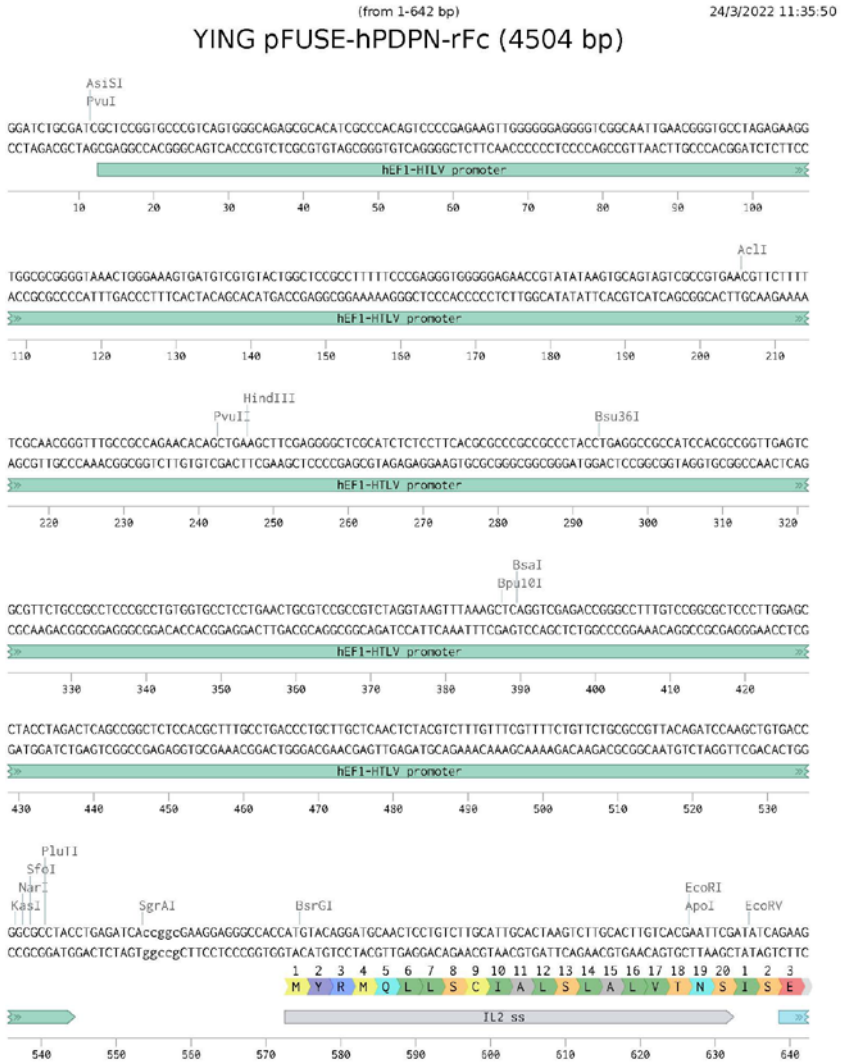
23/3/2022 13:58:23



https://benchling.com/eleyana/f//lib_8QFXPMYM-nanobodies/seq_r1P165mf-twist-bioscience-nb4-dimer-synthesized-dna/edit

2/2

APPENDIX IX- human podoplanin- rabbit Fc DNA sequence



https://benchling.com/eleyrna/f/lib_NGqTTrco-clec-2/seq_dAA3cVHY-ying-pfuse-hpdpn-rfc/edit

1/7

YING pFUSE-hPDPN-rFc (4504 bp) (from 643-1177 bp)

24/3/2022 11:35:50



https://benchling.com/veleyna/f/lib_NGqTTrco-clec-2/seq_dAA3cVHY-ying-pfuse-hpdpn-rfc/edit

2/7

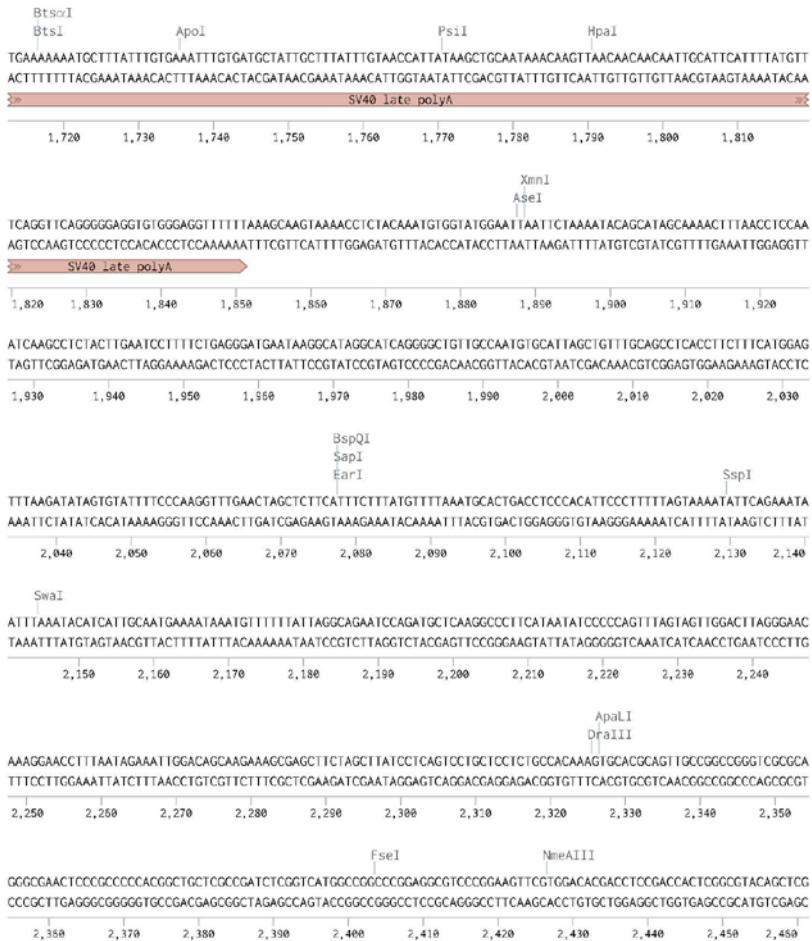


https://benchling.com/veleyna/f/lib_NGqTTrco-clec-2/seq_dAA3cVHY-ying-pfuse-hdpn-rfc/edit

3/7

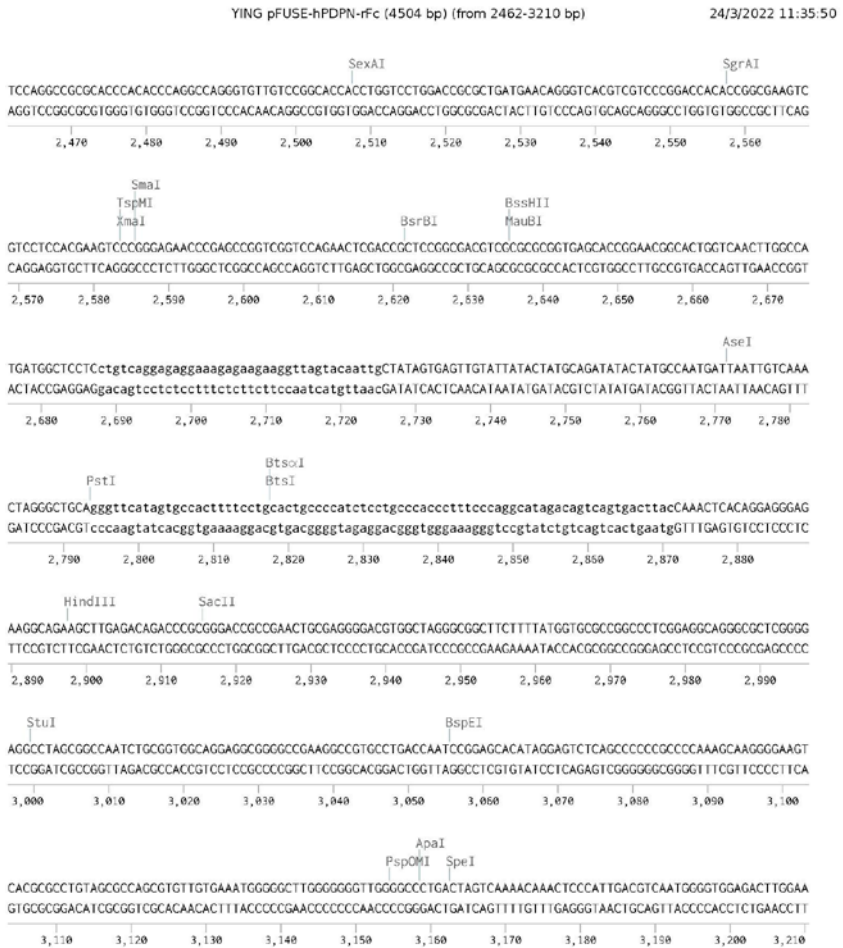
YING pFUSE-hDPN-rFc (4504 bp) (from 1713-2461 bp)

24/3/2022 11:35:50



https://benchling.com/eleyana/f/ib_NGqTTrco-clec-2/seq_dAA3cVHY-ying-pfuse-hdpn-rfc/edit

4/7

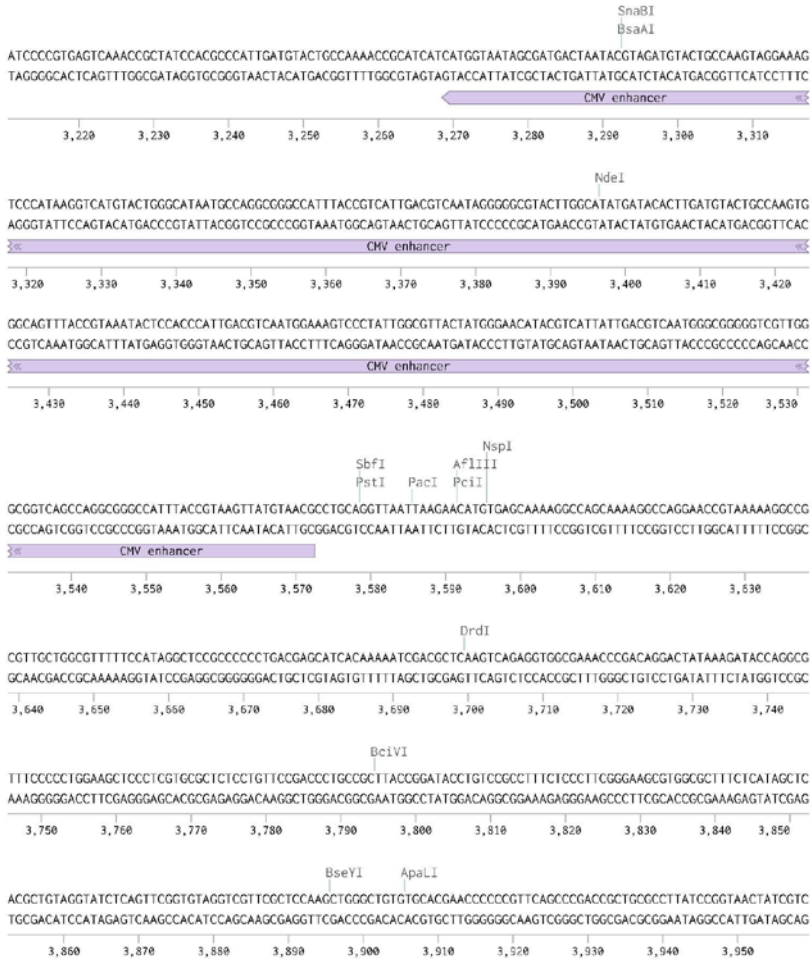


https://benchling.com/eleyrna/f/lib_NGqTTrco-clec-2/seq_dAA3cVHY-ying-pfuse-hdpn-rfc/edit

5/7

YING pFUSE-hDPN-rFc (4504 bp) (from 3211-3959 bp)

24/3/2022 11:35:50

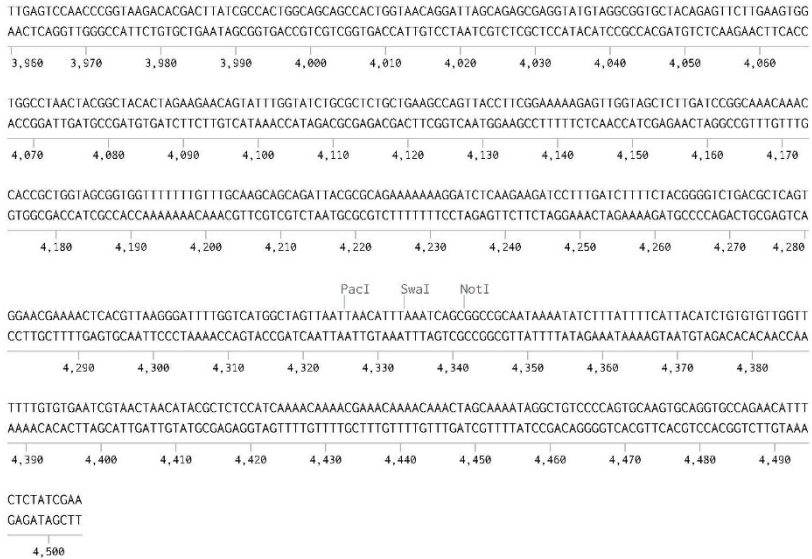


https://benchling.com/eleyrna/f/lib_NGqTTrco-clec-2/seq_dAA3cVHY-ying-pfuse-hdpn-rfc/edit

6/7

YING pFUSE-hDPN-rFc (4504 bp) (from 3960-4504 bp)

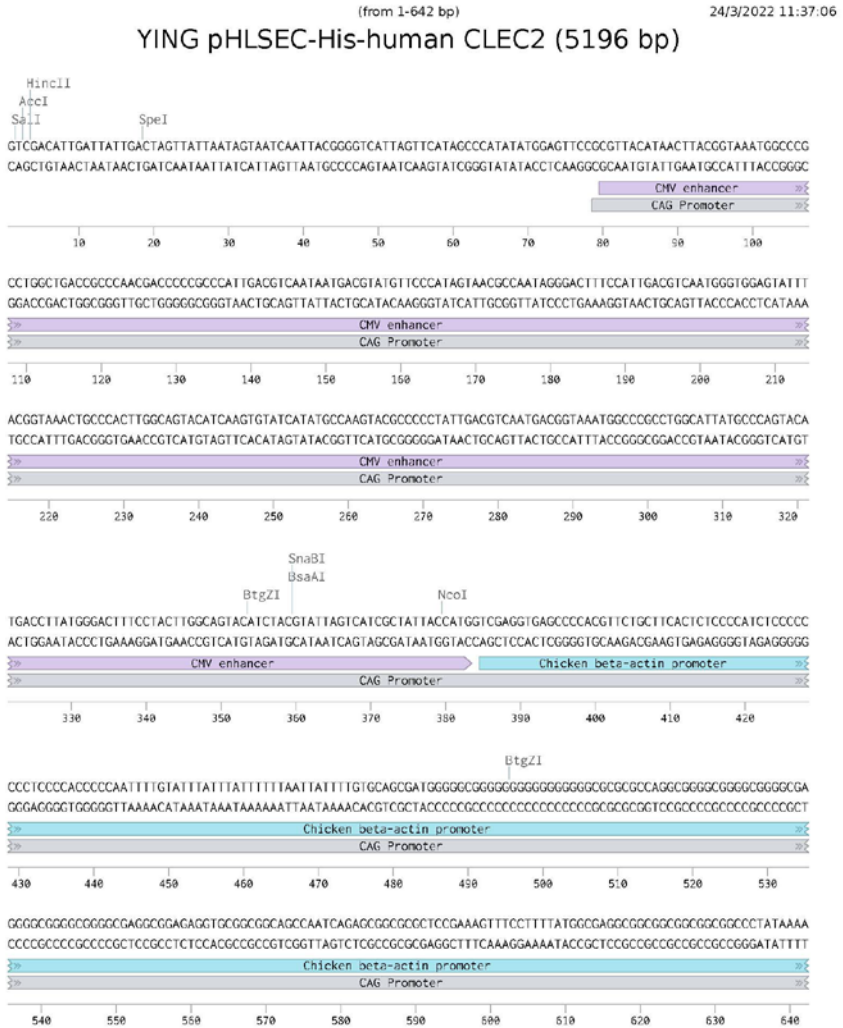
24/3/2022 11:35:50



https://benchling.com/eleyna/f/lib_NGqTTrco-clec-2/seq_dAA3cVHY-ying-pfuse-hdpn-rfc/edit

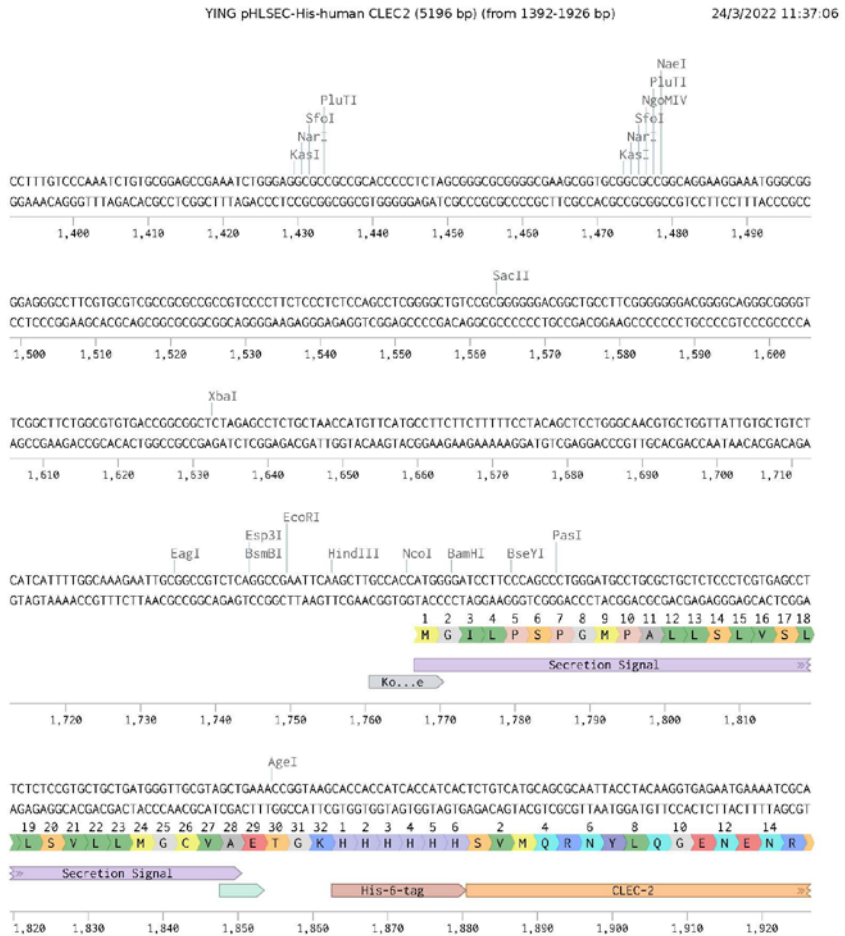
7/7

APPENDIX X- human CLEC-2-His tag DNA sequence



https://benchling.com/eleyyna/f/lib_NGqTTrco-clec-2/seq_fmT5I4Tg-ying-phlsec-his-human-clec2-edit

1/8



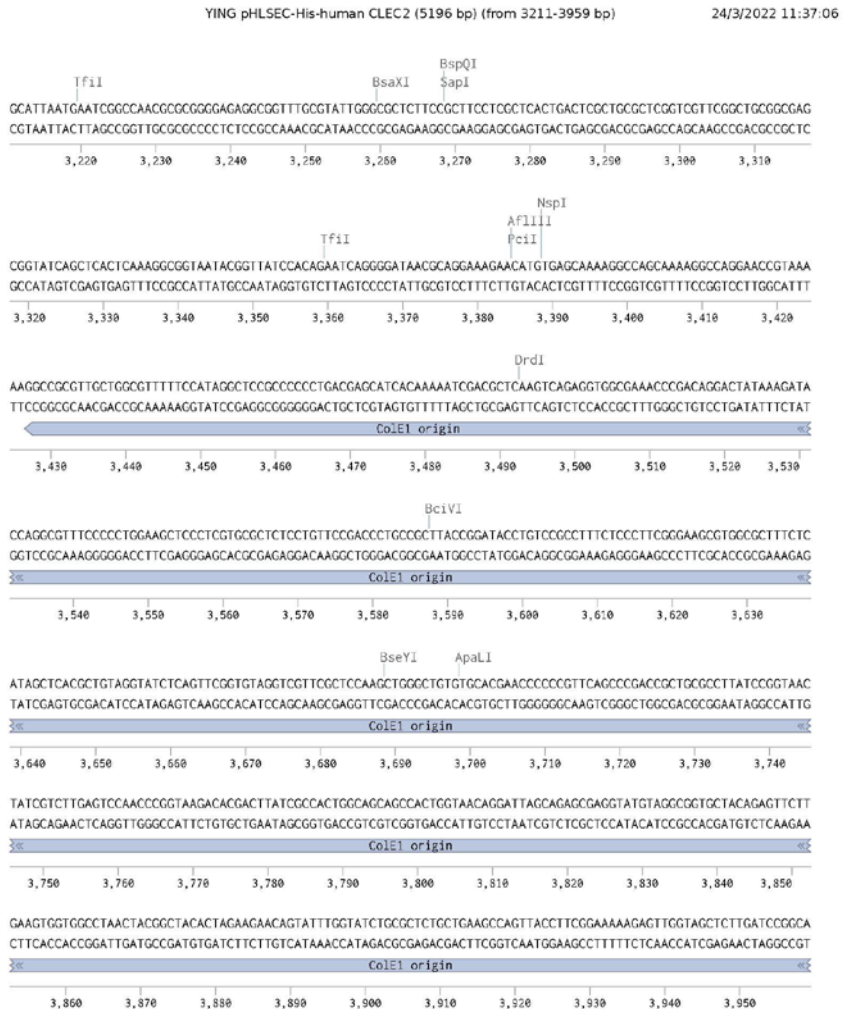
https://benchling.com/veleyna/f/lib_NGqTTrco-clec-2/seq_fMT5I4Tg-ying-phlsec-his-human-clec2/edit

3/8



https://benchling.com/eleyyna/f/llib_NGqTTrco-clec-2/seq_fMT5I4Tg-ying-phlsec-his-human-clec2/edit

5/8

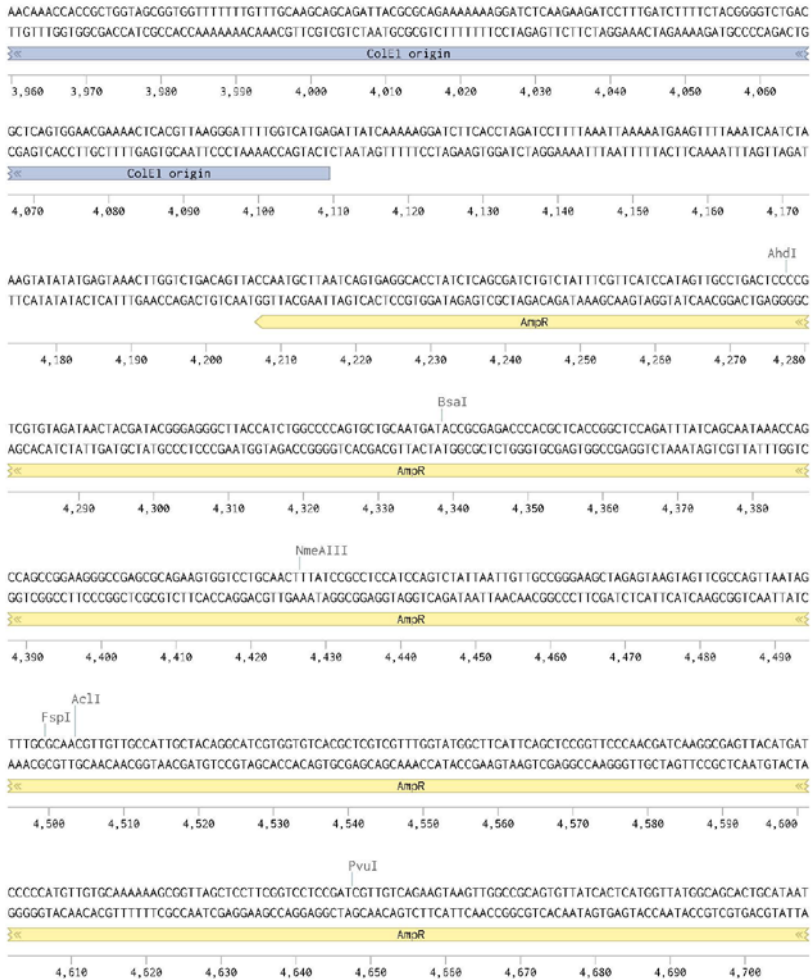


https://benchling.com/eleyyna/f//lib_NGqTTrco-clec-2/seq_fMT5I4Tg-ying-phlsec-his-human-clec2-edit

6/8

YING pHLSEC-His-human CLEC2 (5196 bp) (from 3960-4708 bp)

24/3/2022 11:37:06

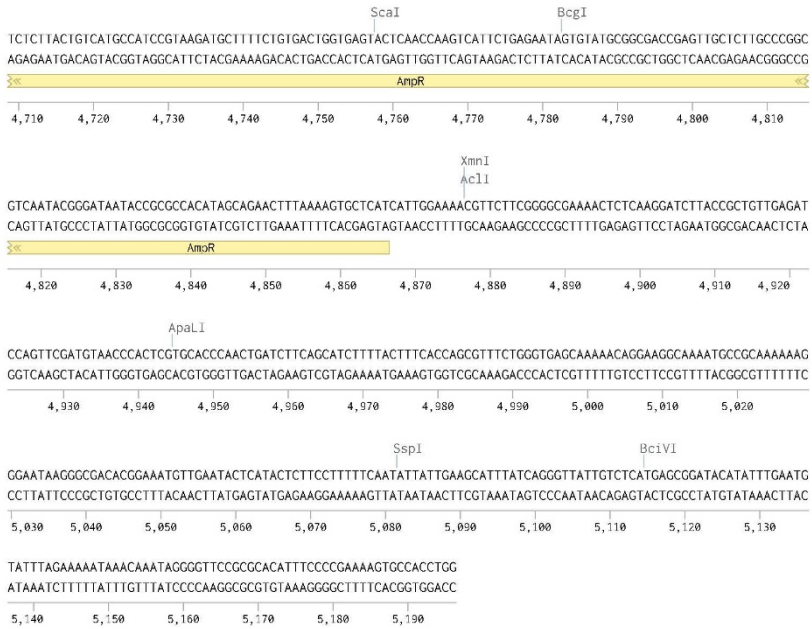


https://benchling.com/veleyna/f/lib_NGqTTrco-clec-2/seq_fMT5I4Tg-ying-phlsec-his-human-clec2-edit

7/8

YING pHLSEC-His-human CLEC2 (5196 bp) (from 4709-5196 bp)

24/3/2022 11:37:06



https://benchling.com/eleyana/f/lib_NGqTTrco-clec-2/seq_fMT5I4Tg-ying-phlsec-his-human-clec2-edit

8/8

APPENDIX XI- List of publications**Publications included in this thesis:**

Morán LA, Di Y, Sowa MA, Hermida-Nogueira L, Barrachina MN, Martin E, Clark JC, Mize TH, Eble JH, Moreira D, Pollitt AY, Loza MI, Domínguez E, Watson SP, García A. Katakine is a new ligand of CLEC-2 that acts as a platelet agonist. *Thromb Haemost.* 2022 Feb 15. DOI: 10.1055/a-1772-1069.

Cheung HYF*, Morán LA*, Sickmann A, Heemskerk JWM, Garcia A, Watson SP. Inhibition of Src but not Syk causes weak reversal of GPVI-mediated platelet aggregation measured by light transmission aggregometry. *Platelets.* 2022 May 9:1-8. doi: 10.1080/09537104.2022.2069235 * Co-first author

Review article:

Damaskinaki FN*, Morán LA*, A Garcia, B Kellam, SP Watson. Overcoming challenges in developing small molecule inhibitors for GPVI and CLEC-2, *Platelets*, 2021 32:6, 744-752, DOI: 10.1080/09537104.2020.1863939 * Co-first author

Publications not included on thesis where the author was a co-author:

Zhi Z, Jooss NJ, Sun Y, Colicchia M, Slater A, Morán LA, Cheung HYF, Di Y, Rayes J, Poulter NS, Watson SP, Iqbal AJ. Galectin-9 activates platelet ITAM receptors glycoprotein VI and C-type lectin-

like receptor-2. *J Thromb Haemost.* 2022 Apr;20(4):936-950. doi: 10.1111/jth.15625.

Martin EM*, Zuidsherwoude M*, Morán LA, Di Y, García A, Watson SP. The structure of CLEC-2: mechanisms of dimerization and higher-order clustering. *Platelets*, 2021 32:6, 733-743, DOI: 10.1080/09537104.2021.1906407

Barrachina MN, Izquierdo I, Hermida-Nogueira L, Morán LA, Pérez A, Arroyo AB, García-Barberá N, González-Conejero R, Troitiño S, Eble JA, Rivera J, Martínez C, Loza MI, Domínguez E, García Á. The PI3K δ Inhibitor Idelalisib Diminishes Platelet Function and Shows Antithrombotic Potential. *International Journal of Molecular Sciences.* 2021; 22(7):3304. <https://doi.org/10.3390/ijms22073304>

Barrachina MN, Hermida-Nogueira L, Morán LA, Casas V, Hicks SM, Sueiro AM, Di Y, Andrews RK, Watson SP, Gardiner EE, Abian J, Carrascal M, Pardo M, García Á. Phosphoproteomic Analysis of Platelets in Severe Obesity Uncovers Platelet Reactivity and Signaling Pathways Alterations. *Arterioscler Thromb Vasc Biol.* 2021 Jan;41(1):478-490. doi: 10.1161/ATVBAHA.120.314485.

Hermida-Nogueira L, Barrachina MN, Morán LA, Bravo S, Diz P, García Á, Blanco J. Deciphering the secretome of leukocyte-platelet rich fibrin: towards a better understanding of its wound healing properties. *Sci Rep.* 2020 Sep 3;10(1):14571. doi: 10.1038/s41598-020-71419-7

Barrachina MN, Morán LA, Izquierdo I, Casanueva FF, Pardo M, García Á. Analysis of platelets from a diet-induced obesity rat model: elucidating platelet dysfunction in obesity. *Sci Rep.* 2020 Aug 4;10(1):13104. doi: 10.1038/s41598-020-70162-3.

Izquierdo I, Barrachina MN, Hermida-Nogueira L, Casas V, Morán LA, Lacerenza S, Pinto-Llorente R, Eble JA, de Los Ríos V, Domínguez E, Loza MI, Casal JI, Carrascal M, Abián J, García A. A Comprehensive Tyrosine Phosphoproteomic Analysis Reveals Novel Components of the Platelet CLEC-2 Signaling Cascade. *Thromb Haemost.* 2020 Feb;120(2):262-276. doi: 10.1055/s-0039-3400295.

APPENDIX XII- MONOGRAPHIC THESIS WITH TOTAL OR PARTIAL REPRODUCTION OF PUBLICATIONS

Publications which content is involved in this thesis:

Morán LA, Di Y, Sowa MA, Hermida-Nogueira L, Barrachina MN, Martin E, Clark JC, Mize TH, Eble JH, Moreira D, Pollitt AY, Loza MI, Domínguez E, Watson SP, García A. Katakine is a new ligand of CLEC-2 that acts as a platelet agonist. *Thromb Haemost.* 2022 Feb 15. DOI: 10.1055/a-1772-1069.

This article was published in the journal: *Thrombosis and Haemostasis*, this journal is related to the field of hematology (Q1) with an impact factor (IF) of 5.723 (2020). This publication has been published in OpenAccess format in 2022.

The author contributed to the article titled: Katakine is a new ligand of CLEC-2 that acts as a platelet agonist is reflected in chapter 4 of this thesis. performing and designing experiments, data analysis, and writing the article. Data associated with this article are found in chapter 5.

The co-authors and affiliations for this article are the following:

Luis A. Morán^{1,2}, Ying Di², Marcin A. Sowa^{1,3}, Lidia Hermida-Nogueira¹, María N Barrachina^{1†}, Eleya Martin², Joanne C. Clark², Todd H. Mize⁴, Johannes A. Eble⁵, David Moreira¹, Alice Y. Pollitt³, María I. Loza¹, Eduardo Domínguez¹, Steve P. Watson², Ángel García¹

¹Center for Research in Molecular Medicine and Chronic Diseases (CIMUS), Universidad de Santiago de Compostela, and Instituto de Investigación Sanitaria (IDIS), Santiago de Compostela, Spain

²Institute of Cardiovascular Sciences, College of Medical and Dental Sciences, University of Birmingham, UK

³Institute for Cardiovascular and Metabolic Research (ICMR), School of Biological Sciences, University of Reading, Reading, UK

⁴Advanced Mass Spectrometry Facility, Biosciences, College of Life and Environmental Sciences, University of Birmingham, UK

⁵Institute for Physiological Chemistry & Pathobiochemistry, University of Münster, Germany

†Current affiliation: Vascular Biology Program, Boston Children's Hospital, Harvard Medical School, Boston, USA

Ying Di, Marcin A. Sowa, Lidia Hermida-Nogueira, María N Barrachina, Eleya Martin, Joanne C. Clark, Todd H. Mize, David Moreira contributed performing experiments, Johannes A. Eble provided key reagents. Alice Y. Pollitt, María I. Loza, Eduardo Domínguez, Steve P. Watson, Ángel García provided supervision, design experiments, write the manuscript.

Cheung HYF*, Morán LA*, Sickmann A, Heemskerk JWM, Garcia A, Watson SP. **Inhibition of Src but not Syk causes weak reversal of GPVI-mediated platelet aggregation measured by light transmission aggregometry.** *Platelets*. 2022 May 9:1-8. doi: 10.1080/09537104.2022.2069235 * Co-first author.

This article was published in the journal: *Platelets*, this journal has an impact factor (IF) of 3.862 (2020). This publication has been published in OpenAccess format in 2022.

The article titled Inhibition of Src but not Syk causes weak reversal of GPVI-mediated platelet aggregation measured by light transmission aggregometry is reflected in Chapter 7 of this thesis.

In this article, Hilaire Yam Fung Cheung and I have equally contributed to the development of this study. We both contributed writing the manuscript, performed experiments and analysed the data. Sickmann A, Heemskerk JWM, Garcia A, and Watson SP designed the experiments, provided supervision, consumables and wrote the manuscript

List of authors and affiliations are the following:

Hilaire Yam Fung Cheung ^{1 2 3}, Luis A Moran ^{1 4}, Albert Sickmann ², Johan W M Heemskerk ³, Ángel Garcia ⁴, Steve P Watson ¹

¹Institute of Cardiovascular Sciences, College of Medical and Dental Sciences, University of Birmingham, Birmingham, UK.

²Department of Bioanalytics, Leibniz-Institut für Analytische Wissenschaften-ISAS-e.V, Dortmund, Germany.

³Department of Biochemistry, Cardiovascular Research Institute Maastricht (CARIM), Maastricht University, Maastricht, The Netherlands.

⁴Center for Research in Molecular Medicine and Chronic Diseases (CIMUS), Universidad de Santiago de Compostela, and Instituto de Investigación Sanitaria (IDIS), Santiago de Compostela, Spain.

Luis A Morán

Declaration of conflict of interest

The author declares no conflict of interest.

Santiago de Compostela, Spain, 30th of March 2022

Luis A. Morán



Platelets are anucleate cells derived from megakaryocytes, which play an important role in the regulation of haemostasis and thrombosis at the injury site; they are also involved in other physiological processes, known as thromboinflammation. This process is modulated by platelet receptors, including CLEC-2. In this study we searched for novel ligands for the platelet receptor CLEC-2, identifying a new platelet agonist, called katacine, which induces strong platelet aggregation through CLEC-2. We also developed multimeric nanobodies against CLEC-2 and we suggested that tetrameric structures are needed to induce platelet aggregation, while lower orders of oligomerisation are able to prevent platelet aggregation. The novel tools will facilitate further research on CLEC-2 function and the mode of activation of CLEC-2.